Report 33651F
30 September 1981

NASA

DESIGN, FABRICATION, TEST, AND DELIVERY OF A HIGH-PRESSURE OXYGEN/RP-1 INJECTOR

Final Report

By

L. Schoenman
R. S. Gross
Aerojet Liquid Rocket Company

Prepared For

National Aeronautics and Space Administration
George C. Marshall Space Flight Center
Huntsville, Alabama 35812

Contract NAS 8-33651

Report 33651F
30 September 1981

DESIGN, FABRICATION, TEST, AND DELIVERY OF A HIGH-PRESSURE OXYGEN/RP-1 INJECTOR

Final Report

By

L. Schoenman
R. S. Gross
Aerojet Liquid Rocket Company

Prepared For

National Aeronautics and Space Administration
George C. Marshall Space Flight Center
Huntsville, Alabama 35812

Contract NAS 8-33651

1. Report No.	2. Government Accession No.	3. Recipient's Catalog No.
33651F		

4. Title and Subtitle	5. Report Date
Design, Fabrication, Test, and Delivery of A High-Pressure Oxygen/RP-1 Injector	30 September 1979
	6. Performing Organization Code

7. Author(s)	8. Performing Organization Report No.
L. Schoenman and R. S. Gross	
	10. Work Unit No.

9. Performing Organization Name and Address	11. Contract or Grant No.
Aerojet Liquid Rocket Company Post Office Box 13222 Sacramento, California 95813	NAS 8-33651
	13. Type of Report and Period Covered
12. Sponsoring Agency Name and Address	Contractor Report, Final
National Aeronautics and Space Administration Washington, D.C. 20546	14. Sponsoring Agency Code

15. Supplementary Notes

Project Manager, C. R. Bailey, Propulsion Division
NASA-Marshall Space Flight Center
Marshall Space Flight Center, Alabama 35812

16. Abstract

This final report presents a summary of the design analyses for a liquid rocket injector using oxygen and RP-1 propellants at high chamber pressures of 20,682 kPa (3000 psia). This analytical investigation includes combustion efficiency versus injector element type, combustion stability, and combustor cooling requirements. The design and fabrication of a subscale injector/acoustic resonator assembly capable of providing a nominal thrust of 222K N (50,000 lbF) is presented.

PRECEDING PAGE BLANK NOT FILMED

17. Key Words (Suggested by Author(s))	18. Distribution Statement
Liquid Rocket Injector LOX/RP-1 Combustion Combustion Stability	Unclassified-Unlimited

19. Security Classif. (of this report)	20. Security Classif. (of this page)	21. No. of Pages	22. Price*
Unclassified	Unclassified	91	

FOREWORD

This is the final report submitted for the "Design, Fabrication, Test, and Delivery of a High-Pressure/RP-1 Injector" program as per the requirements of Contract NAS 8-33651. The work is being perfomred by the Aerojet Liquid Rocket Company (ALRC) for the NASA-George C. Marshall Space Flight Center (MSFC . The contract period of performance is 1 January 1980 through 15 July 1981.

The program goal is to provide combustion device technology required for the development of high-pressure liquid oxygen/hydrocarbon (LOX/HC) booster engines. The specific end product of this contract is a stable, high-performing, and compatible injector for 3000 psia chamber pressure operation, using liquid oxygen and liquid RP-1 as the propellants.

The NASA/MSFC project manager is Mr. Curtis R. Bailey. The ALRC program manager is Mr. J. W. Salmon, and the project engineers are Mr. R. S. Gross and, as of April 1981, Mr. L. Schoenman. The program lead analyst and mechanical designer are Mr. J. I. Ito and Mr. K. Y. Wong, respectively.

TABLE OF CONTENTS

LIST OF TABLES

LIST OF FIGURES

LIST OF FIGURES (cont.)

LIST OF PRINCIPAL SYMBOLS

EB	=	Electron Beam Welding
ED	=	Electrical Discharge Machining
ERE	=	Energy Release Efficiency
HC	=	Hydrocarbon
HDF	=	High-Density Fuel
LOL	=	Like-on-Like
LOX	=	Liquid Oxygen
MMH	=	Monomethylhydrazine
MR	=	Mixture Ratio
OMS	=	Orbital Maneuvering System
PAT	=	Preatomized Triplet
PN	=	Part Number
RP-1	=	Rocket Propellant No. 1
SI	=	System International
STS	=	Space Transportation System
TCE	=	1,1,1-trichloroethane
TLOL	=	Transverse Like-on-Like
XDT	=	X-Doublet
C*	=	Characteristic velocity
Cd	=	Discharge coefficient
CSM	=	Combustion Stability Monitor
D	=	Diameter
ΔP/psid	=	Pressure drop
E_m	=	Mixing efficiency
ε_{sl}	=	Sea-level area ratio
F	=	Thrust
fps	=	Feet per second
lbF	=	Pounds thrust
Isp	=	Specific impulse
Isp_{ODE}	=	Specific impulse, one-dimensional equilibrium
K	=	Thousand
°K	=	°Kelvin
kPa	=	Kilo pascals

LIST OF PRINCIPAL SYMBOLS (cont.)

Kw	=	Flow coefficient, (Kw) $= \left(\frac{\dot{w}\ (kg/sec)}{\sqrt{\Delta P\ (kPa)\ Sg}}\right)$ or $\left(\frac{\dot{w}\ (lb/sec)}{\sqrt{\Delta P\ (psi)\ Sg}}\right)$
L'	=	Length (prime)
1L	=	First longitudinal mode of instability
1T	=	First tangential mode of instability
λ_{atom}	=	Droplet atomization length
M	=	Million
μ	=	Micro
mps	=	Meter per second
N/m^2	=	Newton per square meter
N	=	Newtons
ρ	=	Density
P	=	Pressure
Pc	=	Chamber pressure
psia	=	Pounds per square inch absolute
°R	=	°Rankine
r_m	=	Mass median droplet radius
σ_g	=	Geometric distribution of drop sizes
Sg	=	Specific gravity
T	=	Temperature
τ_g	=	Gas resonance time
τ_f	=	Fuel sensitive time lag for stability analysis
τ_{ox}	=	Oxidizer sensitive time lag for stability analysis
θ_f	=	Fuel impingement angle
V	=	Velocity
$\dot{w}$	=	Flowrate lb/sec

Subscript:

ox	=	Oxidizer
f	=	Fuel

I. INTRODUCTION

A. BACKGROUND

Over the past several years, increasing priority has been given to the development of an economical and practical Space Transportation System (STS). Numerous NASA-sponsored and ALRC in-house studies have identified high-pressure LOX/hydrocarbon booster engine stages to have significant envelope, weight, and payload advantages over current booster systems. High-pressure combustion is a critical technology to the development of a LOX/hydrocarbon booster engine. In these studies, various hydrocarbon and amine fuels have been considered, including RP-1, RJ-5, propane, hydrazine, monomethylhydrazine (MMH), and methane. On a comparative basis, RP-1 offers density, cost, and availability advantages over some of the other fuels. Unfortunately, no combustion and heat transfer data for the LOX/RP-1 combination at chamber pressures approaching 20,682 to 27,576 kPa (3000 to 4000 psia) has resulted from these study efforts.

This contracted effort supports the previous NASA/MSFC in-house booster technology programs by providing an injector for use with liquid oxygen and RP-1 propellants at chamber pressures to 20,682 kPa (3000 psia). The injector will subsequently be tested at MSFC, using a water-cooled calorimeter chamber over a chamber pressure range of 13,788 to 16,546 kPa (2000 to 2400 psia) and a hydrogen-cooled axial milled-slot chamber at pressures up to 20,682 kPa (3000 psia). Data from this test program will be an important step toward extending the existing predictive capabilities and hardware technology relevant to the LOX/RP-1 booster application.

B. OBJECTIVES

To meet the program objectives, demonstration of the following technical tasks was required:

I, B, Objectives

- Delivery to MSFC of a high-performance, stable injector for use with LOX/RP-1 propellants.

- Interfacing of the injector assembly with the calorimetric chamber for operation at 13,788 to 16,546 kPa (2000 to 2400 psia).

- Interfacing of the injector assembly with the hydrogen-cooled axial milled-slot chamber for operation at 20,682 kPa (3000 psia).

- Demonstrated C* efficiency >97%.

- Stable combustion; allowable chamber pressure oscillations $\pm$ 5% Pc.

In order to accomplish these objectives, the program was divided into the following four major tasks:

Task I - Analysis and Preliminary Design
Task II - Detailed Design and Fabrication, Assembly, and Flow Check
Task III - Delivery
Task IV - Reviews and Reports

The objective of Task I, Analysis and Preliminary Design, was to identify those injector concepts capable of meeting the design requirements defined in Table I-I while maintaining compatibility with the NASA chamber interface shown in Figure I-1.

The objective of Task II, Detailed Design and Fabrication, was to accomplish the detailed analysis, design, fabrication, and cold-flow verification of the selected injector concept.

TABLE I-I

LOX/RP-1 INJECTOR DESIGN REQUIREMENTS

Chamber Pressure	13,788 to 20,682 kPa	(2000 to 3000 psia)
Fuel:		RP-1
Temperature		Ambient
Max. Interface Pressure	27,576 kPa	(4000 psia)
Oxidizer:		Oxygen
Temperature	103°K	(185°R)
Max. Interface Pressure	27,576 kPa	(4000 psia)
Propellant Mixture Ratio		2.8
Characteristic Velocity Efficiency		>97%
Allowable Chamber Pressure Oscillations		$\leq \pm 5\%$ P_c
Combustion Chamber:		
Throat Diameter	8.41 cm	(3.31 in.)
Chamber Diameter	14.38 cm	(5.66 in.)
Length (Injector to Throat)	35.48 cm	(13.97 in.)

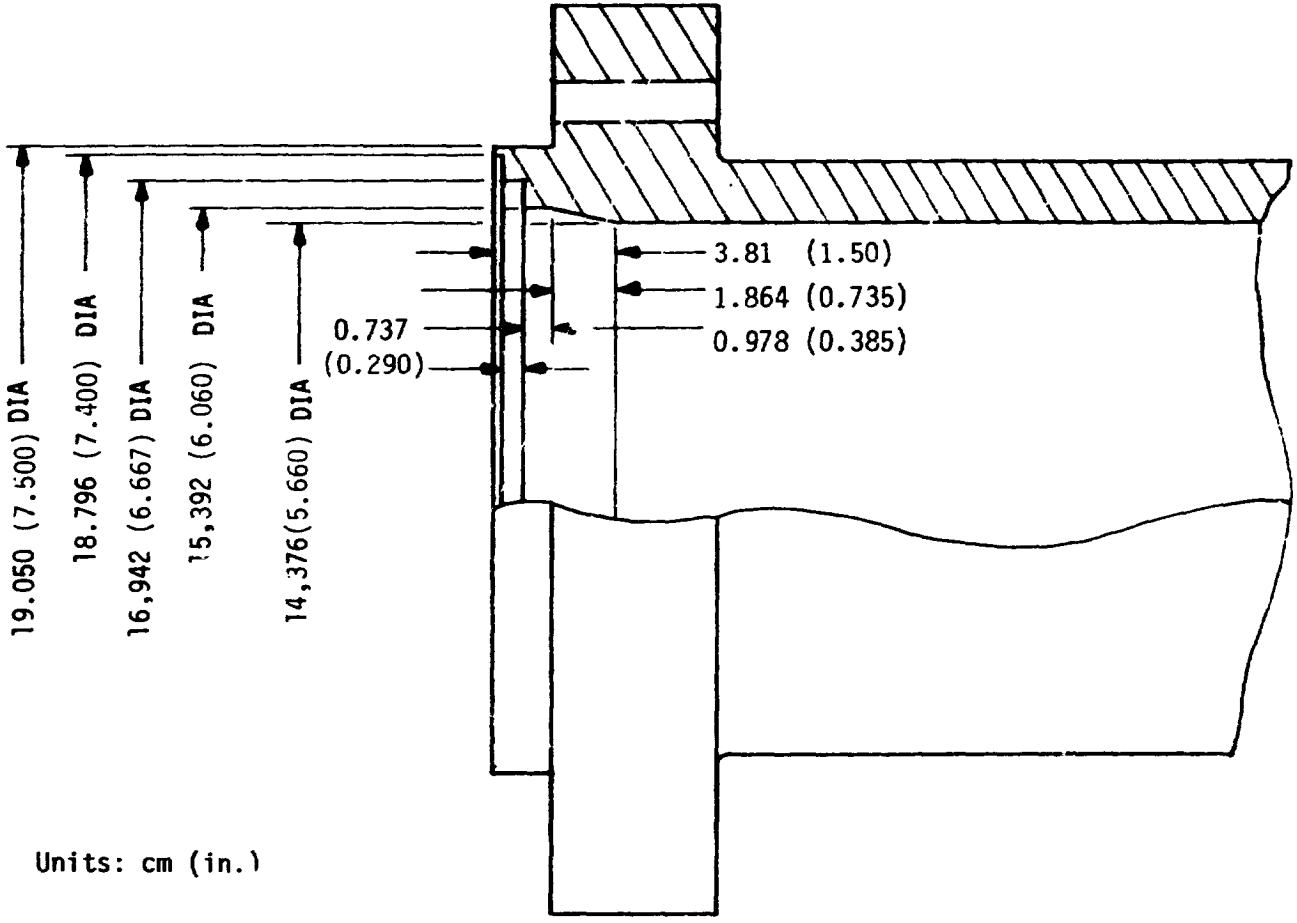

Figure I-1. NASA Combustion Chamber Interface

I, B, Objectives

The objective of Task III, Delivery, was to accomplish the delivery of the completed injector assembly to MSFC. This included a minimum of six sets of seals and four sets of working drawings.

The above tasks were to be supported and documented by the review and reporting requirements of Task IV.

II. SUMMARY

A. DESIGN DESCRIPTION

The recommended injector design, shown in Figures II-1 and II-2, consists of a preatomized triplet (PAT) injector core pattern, together with a tangential fan X-doublet (XDT) barrier compatibility element. This design was based upon the results of the Task I (Analysis and Preliminary Design) effort, calibrated with hot-fire test data derived from the High-Density Fuel (HDF) Program (NAS 3-21030) during which both PAT and transverse like-on-like (TLOL) patterns were evaluated at chamber pressures of 8,272 and 13,788 kPa (1200 and 2000 psia), respectively (see Ref. 1).

The subscale injector design incorporates the two outer rows of XDT-type elements to protect the uncooled resonator and head end of the cooled chamber.

The acoustic resonator cavity is designed to attenuate the expected radial and tangential modes of high-frequency instability. The cavity is formed by the assembly of the injector subassembly (PN 1193158) and the resonator ring assembly (PN 1193155) and has variable tune capability. This fine-tuning feature allows the cavities to be reset to match the actual frequency ranges and cavity sound speeds, measured in the early test, in the event they differ from the predicted design values.

The resonator ring contains provision for sufficient high-frequency pressure measurement instrumentation to allow the optimum cavity settings to be calculated from the early tests.

The small central tube is provided within the injector body to introduce an ignition fluid comprised of a 15/85 blend of TEA/TEB.

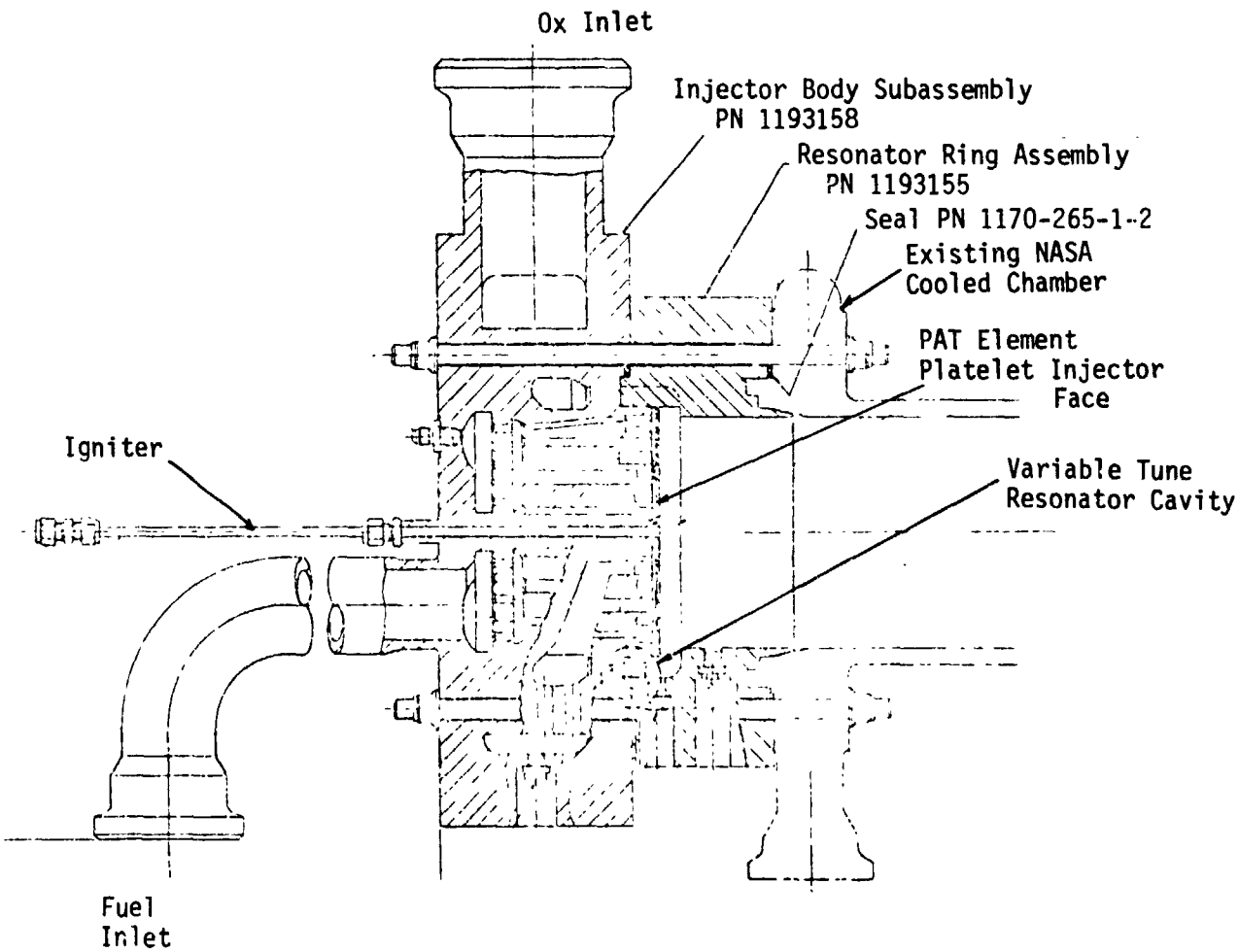

Figure II-1. LOX/RP-1 Injector Assembly PN 1193106

Figure II-2. Photographs of Injector and Resonator

II, Summary (cont.)

B. DESIGN PHILOSOPHY

The primary areas of technical concern to the high-pressure LOX/RP-1 injector program are summarized in order of decreasing priorities in Table II-I. First and foremost is the fact that the acquisition of data is essential for the development of new technology. This requires that the test hardware be sufficiently durable to withstand a minimum test program and that adequate instrumentation for acquiring the necessary data be provided.

In order to select the optimum design recommendation from among many possible parallel approaches, the decision-making process must assess the REWARD/RISK payoff. Technological advancement is the desired benefit from this type of program. Hopefully, the setbacks and disappointments are acceptable, identifiable, and solvable and do not detract from the demonstrated accomplishments.

The prevention of combustion instability is unquestionably the greatest technical challenge and can be a significant cost driver in future LOX/HC engine development programs. Thus, stability must be demonstrated on this technology program. Futhermore, as demonstrated by the transverse platelet like-on-like element (TLOL) injector test results from the recent High-Density Fuel (HDF) Program (NAS 3-21030), even a marginally unstable injector will summarily and prematurely terminate the test program.

It can be shown analytically that, for a given injector atomization characteristic, operating at higher Pc increases droplet vaporization rate and diminishes high-frequency combustion stability margin. The TLOL-2000* injector (NAS 3-21030) was definitely less stable than the TLOL-1200*, which verifies this prediction. Increasing the total element quantity or

*1200 and 2000 designate operating pressure in psia

TABLE II-I

SUMMARIZED TECHNICAL RISK/REWARD ASSESSMENT

TECHNICAL CONCERNS	SHORT TERM RISK	LONG TERM RISK	DESIGN APPROACH TO SOLVE	DESIGN CONSEQUENCE	BACKUP TEST EXPERIENCE	DESIRED LONG-TERM BENEFIT
High-frequency combustion instability	High frequency instability @ Hi Pc will fail injector before test data acquisition is complete		Select injection element with proven high frequency stable combustion characteristics	Select Preatomized Triplet (PAT)	PAT 2000 Stable combustion injector refirable after 7 tests and 61 sec duration	Early technology identification of stable, face-compatible injection element could save 5-10 years and $ billions from NASA LO_2/HC Booster Development Program
		Higher performance element may be stable @ 40K but is non-scalable to [illegible] booster	Place primary emphasis upon element with potential application to prototype booster	PAT is viable candidate for booster stability		
High Density Fuel Analysis predictions and test data verified [illegible] LO_2/RP-1 engine will be unstable without damping	40K-SFS engines will also be unstable without damping		Baffle or acoustic cavities are required		TLOL-2000 Unstable face, non-refirable after 5 tests, 6 sec duration	
		Baffles require cooling, degrade performance, unproven cycle life for STS reuse requirements		Use acoustic cavities like HDF program with PAT element	TLOL-1,00 Marginal instability refire not recommended after 9 tests, 64 sec duration	
Injector face incompatibility	Injector failure before testing completed		Select elements with demonstrated injector face compatibility	Select PAT		
		Selected element may not satisfy [illegible] requirement	Change face plate material, incorporate active cooling, etc.	Defer until later		
Existing calorimeter chamber interface does not have provision for acoustic cavity			Incorporate acoustic cavity, [illegible] component between injector & chamber interface	Acoustic cavity [illegible] compatibility for uncooled cavity	HDF heat sink cavities limited to [illegible] sec duration	Verify hypothesis: Demonstrate higher booster Isp can be delivered by reducing chamber heat flux, operating at higher Pc, higher Isp ODE in spite of [illegible] lower ηC*
Regen cooled cavities cannot use uncooled variable tuning blocks and limit instrumentation capability	Uncooled blocks will melt. Non tunable		Use uncooled cavities and uncooled blocks	Provide XDT barrier compatibility row	Platelet aerobee demonstrated low XDT barrier gas temp	
					PAT calorimeter data indicates low forward heat flux but requires [illegible] additional cooling	Redirect system optimization studies, redefine IPA technology requirements, alter baseline LO_2/HC booster specifications.
XDT Barrier degrades performance	ηC* [illegible] @ 40K effect, contract SOW requirement		Accept [illegible]			
		LONG TERM GAIN [illegible] @ [illegible] 6.67MN ([illegible] lb) thrust ΔIsp ODE +5% due to higher allowable Pc for same throat heat flux		Incorporate XDT barrier compatibility	PAT calorimeter heat flux data indicate strong dependence on test mixture ratio and verify PAT mixing E_m data	
Low [illegible] C* performance	chamber heat flux not representative of high efficiency LO_2/RP-1 injector		See updated C* prediction for PAT [illegible] (table [illegible])	Fabricate as designed		Verify combustion stability @ Pc 20,682 kPa (3000 psia). Thermal compatibility of injector/chamber
			Improve PAT E_m	Future cold flow [illegible] required	OMS & ITIP subscale uni element development experience	
		Upgraded high performance injector may unstable	Maintain [illegible] atomization vaporization characteristics, only improve mixing	Use proven element, retaining pattern orientation	OMS & ITIP experience indicates finer atomization faster vaporization degrades high frequency instability, better mixing has only second order effect on high frequency	Quantify performance improvement required if C* not achieved. Identify next step of LO_2/RP-1 injector technology program [illegible] flow, E_m optimization
[illegible] C* [illegible]	None	See above ([illegible] C*)				
Not calibrated [illegible] stability Model predict stability for Pc [illegible] 856 kPa ([illegible] psia). Since HDF PAT did not go [illegible] as predicted, cannot verify < 15,856 kPa ([illegible] psia)	[illegible] may limit operation [illegible] 15,856 kPa ([illegible] psia), may require external injector cooling at [illegible] chamber lengths [illegible] 15,856 kPa ([illegible] psia) catastrophic failure not predicted		Test with CSM tuned to include [illegible]	Verify PAT time lag, calibrate [illegible] Model. Modify [illegible] and [illegible] if required to secure [illegible] stability at desired nominal operating point in 2nd generation injector		Provide calibrated stability models for all modes for future LO_2/HC booster injector development program

reducing the orifice diameter results in finer atomization distributions which vaporize faster and degrade stability. There is much historical data supporting the prediction that "higher performance injectors" are less stable. LOX/RP-1 technology data from the 1960's have indicated that unlike impinging triplets and unlike doublets were less stable than like-on-like doublets. Recent analytical insight has attributed this stability difference to their drop size distributions. Triplets and unlike doublets produce more fine and more coarse droplets (σ_y = 3.6) compared to their mass median than like doublets (σ_y = 2.3). The preatomized triplet (PAT) element indicates more uniform distribution than the like doublet, based on experimental d(ERE*)/dx and d(%RP-1 Vap.)/dx data obtained for the TLOL-1200 and PAT-2000 injectors between 27.94-cm (11-in.) and 38.1-cm (15-in.) chamber L'. The fact that the PAT injector was considerably more stable than the doublet also supports this performance-derived conclusion.

When it becomes necessary to extrapolate this subscale combustion technology data obtained with ~12.7-cm (5-in.) diameter injectors to prototype boosters (~50.8-cm (20-in.) injector diameter), the transverse mode acoustic response frequencies will approximately decrease by a factor of 4:1. Thus, injectors which require extensive acoustic cavity tuning effort to stabilize at these subscale technology thrust levels are assured of being dynamically unstable without extensive injector baffling in full-scale booster applications. As shown in Table II-I, baffles degrade performance. The low performance (93.8% C*) of the LOX/RP-1 F-1 engine is proof of the above. Thus, for booster applications, it is best to select elements producing the most uniform atomization distribution. These injectors will be most stable, which not only minimizes the short-term risk of premature injector failure due to combustion instability, but also provides greatest promise for full-scale application. These injectors are least likely to suffer from later

*ERE = Energy Release Efficiency

II, B, Design Philosophy (cont.)

performance degradation as the result of either de-optimizations required to achieve stability in larger-diameter engines or due to baffle cooling losses. On the basis of the PAT Injector element was selected over all other candidates.

III. TECHNICAL DISCUSSION

A. DESIGN ANALYSES

1. Design Requirements

The contractual design and interface requirements for the injector to be delivered are documented in Table I-I and Figure I-1. The imposed geometric and pressure parameters result in an assembly that delivers ≈222,400 N (≈50,000 lb) of thrust at a chamber pressure of 20,682 kPa (3000 psia). The propellant flowrates at these conditions are as follows:

RP-1	17.10 kg/sec	(37.7 lb/sec)
LOX	47.90 kg/sec	(105.6 lb/sec)

The design analyses which follow translate these requirements into specific geometric configurations and define the resulting required inlet pressures and stabilizing devices for maintaining stable combustion.

2. Pattern Selection

The injector pattern selection plays a critical role in meeting both the 97% C* efficiency and combustion stability goals. Section II,B, Design Philosophy, provides a discussion of the interaction of these parameters based on a broad range of test experience and data.

Figure III-1 depicts the injection element screening process for arriving at the recommended designs. This process requires that, as a minimum, uni-element cold-flow data and some hot-fire data be available for an element concept before it can qualify as a candidate. Untested minor modifications to proven elements are considered acceptable if they can be analytically shown to result in an improvement over previous experience.

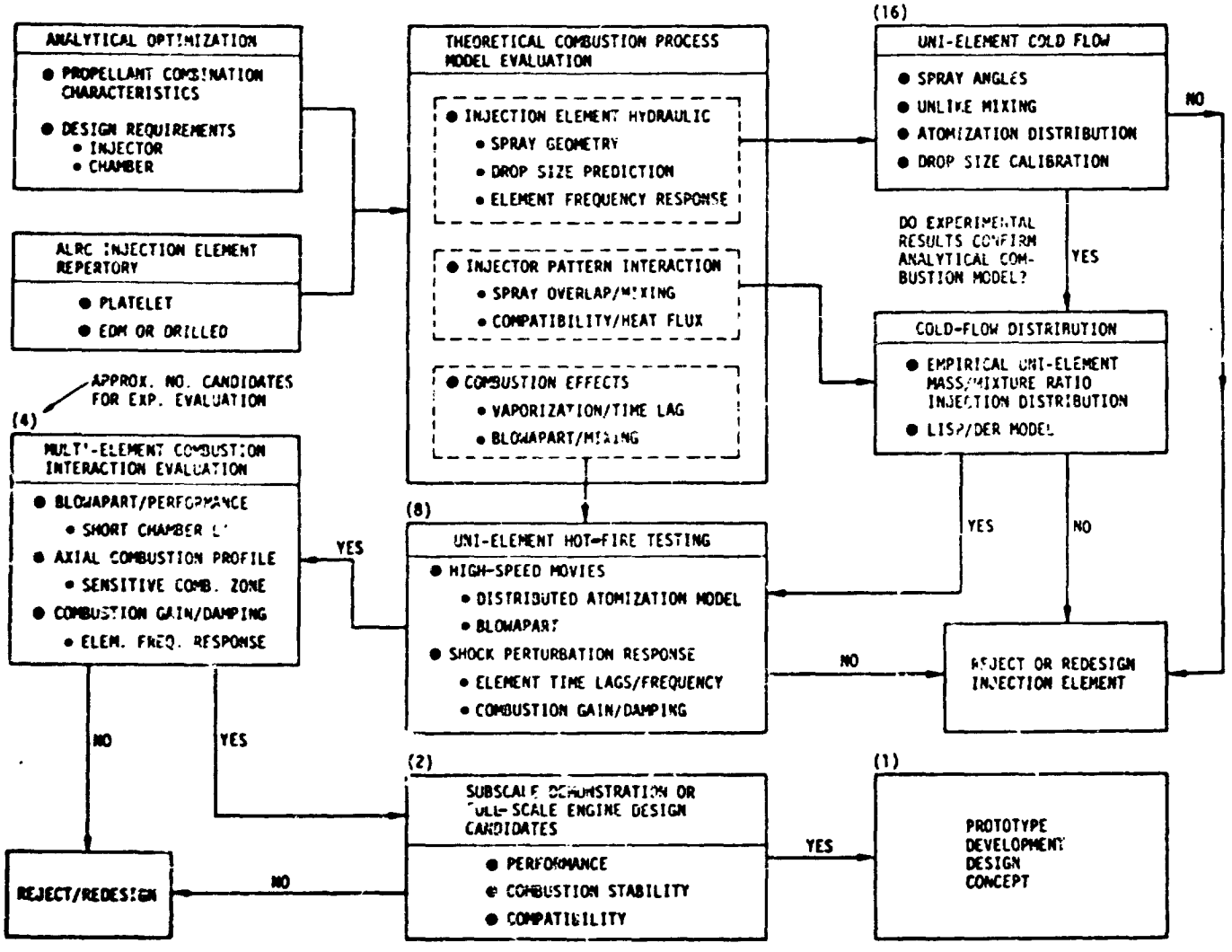

Figure III-1. ALRC Injection Element Screening Process - Summary

III, A, Design Analyses (cont.)

Figure III-2 defines the categories of element concepts considered applicable to the LOX/RP-1 booster engine, along with comments on their features.

Figure III-3 illustrates the various injection element configurations and their resulting spray patterns. Figures III-4 and III-5 further define the geometric characteristics of the TLOL and PAT elements which are prime candidates for the high-performance core elements. Figure III-5 also defines the characteristics of the recommended XDT barrier compatibility elements.

HIGH-PERFORMANCE CORE ELEMENTS

The NAS 3-21030 data are the best current analytical/experimental correlations for both the TLOL-1200 and PAT-2000 injectors. Ambient and heated fuel temperature and both 27.94-cm (11-in.) and 38.10-cm (15-in.) length chambers were tested. These data are documented in Reference 1. By testing these injectors over a range of mixture ratios from approximately 2 to 4, it was possible to separate mixing and vaporization losses, yielding both % E_m and % RP-1 vaporization efficiency. Due to its volatility, the LOX vaporization efficiency was assumed to be 100% at all conditions. Excellent correlations were evident between Pc-based % C* and thrust-based % ERE at the sea level nozzle area ratio (ε_{sl}) of 5.8:1. The exception was the L' = 27.94-cm (11-in.) TLOL-1200 data, where the C* data became progressively more invalid late in the test program due to suspected throat delamination of the NASA-supplied slotted/electroformed chambers.

Due to the large mixing losses associated with these first-generation injectors, % C* and % ERE are not exactly equal, nor will % ERE be

ELEMENT TYPE

° Preatomized Triplet	- High Performance. Good Injector Face Compatibility and Good Stability Characteristics.
° X-Doublet (XDT)	- Excellent Chamber Wall Compatibility. Low Performance.
° Platelet Aerobee Mixed-Element Pattern-See Figure III-3	- Excellent Theoretical Stability Potential; High Performance; Face Compatibility Unknown.
° V-Doublet	- Excellent Theoretical High-Frequency Stability Demonstrated with Storables (OMS); Good Performance; Face Compatibility Unknown.
° TLOL/EDM-LOL	- Thus Far Limited < 8272 kPa (1200 psia) Chamber Pressure by Stability and Injector Face Incompatibility. Was Baseline 1960 Technology Standard.

Figure III-2. Candidate LO_2/HC Injection Element Concepts

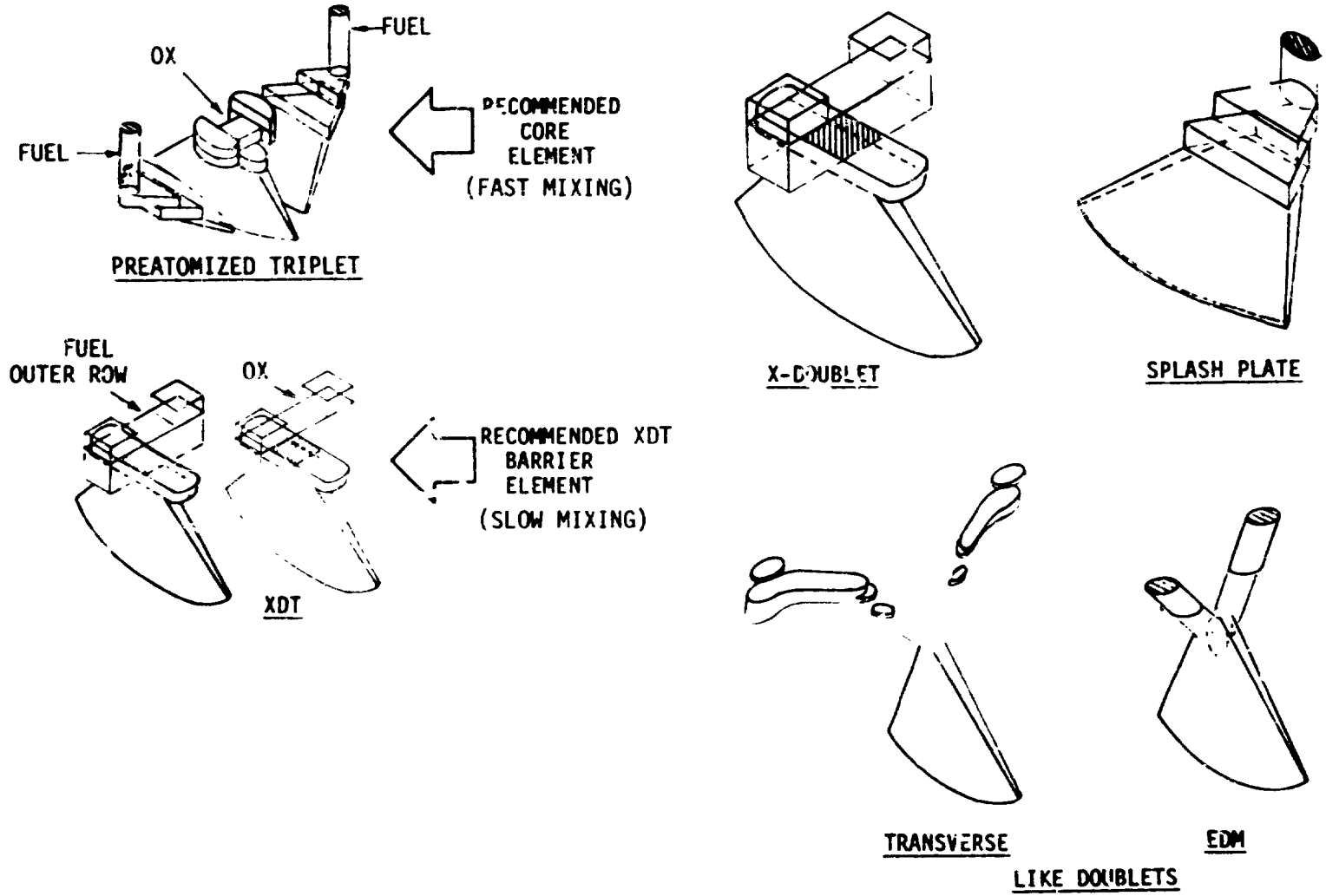

Figure III-3. Proposed Injection Element Concepts

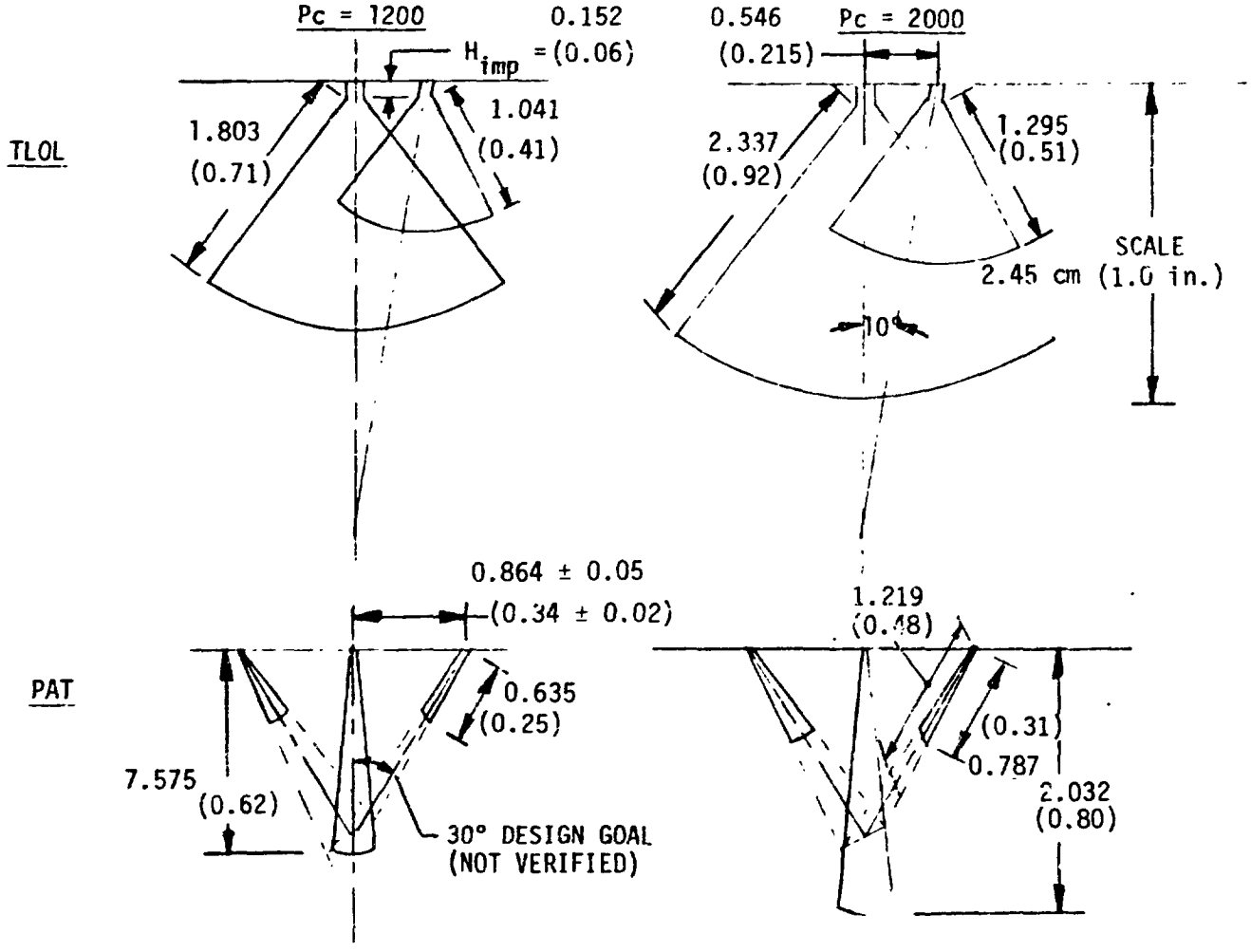

Figure III-4. Spray Atomization Pattern Schematic

PATTERN:	PREATOMIZED TRIPLET		TLOL EDM-LOL		PLATELET AEROBEE			BARRIER COMPATIBILITY	
CIRCUIT:	OXID	FUEL	OXID	FUEL	FUEL	OXID	FUEL	OXID	FUEL
BARRIER									
ELEMENT	XDT ←					→ XDT		XDT	XDT
QUANTITY	96 ←					→ 96		96	96
% MASS	20 ←					→ 20		20	20
CORE									
ELEMENT	XDT	S/P	LOL	LOL	TLOL	TLOL	S/P*		
QUANTITY	72	144	72	72	48	48	48		
% MASS	80	80	80	80	40	80	40		
Pc = 3000 kPa									
$\dot{W}_j$ (kg/sec)	38.3	13.7	38.3	13.7	6.85	38.3	6.85	9.57	3.40
ΔP (kPa)	6204	4481	6204	4481	4481	6204	4481	6204	4481
V_j (mps)	106.7	106.7	85.3	85.3	85.3	85.3	106.7	106.7	106.7
D_{orif} (cm)	0.274	0.142	0.231	0.157	0.137	0.282	0.175	0.119	0.084
r_{atom} (cm)	3.56	1.68	5.03	1.98	2.82	6.71	1.55	1.40	0.79
r_m ($\times 10^{-3}$ cm)	5.08	3.56	6.86	5.59	3.56	8.64	3 56	2.44	2.16

*Splash plate

Figure III-5. Injector Characteristics of Proposed Pattern Options (SI Urits)
(Sheet 1 of 2)

PATTERN:	PREATOMIZED TRIPLET		TLOL EDM-LOL		PLATELET AEROBEE			BARRIER COMPATIBILITY	
CIRCUIT:	OXID	FUEL	OXID	FUEL	FUEL	OXID	FUEL	OXID	FUEL
BARRIER									
ELEMENT	XDT ←					→ XDT		XDT	XDT
QUANTITY	96 ←					→ 96		96	96
% MASS	20 ←					→ 20		20	20
CORE									
ELEMENT	XDT	S/P	LOL	LOL	TLOL	TLOL	S/P*		
QUANTITY	72	144	72	72	48	48	48		
% MASS	80	80	80	80	40	80	40		
Pc = 3000 psia									
$\dot{W}_j$ (lbm/sec)	85.4	30.2	85.4	30.2	15.1	84.5	15.1	21.1	7.5
ΔP (psid)	900	650	900	650	650	900	650	900	650
V_j (fps)	350	350	280	280	280	280	350	350	350
D_{orif} (in.)	0.108	0.056	0.091	0.062	0.054	0.111	0.069	0.047	0.033
λ_{atom} (in.)	1.40	0.66	1.98	0.78	1.11	2.64	0.61	0.55	0.31
r_m ($\times 10^{-3}$ in.)	2.0	1.4	2.7	2.2	1.4	3.4	1.4	0.96	0.85

*Splash plate

Figure III-5. Injector Characteristics of Proposed Pattern Options (Englisn Units)
(Sheet 2 of 2)

a unique function of test mixture ratio alone. Mixing losses for any E_m <100% will always maximize at the peak performance mixture ratio since performance drops off on both the fuel-rich and oxidizer-rich stream tubes. Thus, delivered C* efficiency minimizes at O/F = 2.3 since that is where C* optimizes. Specific impulse peaked at O/F ∿2.5 for the nozzle expansion ratio (ε_{sl} = 5.8) tested, and, hence, the ERE mixing efficiency minimizes near this mixture ratio.

Flight configuration boosters will probably utilize ε∿40 nozzle expansion ratios whose Isp peaks around O/F = 2.8. Hence, the delivered % C* at O/F = 2.3 or the present % ERE at O/F = 2.5 with the 5.8 sea-level nozzle will be representative of the flight nozzle % ERE to be expected at O/F = 2.8 rather than the current % ERE at O/F = 2.8 with the ε = 5.8 nozzle or the % C* at O/F = 2 8. The expected operating efficiencies are documented in Table III-I. The PAT-3000 (Core) column, entitled "Old E_m," shown in the table, is based on the HDF (NAS 3-21030) calibrated RP-1 vaporization model and uses the HDF-PAT E_m value of 73%. Note, however, that the values previously quoted for % C* were actually for % ERE at O/F = 2.8 with the prototype booster flight expansion ratio nozzle. This represented the absolute minimum ERE combustion efficiency, not % C* at O/F = 2.8 as previously reported. Even with the old prediction model, the PAT-3000 Core C* efficiency at O/F = 2.8 was predicted to be 97.0% ± 0.2%, depending upon whether ambient or heated RP-1 was tested.

The second point of difference between the HDF PAT-2000 and the MSFC PAT-3000 is that two design modifications were incorporated. First, the unlike fuel impingement angle was increased from a 60° total included angle to 90°. Uni-element LOX/HC hot-fire photographic data (NAS 9-15724) with PAT elements show that the combustion gases between the LOX and HC sprays retard fuel penetration into the LOX spray; thus, increasing the fuel impingement angle will most probably improve inter-element E_m. The second

TABLE III-I

UPDATED LO_2/RP-1 PERFORMANCE PREDICTION SUMMARY

PROGRAM: CONTRACT NO:	High-Density Fuel Comb. & Cooling NAS 3-21030				Hi Pc LO_2/RP-1 Injector Prediction NAS 8-33651		
INJECTOR	TLOL - 1200		PAT - 2000		PAT - 3000 (CORE) ELEMENTS (80% Mass)	OLD E_m	XDT (BARRIER, ELEMENT (20% Mass)
Fuel Imp. Ang., $2\theta_f$	N/A		60°		90°	90°	0°
Cant Angle, θ_{cant}	0		29°5		37°30	37°30'	30°
Mix. Eff., % E_m	82		73		80±7	73	60
$\bar{T}_{RP-1}$ = 70°F							
L' cham., cm (in.)	27.94 (11)	38.10 (15)	27.94 (11)	38.10 (15)	35.56 + 8.64 (14.0 + 3.4)	44.20 (17.4)	44.2 (17.4)
%RP-1 Vap.	93.5	96	92	98	98	98	100
% C*	Invalid	97.7	94.8	96.7	98.1 ± 1.3	96.2	94.7
% ERE (ε_{SL}~5.8)	96.0	97.2	94.5	96.5	97.5 ± 1.6	95.9	93.2
% ERE (ε_{flight}~40)	95.9	97.0	94.0	95.6	97.2 ± 1.7	95.5	92.5
$\bar{T}_{RP-1}$~240°F							
%RP-1 Vap.	95	Not Tested	97	99+	99+	99+	100
% C*	Invalid		96.0	97.4	98.5 ± 1.3	97.2	94.7
% ERE (ε~5.8)	96.4		95.8	97.0	97.9 ± 1.6	96.3	93.2
% ERE (ε~40)	96.2		95.1	96.5	97.7 ± 1.7	96.0	92.5

design modification was that the new pattern rotated the PAT element to increase a spray fan alignment relative to the chamber wall. Smaller angles result in better chamber wall compatibility but minimize inter-element spray overlap between fuel-rich and oxidizer-rich zones from adjacent elements. The HDF PAT-2000 injector has a uniform core without special compatibility elements. The MSFC PAT-3000 injector pattern rotated the element 37°30' to the chamber wall to further improve the spray overlap, as compared to the 24° and 34° rotation used on the PAT-2000. While these modifications seem to improve E_m, in the absence of mathematical models for quantitatively predicting the magnitude of improvement, it was initially decided to use the same 73% E_m prediction for all PAT injectors and to retain these values until a uni-element cold-flow optimization program could quantify the E_m improvement magnitude or until it could be replaced by a better experimental hot-fire E_m value with the new injector.

An attempt has since been made to try and estimate the E_m improvement. It was assumed that the mixing deficiency, $1-E_m$, is proportional to $180°-2\theta_f$. Using this analogy, E_m was calculated to increase from 73% to 80%. The "tolerance" on this improvement was assumed to be $\pm$ 100% of the change, or $E_m = 80\% \pm 7\%$. The % C* and % ERE's at both $\varepsilon_{sl} \sim 5.8$ and $\varepsilon_{flight} \sim 40$ are shown in Table III-I for this revised analytical assumption. The resultant core performance efficiency predictions range from >98% C* to between 97-98% ERE efficiencies. However, the core efficiency must be reduced by 1% in the subscale version due to the interaction with the XDT barrier compatibility row. This 1% reduction may not be present in the full-scale design. As noted in Table II-I, the prototype booster cooling loss due to an XDT barrier compatibility row is significantly reduced due to the larger chamber diameter and reduced barrier mass fractions.

OUTER ROW COMPATIBILITY ELEMENTS

A compatibility barrier would not only permit testing with the existing marginally cooled combustion chamber head end but could also provide performance advantages for real engine applications. The compatibility row around a hot core permits operation up to 27,576 kPa (4000 psia) chamber pressure while maintaining heat fluxes comparable to 13,788 kPa (2000 Pc). The higher booster nozzle area ratio for a given envelope delivers 4-5% higher Isp at the higher chamber pressure and more than offsets the barrier cooling losses. Furthermore, in a 2.224 to 4.448M N (500K to 1 M lbF) thrust booster engine, the barrier mass fraction required to achieve chamber compatibility is considerably reduced. Therefore, by incorporating chamber compatibility elements with significantly reduced barrier mass fraction due to the larger booster chamber diameter, the cooling performance penalty is only on the order of 1/2% Isp. This indicates that the improvement possible at higher Pc (from the standpoint of higher theoretical performance attributable to the higher area ratio nozzle) more than offsets the loss from the use of barrier cooling. Additional analyses conducted during Task II have further refined the estimated barrier cooling performance loss attributable to the XDT element to approximately a 1% performance penalty.

3. Stability Analyses

This section summarizes the results of the stability analyses conducted for the LOX/RP-1 combustor design selected. Stability margins for the chug, longitudinal (1L), and high-frequency modes were predicted using the standardized computer models, calibrated to the existing high-pressure LO_2/RP-1 test results documented in Reference 1. Table III-II defines the injector element design data employed in these analyses.

TABLE III-II

SI Units

LOX/RP-1 INJECTOR DATA

PAT CORE ELEMENTS - 80% Mass Flow

Pc = 20682 kPa				Pc = 13788 kPa			
T_{ox}	= 102°K	T_f	= 294°K	T_{ox}	= 102°K	T_f	= 294°K
ρ_{ox}	= 1128 kg/m^3	P_f	= 801 kg/m^3	ρ_{ox}	= 1122	ρ_f	= 801
Sg_{ox}	= 1.07	Sg_f	= 0.80	Sg_{ox}	= 1.122	Sg_f	= 0.80
ΔP_{ox}	= 4136 kPa	ΔP_f	= 3102 kPa	ΔP_{ox}	= 1841	ΔP_f	= 1379
V_{ox}	= 88.4 mps	V_f	= 88.4 mps	V_{ox}	= 58.7	V_f	= 58.8
D_{ox}	= 0.2819 cm	D_f	= 0.145 cm	D_{ox}	= 0.2819	D_f	= 0.145
C_{dox}	= 0.60 cm	C_{df}	= 0.69 cm	C_{dox}	= 0.60	C_{df}	= 0.69
$\lambda_{ox, atom}$	= 3.52 cm	$\lambda_{f, atom}$	= 1.684 cm	$\lambda_{ox, atom}$	= 3.366*	$\lambda_{f, atom}$	= 1.610*
$r_{m,ox}$	= 0.0053 cm	$r_{m,f}$	= 0.0076 cm	$r_{m,ox}$	= 0.0056*	$r_{m,f}$	= 0.0079
		θ_f	= 45°			θ_f	= 45°

XDT BARRIER ELEMENTS - 20% Mass Flow

Pc = 20682 kPa				Pc = 13788 kPa			
T_{ox}	= 102°K	T_f	= 294°K	T_{ox}	= 102°K	T_f	= 294°K
ρ_{ox}	= 1128 kg/m^3	ρ_f	= 801 kg/m^3	ρ_{ox}	= 1122	ρ_f	= 801
Sg_{ox}	= 1.128	Sg_f	= 0.80	Sg_{ox}	= 1.122	Sg_f	= 0.80
ΔP_{ox}	= 2922 kPa	ΔP_f	= 3102 kPa	ΔP_{ox}	= 1746	ΔP_f	= 1379
V_{ox}	= 83.8 mps	V_f	= 88.4 mps	V_{ox}	= 55.8	V_f	= 58.8
D_{ox}	= 0.130 cm	D_f	= 0.089 cm	D_{ox}	= 0.130	D_f	= 0.089
C_{dox}	= 0.60 cm	C_{df}	= 0.60 cm	C_{dox}	= 0.60	C_{df}	= 0.60
$\lambda_{ox, atom}$	= 1.494 cm	$\lambda_{f, atom}$	= 0.729 cm	$\lambda_{ox, atom}$	= 1.427	$\lambda_{f, atom}$	= 0.699
$r_{m,ox}$	= 0.0027 cm	$r_{m,f}$	= 0.0038 cm	$r_{m,ox}$	= 0.0028	$r_{m,f}$	= 0.0041

*For Pc < 13788 kPa assume λ_{atom} and r_m are essentially constant.

TABLE III-II (cont.) English Units

LOX/RP-1 INJECTOR DATA

PAT CORE ELEMENTS - 80% Mass Flow

Pc = 3000 psia				Pc = 2000 psia			
T_{ox}	= -275°F	T_f	= 70°F	T_{ox}	= -275°F	T_f	= 70°F
ρ_{ox}	= 70.4 lbm/ft^3	ρ_f	= 50 lbm/ft^3	ρ_{ox}	= 69.4	ρ_f	= 50
Sg_{ox}	= 1.128	Sg_f	= 0.80	Sg_{ox}	= 1.112	Sg_f	= 0.80
ΔP_{ox}	= 569 psi	ΔP_f	= 450 psi	ΔP_{ox}	= 257	ΔP_f	= 200
V_{ox}	= 275 fps	V_f	= 290 fps	V_{ox}	= 186	V_f	= 193
D_{ox}	= 0.110 in.	D_f	= 0.057 in.	D_{ox}	= 0.110	D_f	= 0.057
C_{dox}	= 0.60 in.	C_{df}	= 0.69 in.	C_{dox}	= 0.60	C_{df}	= 0.69
$\lambda_{ox,\ atom}$	= 1.386 in.	$\lambda_{f,\ atom}$	= 0.663 in.	$\lambda_{ox,\ atom}$	= 1.325*	$\lambda_{f,\ atom}$	= 0.634*
$r_{m,ox}$	= 0.0021 in.	$r_{m,f}$	= 0.0030 in.	$r_{m,ox}$	= 0.0022*	$r_{m,f}$	= 0.0031*
		θ_f	= 45°			θ_f	= 45°

XDT BARRIER ELEMENTS - 20% Mass Flow

Pc = 3000 psia				Pc = 2000 psia			
T_{ox}	= -275°F	T_f	= 70°F	T_{ox}	= -275°F	T_f	= 70°F
ρ_{ox}	= 70.4 lbm/ft^3	ρ_f	= 50	ρ_{ox}	= 69.4	ρ_f	= 50
Sg_{ox}	= 1.128	Sg_f	= 0.80	Sg_{ox}	= 1.112	Sg_f	= 0.80
ΔP_{ox}	= 569 psi	ΔP_f	= 450	ΔP_{ox}	= 257	ΔP_f	= 200
V_{ox}	= 275 fps	V_f	= 290	V_{ox}	= 186	V_f	= 193
D_{ox}	= 0.051 in.	D_f	= .035	D_{ox}	= 0.051	D_f	= 0.035
C_{dox}	= 0.60 in.	C_{df}	= 0 60	C_{dox}	= 0.60	C_{df}	= 0.60
$\lambda_{ox,\ atom}$	= 0.588 in.	$\lambda_{f,\ atom}$	= 0.287	$\lambda_{ox,\ atom}$	= 0.562	$\lambda_{f,\ atom}$	= 0.275
$r_{m,ox}$	= 0.00105 in.	$r_{m,f}$	= .0015	$r_{m,ox}$	= 0.0011	$r_{m,f}$	= 0.0016

*For Pc < 2000 psia assume λ_{atom} and r_m are essentially constant.

III, A, Design Analyses (cont.)

CHUG MODES

Correlation of the High-Density Fuel (HDF) test results (Ref. 1) with chug predictions revealed the need to modify the standard combustion time lag calculation to account for LOX/RP-1 propellants. The fuel atomization length and droplet radius calculated by the methods of Reference 2 were multiplied by a factor of 1.5, an empirical correction based on HDF performance results. In addition, the total time lags were evaluated at 20% of propellant vaporization plus a "mixing" time lag of 0.1 ms instead of at just the conventional 20% vaporization time.

The injector is predicted to be chug-stable at its operating points of Pc = 20,682 kPa (3000 psia), MR = 2.8 and Pc = 13,788 kPa (2000 psia), MR = 2.8. Eight other operating points were examined to determine the lower chamber pressure limit. A minimum chug-stable chamber pressure limit of 12,340 kPa (1790 psia) is predicted for a mixture ratio of 2.8. A 420 Hz instability mode is predicted for lower pressures.

LONGITUDINAL (1L) MODES

The atomization time lags used to make the 1L predictions were arrived at by correlating the HDF 1L test data with analytical predictions. Correlation could be obtained only with the use of distributed atomization time lags. The time lags were distributed according to a logarithmic-normal distribution, with the concentrated atomization time lag as the median. The standard deviation used was 2.3. This is the same standard deviation used by Priem and Heidmann for drop-size distribution as discussed in Reference 2.

III, A, Design Analyses (cont.)

When the selected distributed atomization time lags are used, the PAT injector is predicted to experience 1L instability problems at the low Pc operating point of Pc = 13,788 kPa (2000 psia) and MR = 2.8. The expected 1L frequency mode is 1400 $\pm$ 100 Hz. The nominal operating point of Pc = 20,682 kPa (3000 psia) and MR = 2.8 is predicted to be 1L stable. The lower limit for stable operation is predicted to be about 15,856 kPa (2300 psia) at MR = 2.8. Therefore, initial tests should be at pressures greater than 17,235 kPa (2500 psia).

HIGH-FREQUENCY MODES

The high-frequency modes are predicted to be 1T at 4700 Hz, 2T at 7800 Hz, and 2T + 1L at 7800 Hz.

The injector pressure interaction index (n) used in this analysis is based on the correlation of HDF test results with analytical predictions and has a value of 0.7. Based on HDF test results (Ref. 1), the sensitive time lag (τ) is taken to be the vaporization time of 20% propellant vaporized. The sensitive time lags are τ_f = 0.166 ms and τ_{ox} = 0.0168 ms at 13,788 kPa (2000 psia) and τ_f = 0.115 ms and τ_{ox} = 0.0116 ms at 20,682 kPa (3000 psia). The analysis predicts that a monotune cavity configuration would not be sufficient to damp a 2T + 1L mode. A bitune configuration with a 1T depth of 3.81 cm (1.5 in.) and a 2T depth of 1.728 cm (0.7 in.) is required to damp all the anticipated modes. These depths are based on an estimated cavity sound speed of 610 mps (2000 fps). The cavity width is 1.016 cm (0.4 in.). The analytis indicates that cavity splits of either eight at 1T and four at 2T or nine at 1T and three at 2T will stabilize the injector. The cavity configuration with nine at 1T and three at 2T was selected to avoid 2T mode orientation effects which could occur with the 8-1T and 4-2T configuration (see Figure III-6). Figure III-7 illustrates the geometry of the cavities tuned for 1 and 2T instability modes.

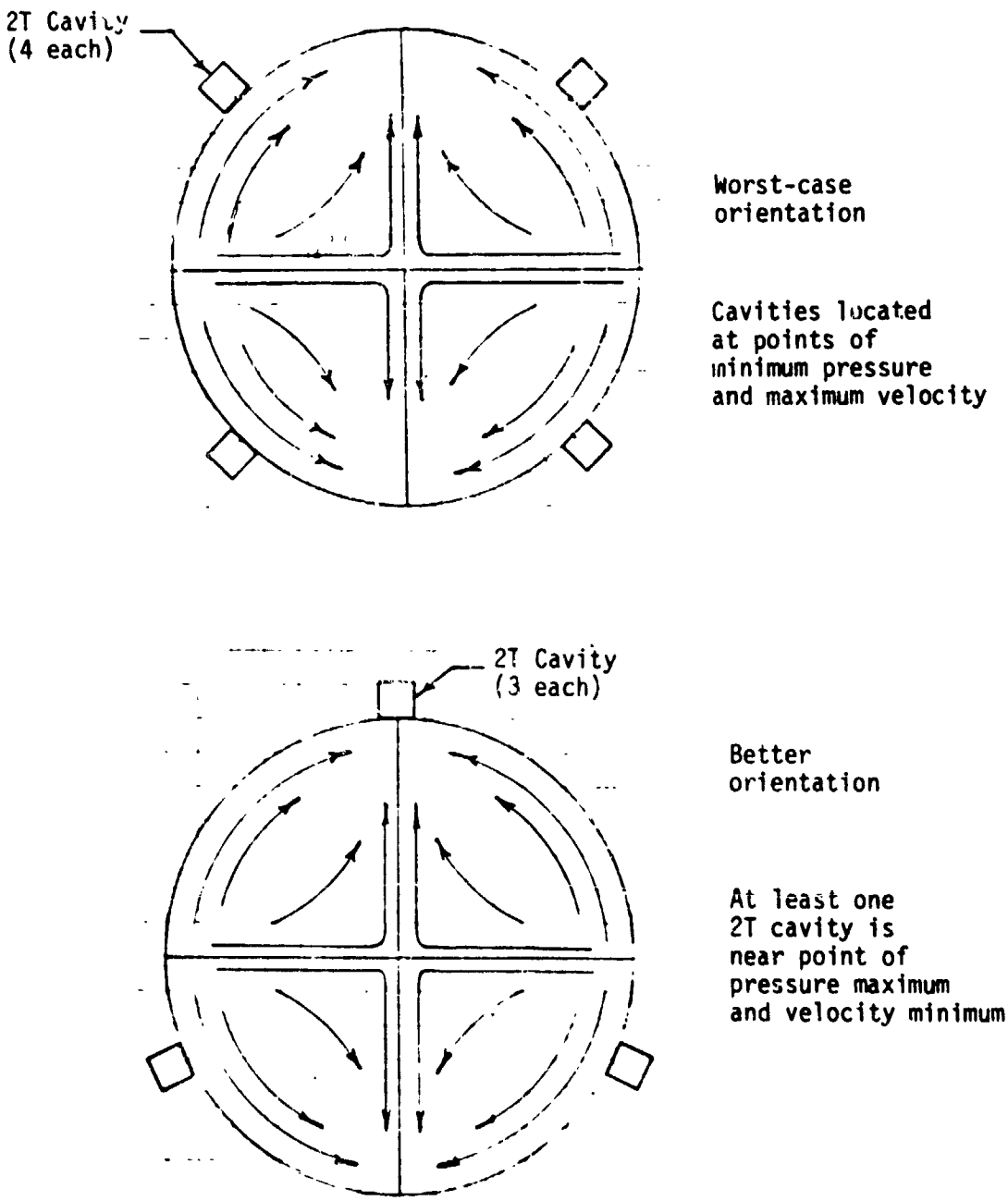

Figure III-6. 2T Mode Orientation

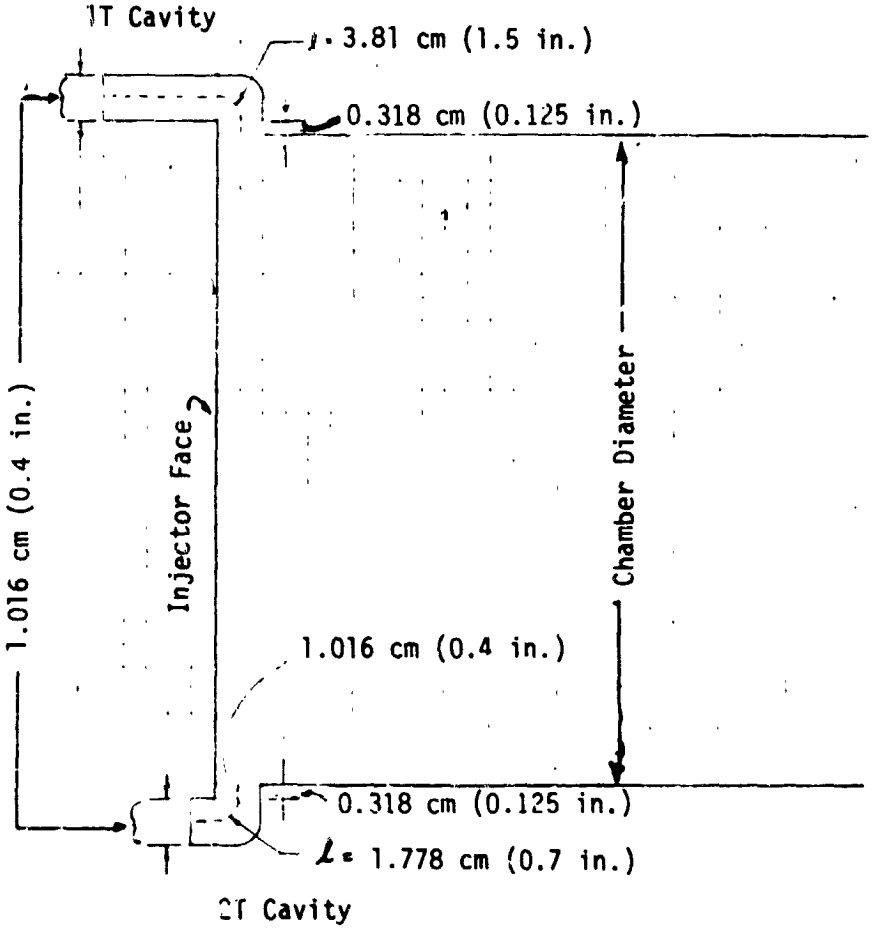

Figure III-7. Acoustic Cavity Detail

STABILITY ANALYSIS CONCLUSIONS AND RECOMMENDATIONS

1. The LOX/RP-1 PAT injector is predicted to be chug-stable at the nominal operating conditions (Pc = 13,788 and 20,682 kPa (2000 and 3000 psia) at MR = 2.8).

2. A chamber pressure chug limit of 12,340 kPa (1790 psia) is predicted for the LOX/RP-1 injector at MR = 2.8. Chugging at 420 Hz is predicted to occur at chamber pressures below this.

3. The injector is predicted unstable in the 1L mode at Pc = 13,788 kPa (2000 psia) and MR = 2.8 and is predicted to be 1L stable at Pc = 20,682 kPa (3000 psia) and MR = 2.8. The 1L instability will be recognized by a 1400 ± 100 Hz frequency. Initial testing should be at 17,235 kPa (2500 psia) or higher to avoid the 1L mode.

4. The injector is predicted to be stable in all high-frequency modes with the use of nine 1T (L = 3.81 cm (1.5 in.), W = 1.016 cm (0.4 in.) and three 2T (L = 1.778 cm (0.7 in.), W = 1.016 cm (0.4 in.) cavities based on an estimated 610 mps (2000 fps) cavity sound speed. The actual cavity sound speed must be determined in the early testing by using the pressure wave relative time of arrival at Kistler transducers located at different positions in the resonator cavity ring.

5. The LOX/RP-1 injector should be tested at the conditions analyzed herein to verify model predictions, deferring the low-pressure tests where potential 1L modes exist until the end.

4. Injector Manifold Hydraulics

The MSFC LOX/RP-1 injector manifold design is conceptually identical to the design used and developed on the HDF program. A comparison of the two injectors is shown in Figure III-8. A detailed description of the manifolding flow paths is provided in Section III,B,3.

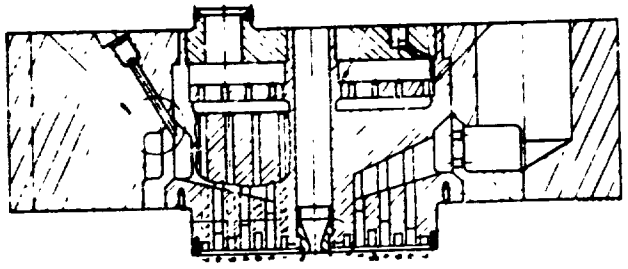

NAS 3-21030
PN 1191403

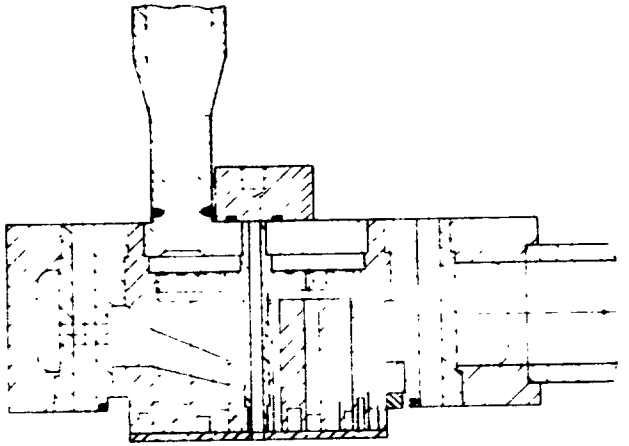

NAS 8-33651

	NAS 3-21030 PN 1191403		NAS 8-33651	
Pc, kPa (psia)	13,788 (2K)		20,682 (3K)	
F, N (lbF)	89,600 (20K)		222,400 (~50K)	
CIRCUIT	OXID	FUEL	OXID	FUEL
W_i kg/sec (lbm/sec)	17.65 (38.9)	6.31 (13.9)	47.90 (105.6)	17.10 (37.7
Inlet Dia., cm (in.)	5.08 (2)	3.81 (1.5)	7.62 (3)	5.08 (2)
Channel Width, cm (in.)	0.51 (0.20)	0.38 (0.15)	0.851 (0.335)*	0.51 (0.20)
Land Width, cm (in.)	0.254 (0.10)	0.254 (0.10)	0.318 (0.125)	0.318 (0.125)
Manifold Distribution Orifice				
Quantity	90	84	32*	60
Dia., cm (in.)	0.475 (0.187)	0.318 (0.125)	1.031 (0.046)*	0.51 (0.20)

(*Task II Update)

Figure III-8. Comparison of High-Density Fuel and LOX/RP-1 Injector Manifolds

III, A, Design Analyses (cont.)

A detailed hydraulic analysis of the injector manifold was conducted for ALRC PN 1191403, the high-density fuel injector. Changes from this earlier design consist of enlarged inlet lines in order to accommodate the higher engine flowrates. Furtnermore, the hydraulic resistance of the injector manifold distribution orifices was reduced to accommodate the higher flowrate. The predicted velocity distribution and pressure drops in both the fuel and oxidizer circuits of this design are shown in Table III-III at the maximum Pc = 20,682 kPa (3000 psia) operating point. The overall injector manifold resistance is predicted to result in 393 kPa (57 psid) fuel manifold and 607 kPa (88 psid) oxidizer manifold pressure drop at maximum thrust.

B. DETAILED DESIGN DESCRIPTION

This section provides a detailed description of the injector designed to meet the objectives and goals of the program. The design details were developed from the Task I analytical activities covered in Section III,A. A description of the design is accomplished by use of engineering drawings and photographs of the components in various stages of assembly.

1. Assembly Description

The injector assembly, shown in Figures III-9 and III-10, is fabricated completely from 300 series stainless steel, with the exception of the platelet pattern plate and a portion of ring manifolding to which the pattern plate is welded. The latter material is a high-purity nickel. Nickel was selected for the faceplate assembly because it provides the higher thermal conductivity required to provide additional face cooling margin. The nickel-clad rings were required to allow proper welding of the faceplate to the body.

TABLE III-III

INJECTOR MANIFOLD HYDRAULIC SUMMARY

Ref: B/P # 1191403

	FUEL		OXID	
	V_f mps (fps)	ΔP_f kPa (psid)	V_{ox} mps (fps)	ΔP_{ox} kPa (psid)
Inlet Line (Round)	11.3 (37)	137.9 (20)	12.8 (42)	41.4 (6)
(Squashed)	18.6 (61)			
Upper Fuel Dome	14.0-18.3 (46.60)			
Outer Oxidizer Torus	-	-	(In) 12.8 (42)	27.6 (4)
			(Stagnation) 3.66 (12)	
Distribution Plate	19.8 (65)	137.9 (20)	17.7 (58)	165.5 (24)
Inner Oxidizer Ring	-	-	10.4 (34)	27.6 (4)
Radial Oxidizer Manifold	-	-	13.7 (45)	103.4 (15)
Downcomer	14.6 (48)	82.7 (12)	18.9 (62)	186.1 (27)
Channel	7.6-10.7 (25-35)	34.5 (5)	9.1-13.1 (30-43)	55.2 (8)
Total Manifold ΔP kPa (psid)		393 (57)		607 (88)

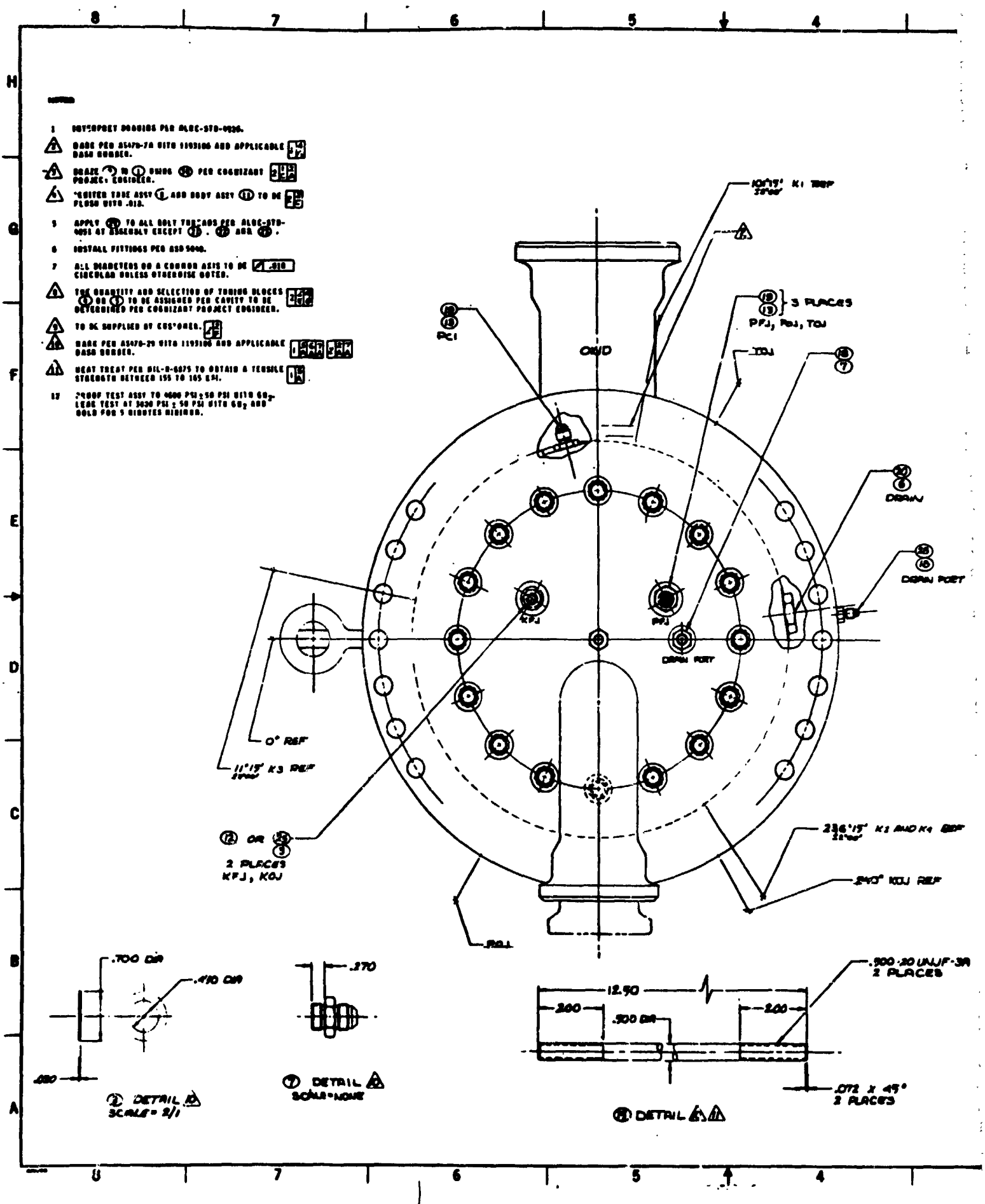

FOLDOUT FRAME

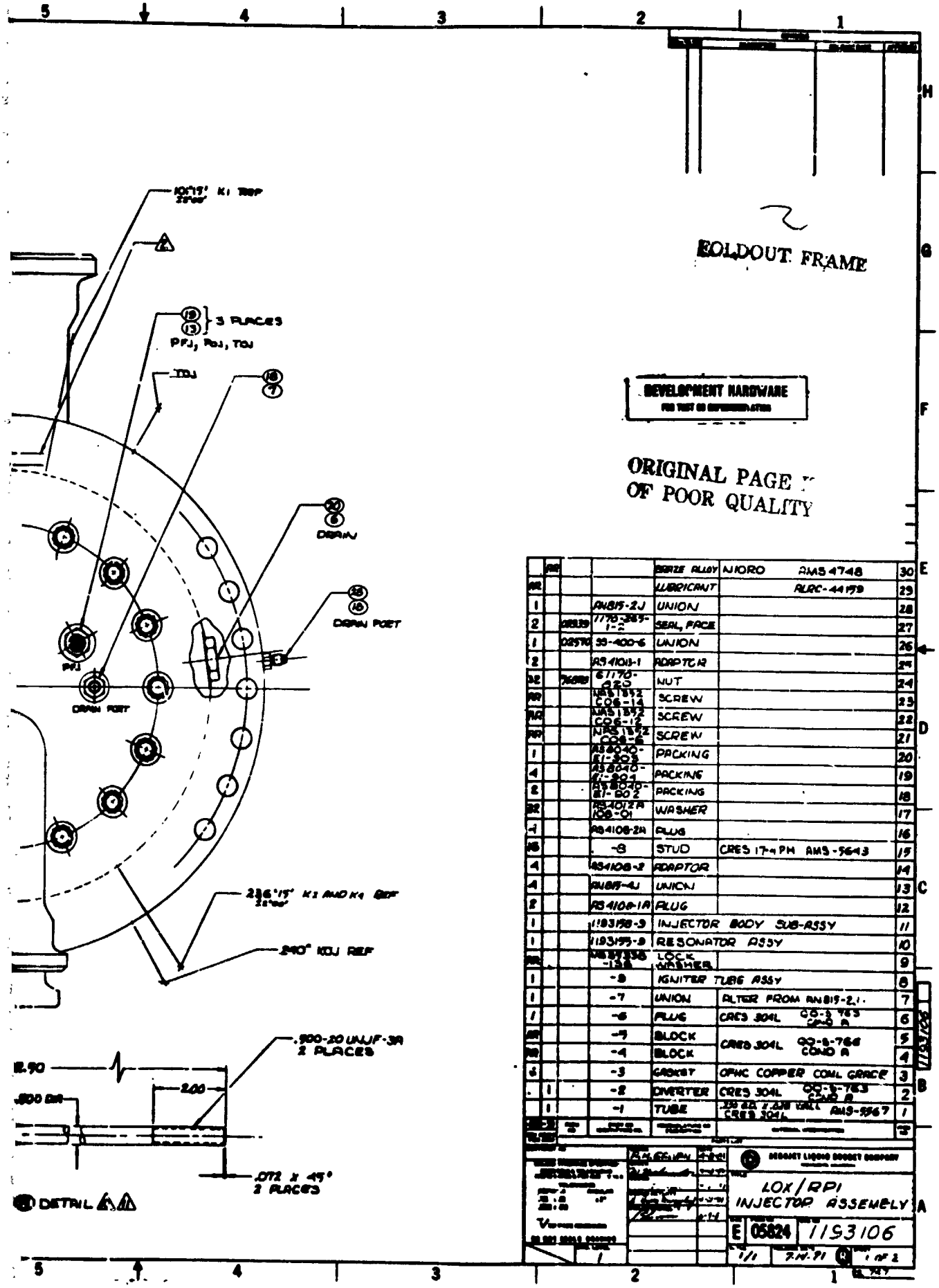

Figure III-9. Injector Assembly (Sheet 1 of 2)

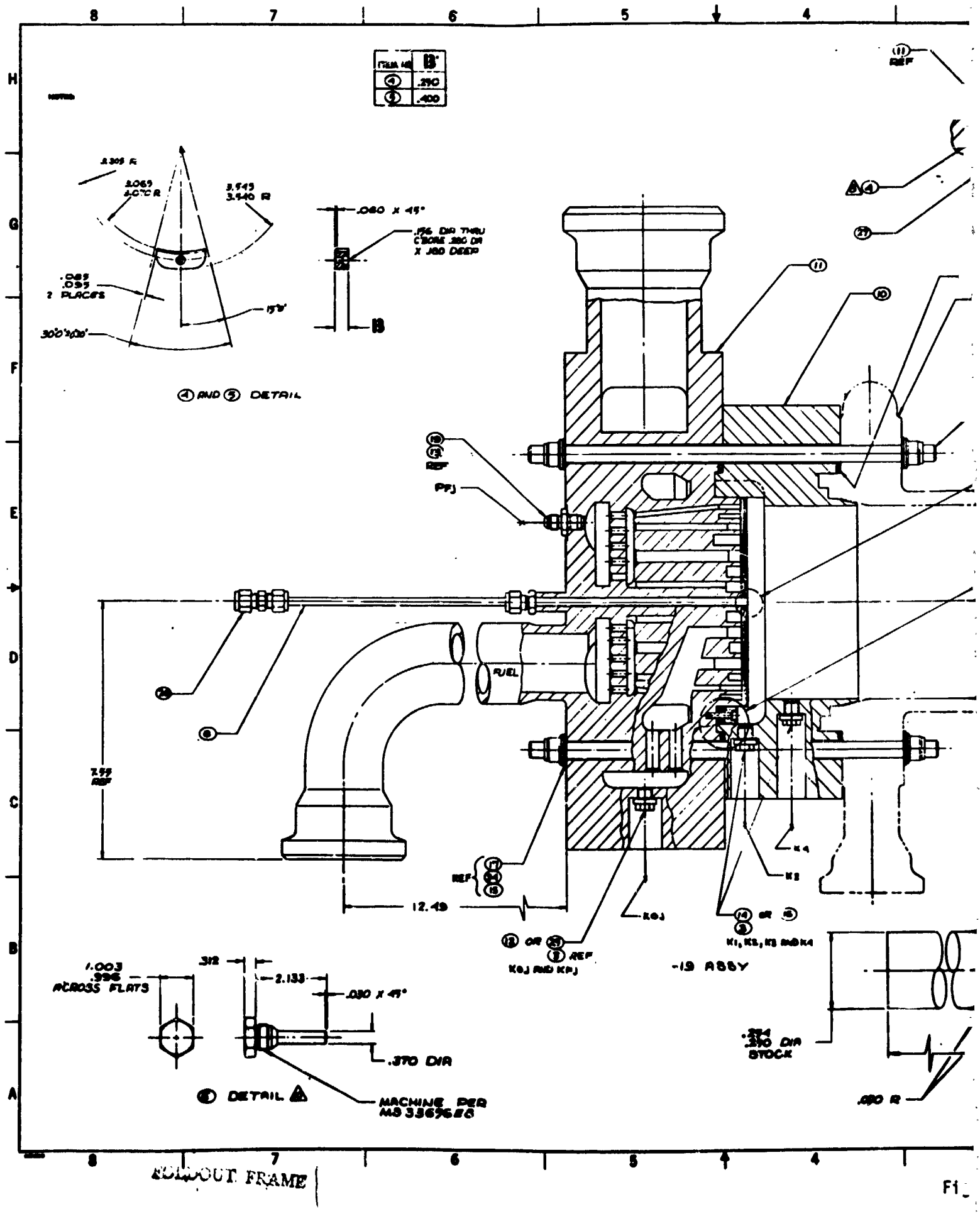

FOLDOUT FRAME

F1

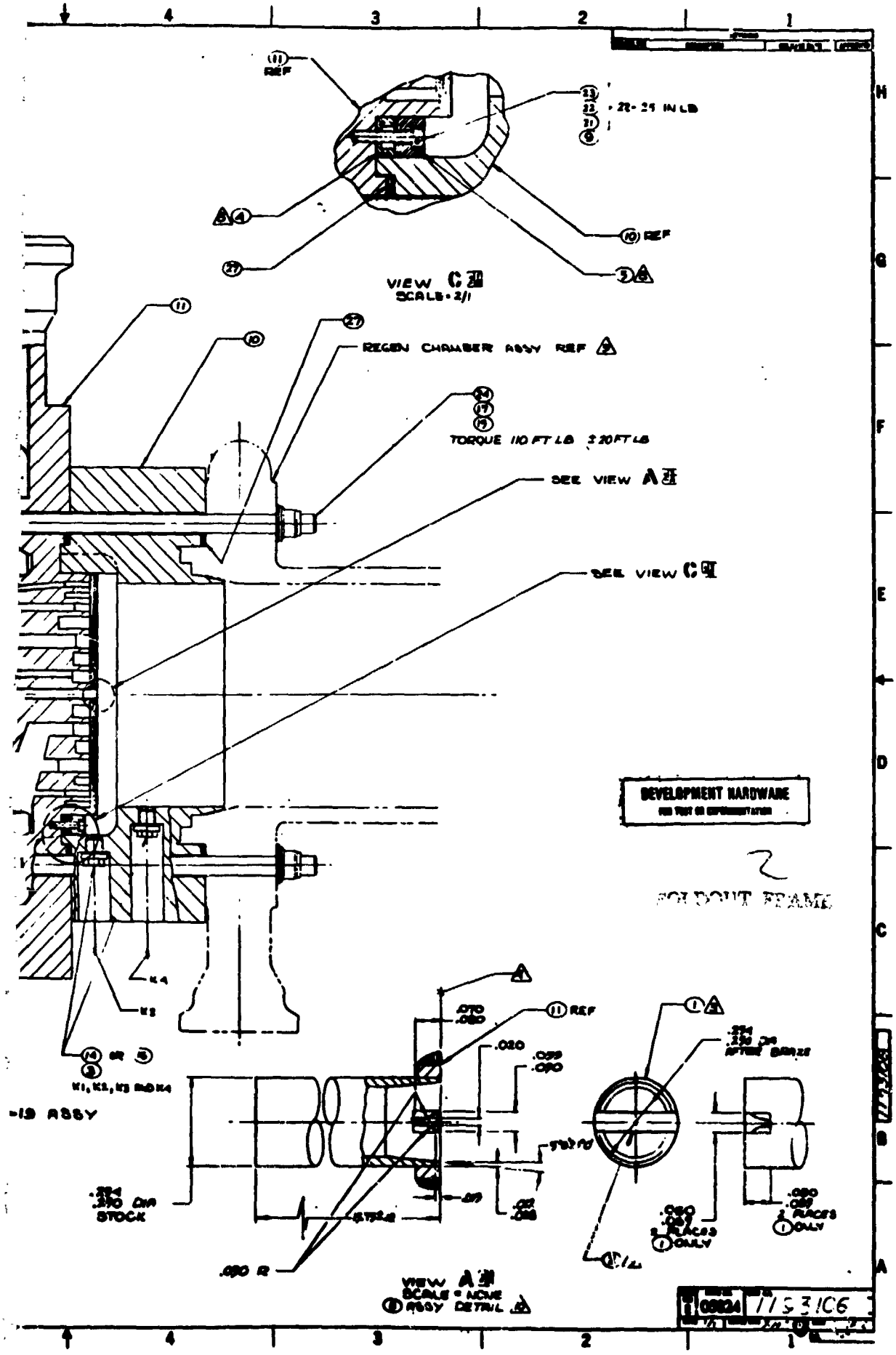

Figure III-9. Injector Assembly (Sheet 2 of 2)

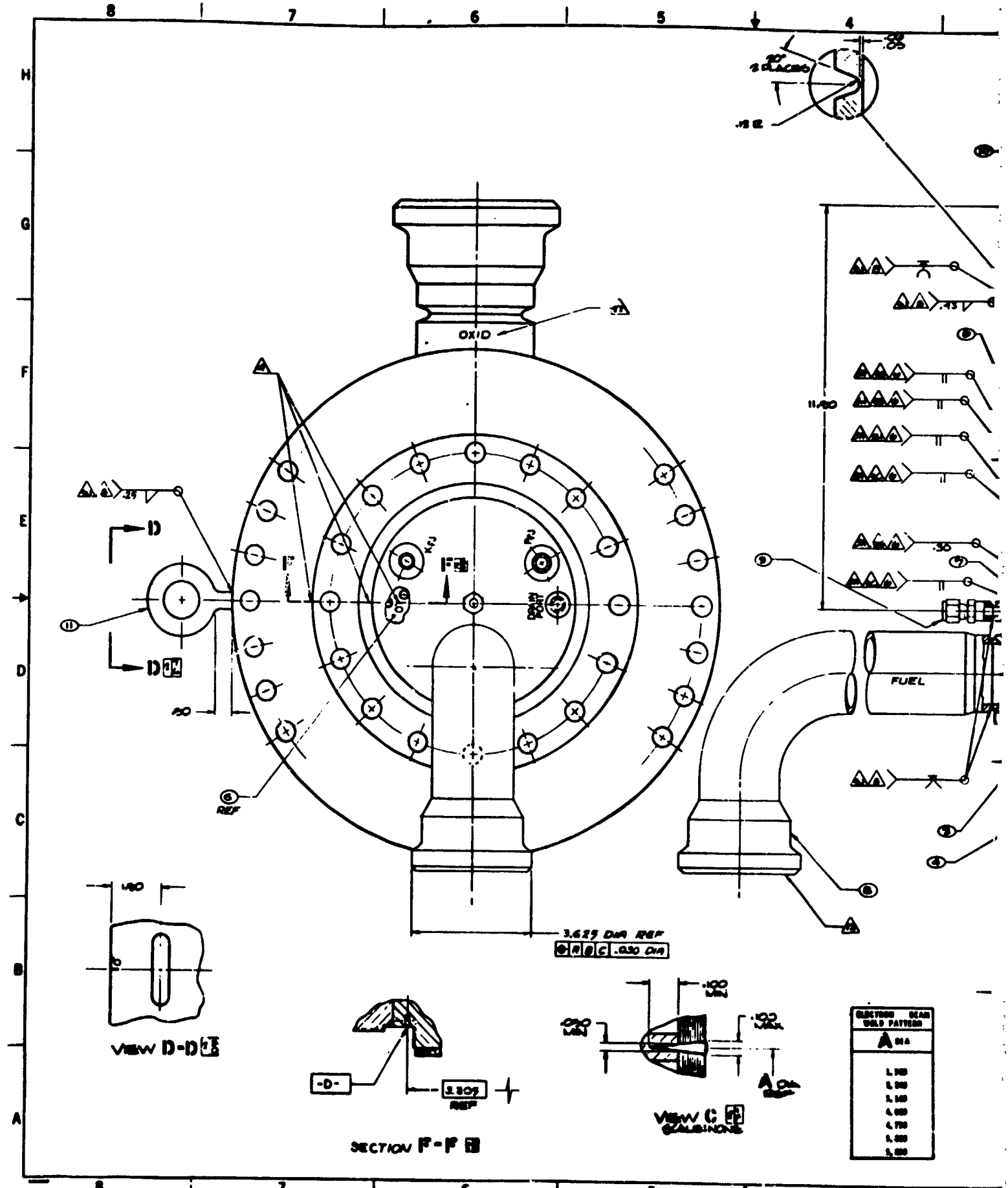
OXID
FUEL
11.490
3.625 DIA REF
.030 DIA
VIEW D-D
SECTION F-F
VIEW C
SCALE:NONE
-D-
REF

Figure I

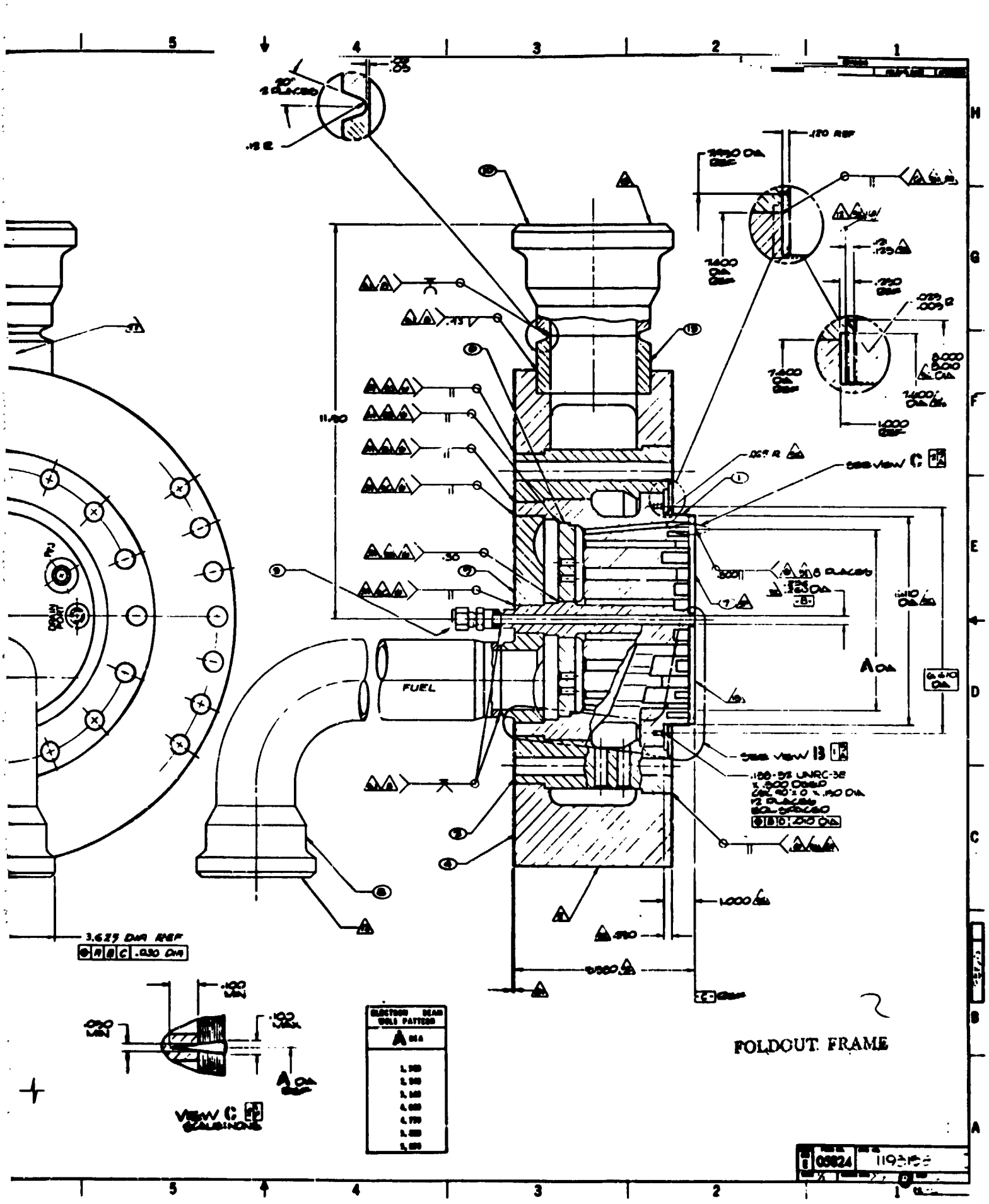

Figure III-10. Injector Body Subassembly (Sheet 1 of 2)

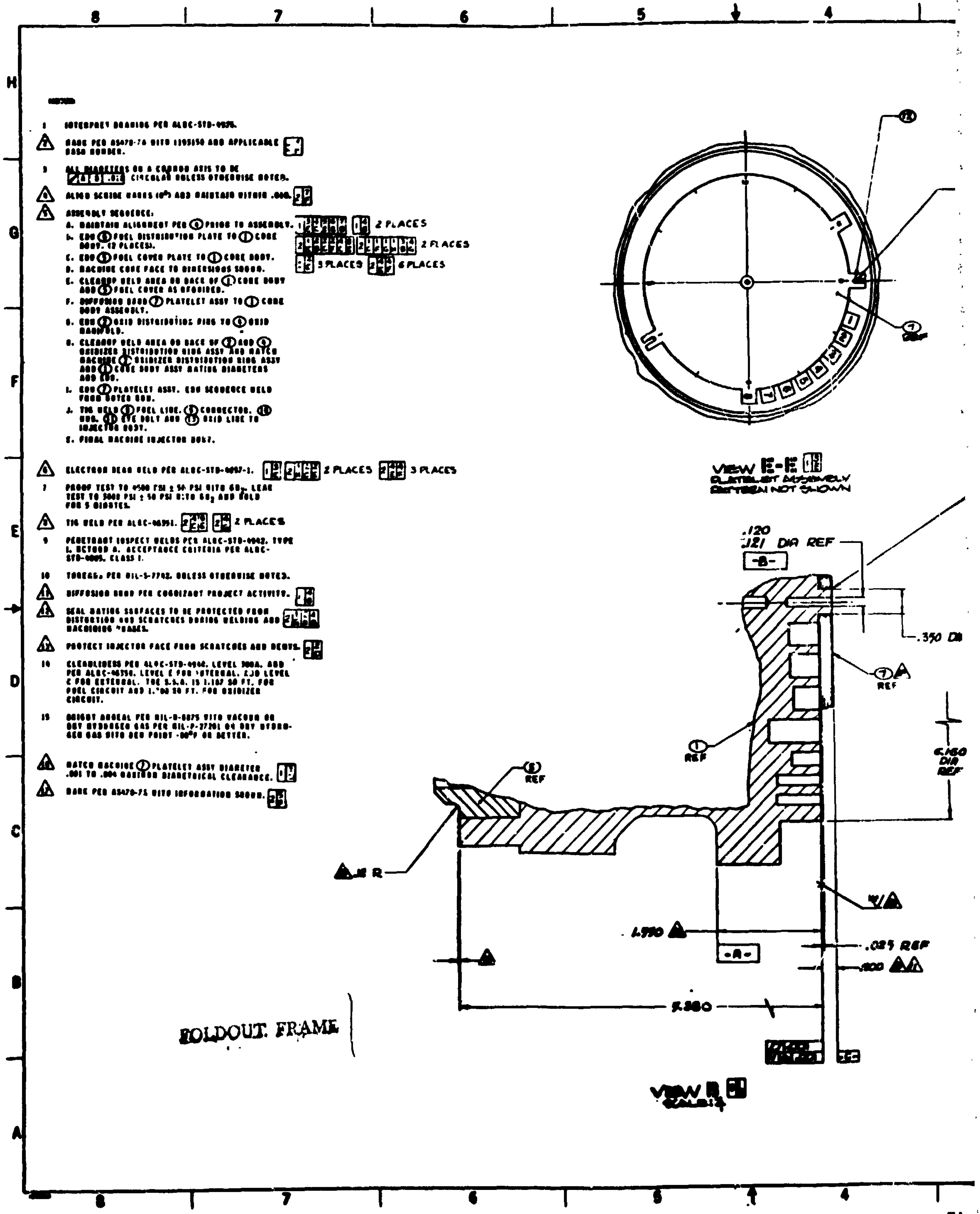

FOLDOUT FRAME

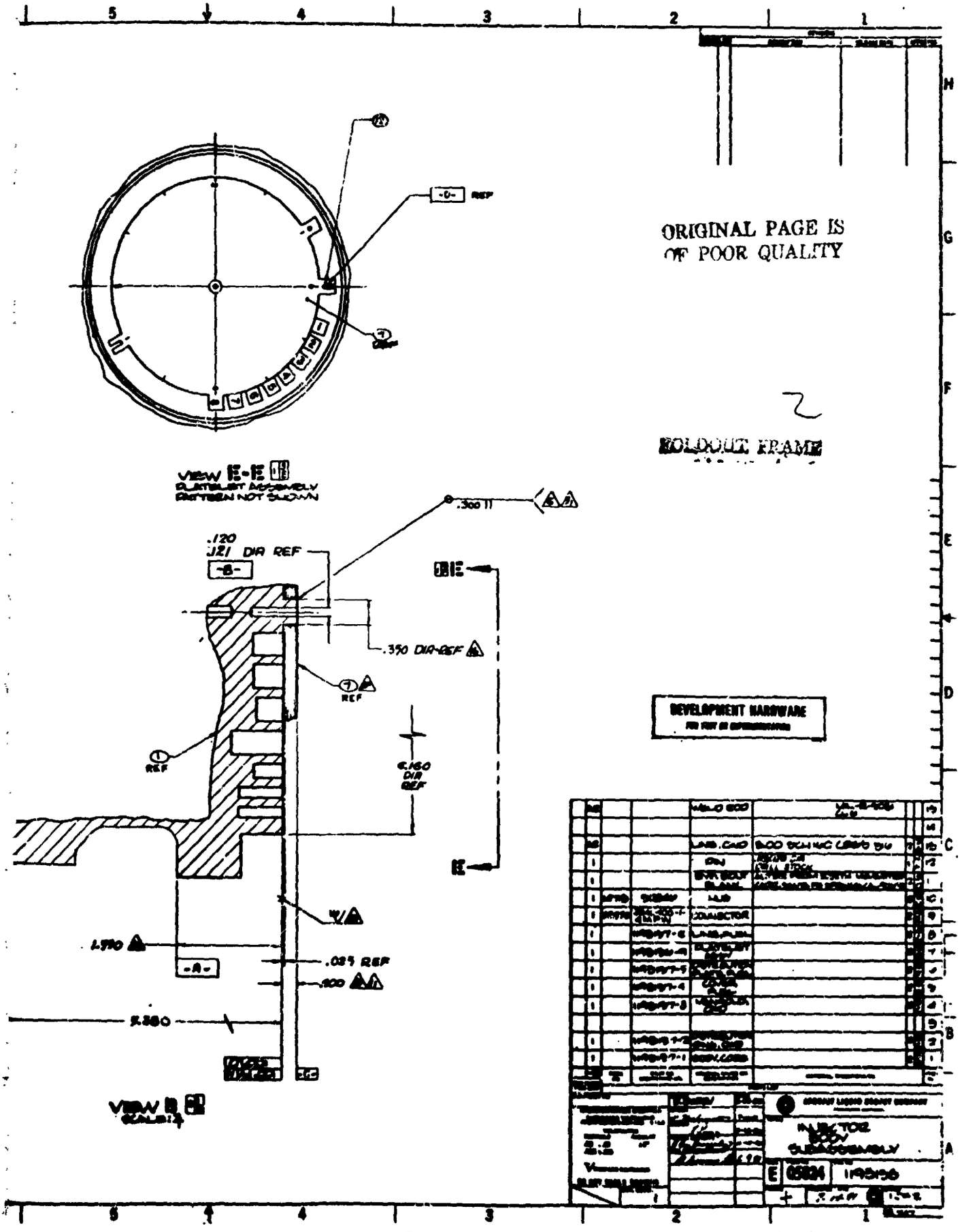

Figure III-10. Injector Body Subassembly (Sheet 2 of 2)

III, B, Detailed Design Description (cont.)

Mating of the injector subassembly (PN 1193158) and the resonator assembly (PN 1193155) produces an L-shaped annular cavity at the periphery of the injector face. The annular cavity is divided into 12 compartments, each containing a removable arc-shaped tuning block which is held in place by a socket head screw. These can be seen in Figure II-2. The segmented cavity prevents tangential modes of combustion instability from developing within the cavity. The removable blocks allow the cavity to be easily retuned if required.

The injector assembly contains ports for measurement of manifold pressures and chamber pressures. Drain ports are provided for removing cleaning solvents from the manifold while the assembly is mounted in a horizontal position, with the lifting eyebolt in the vertically upward orientation. These features can be seen in Figure III-9.

Assembly of the all-welded injector and the resonator ring requires the use of a single spring-activated Teflon face seal. The recommended part (PN 1170-265-1-2) is a RACO brand seal, manufactured by the Fluorocarbon Company. This type of oxygen-compatible seal is specifically designed for use at cryogenic temperatures. The same seal is also used at the interface of the resonator ring and the NASA-supplied cooled chambers.

The injector, resonator, and NASA-supplied cooled chamber flanges are held by sixteen 1.27-cm (0.5-in.) diameter studs which are 31.75 cm (12.5 in.) long. The stud material is 17-4 stainless alloy, heat-treated per MIL H 6875 to condition H-900 to H-1025 in order to provide a tensile stress capability of 1.1×10^6 kPa (160K psi). The actual stress is 0.83×10^6 kPa (120K psi) at the recommended torque value of 149 ± 27 m-N (110 ± 20 ft-lbF). The recommended torque valve assumes the use of Fel- Pro C5A lubricant on the studs. The required torque may be different for other lubricants.

III, B. Detailed Design Description (cont.)

2. Propellant Interfaces

The test stand propellant delivery system interfaces with the injector inlet lines through weld-on Greyloc hubs. The fuel enters the back of the injector through a 5.08-cm (2-in.) Schedule 80 pipe/elbow having a 5.08-cm (2-in.) Greyloc hub (PN 52822). The oxygen enters the side-mounted 7.62-cm (3-in.) pipe via a 7.62-cm (3-in.) Greyloc hub (PN 52846). The Greyloc clamps (not supplied) for the 5.08-cm (2-in.) size (2GR20) are PN's 48502 and 48503 for the 7.62-cm (3-in.) pipe size (3GR25) oxygen line. The seal rings, which should be replaced when the lines are opened, require Greyloc PN's 51236 and 51237 for the fuel and oxygen circuits, respectively.

3. Manifolding

The components which form the manifolding system are shown in Figures III-11 through III-20. The fuel flows from the 5.08-cm (2 in.) inlet line through the back coverplate into an annular distribution manifold (Figures III-12 and III-9). A primary flow distribution plate (PN 1193157), shown in Figure III-13, redistributes the incoming fuel before it enters the injector manifold downcomers. The downcomers, shown in Figures III-14 and III-15, transport the fuel from the plenum located downstream of the primary flow distribution plate to the face rings also shown in Figure III-15. The outermost ring and each alternate face ring moving inward is supplied with fuel. The injector elements are fed directly from the face rings.

The oxygen, entering through a single side-mounted 7.62-cm (3-in.) line (Figure 18), splits into two equal streams and flows circumferentially around the injector core through an annular passage which continuously decreases in the cross-sectioned area. This flow path can be seen in the drawing of Figure II-1.

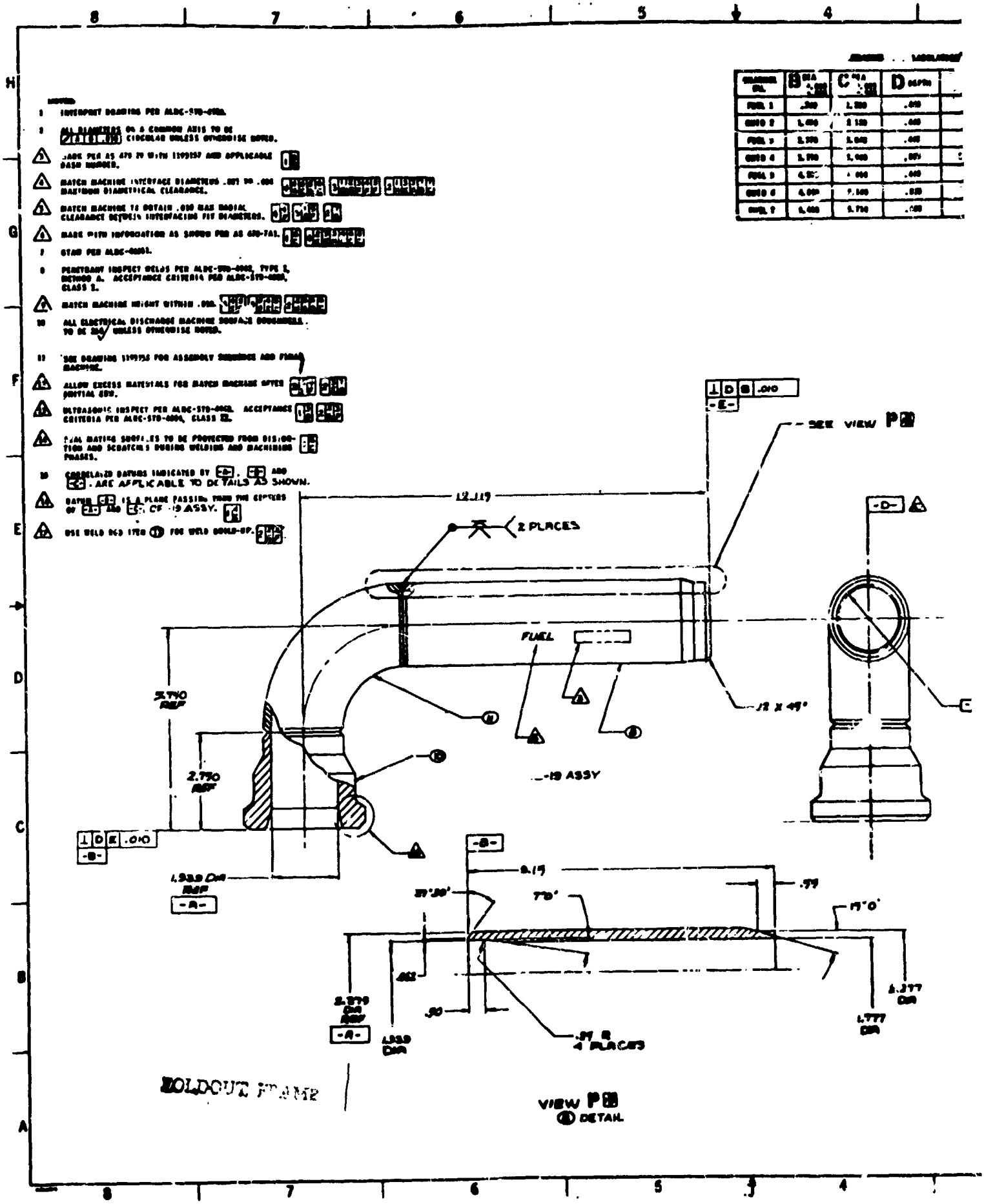

Figure

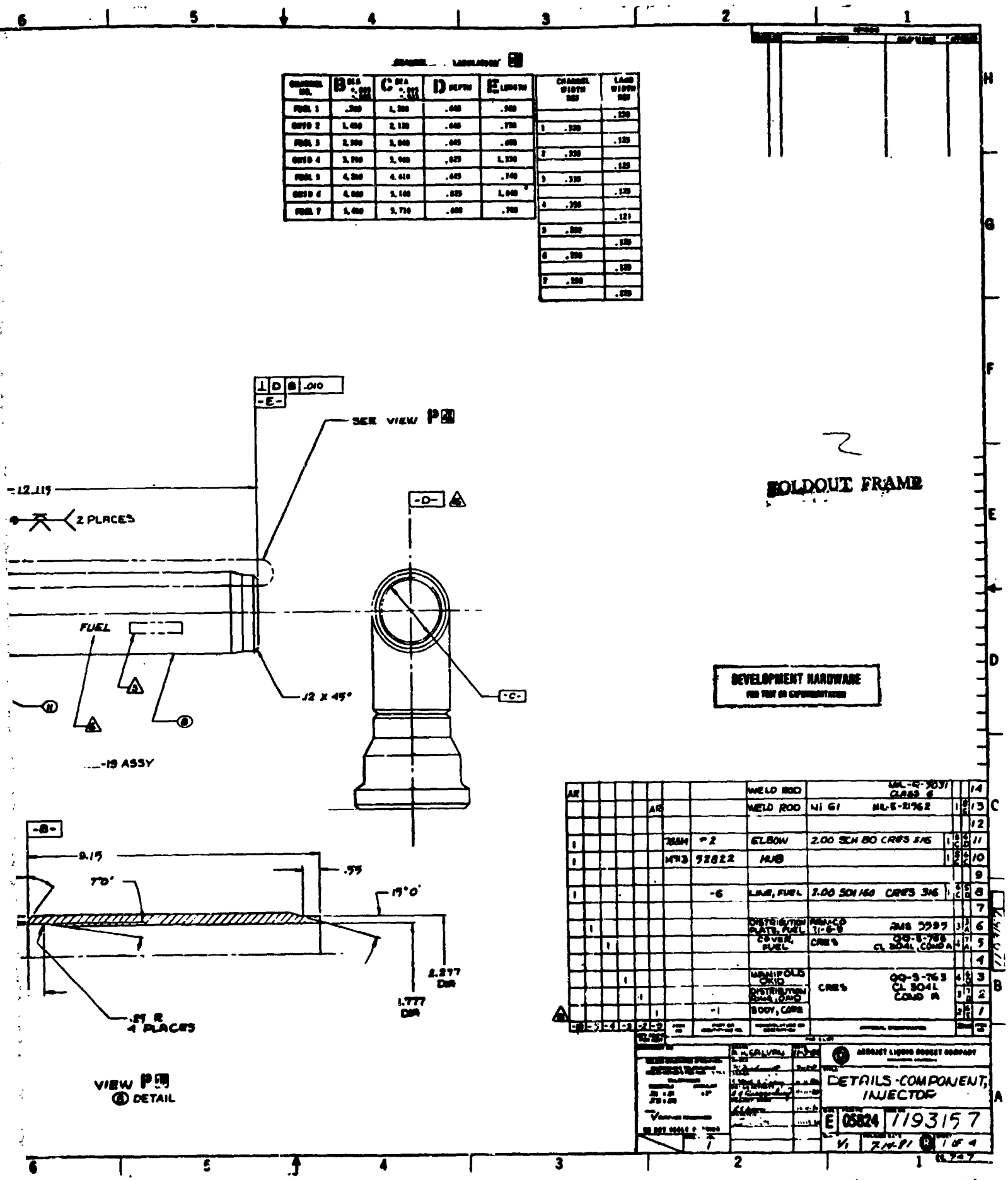

Figure III-11. Injector Components Details (Sheet 1 of 4)

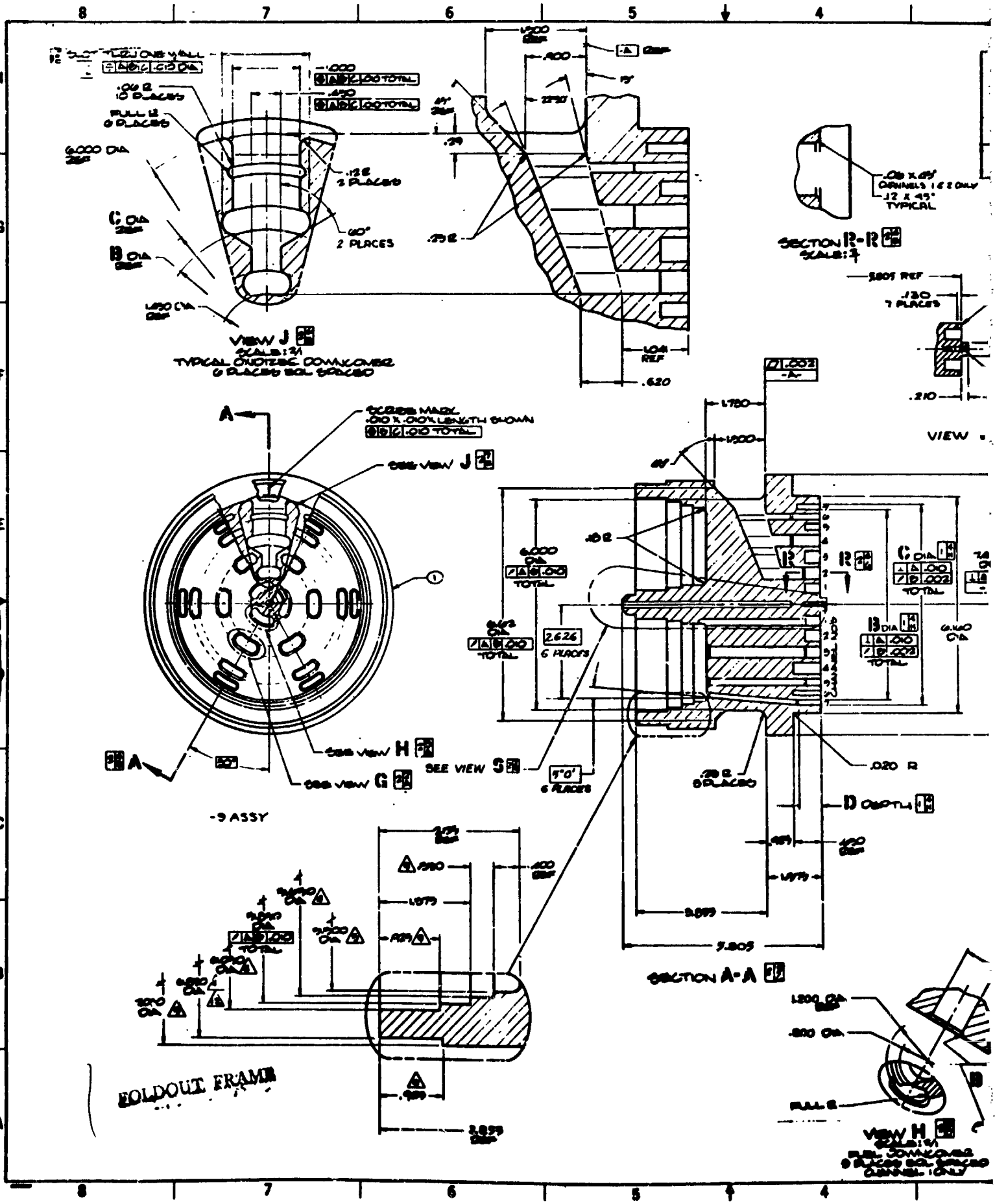
VIEW J
SCALE: 2/1
TYPICAL OUTFLOW DOWNCOMER
6 PLACES EQ. SPACED
SECTION R-R
SCALE: 1/1
VIEW H
SCALE: 2/1
FULL DOWNCOMER
6 PLACES EQ. SPACED
CHANNEL ONLY
SECTION A-A
-9 ASSY
FOLDOUT FRAME

Figure III-

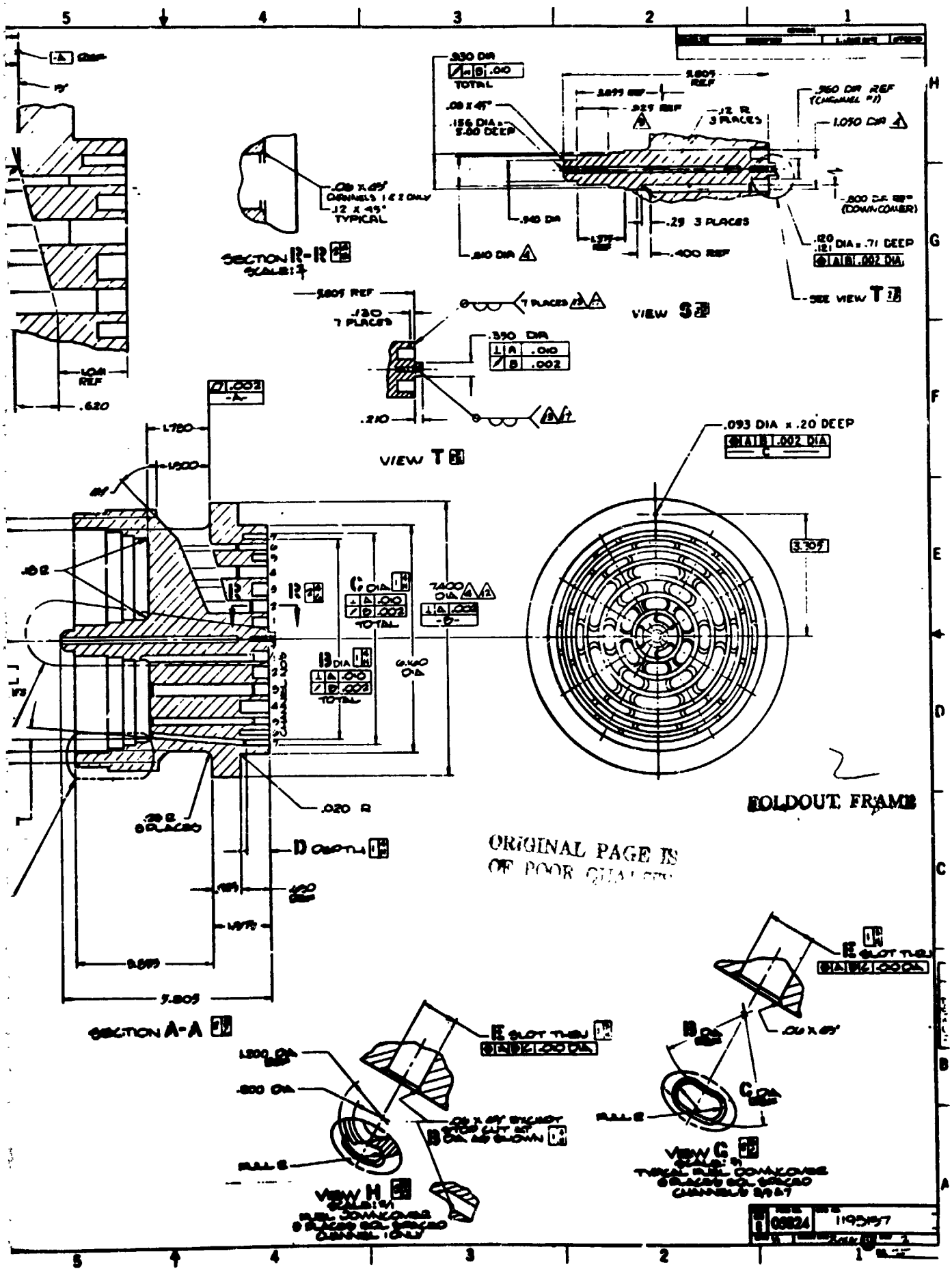

Figure III-11. Injector Components Details (Sheet 2 of 4)

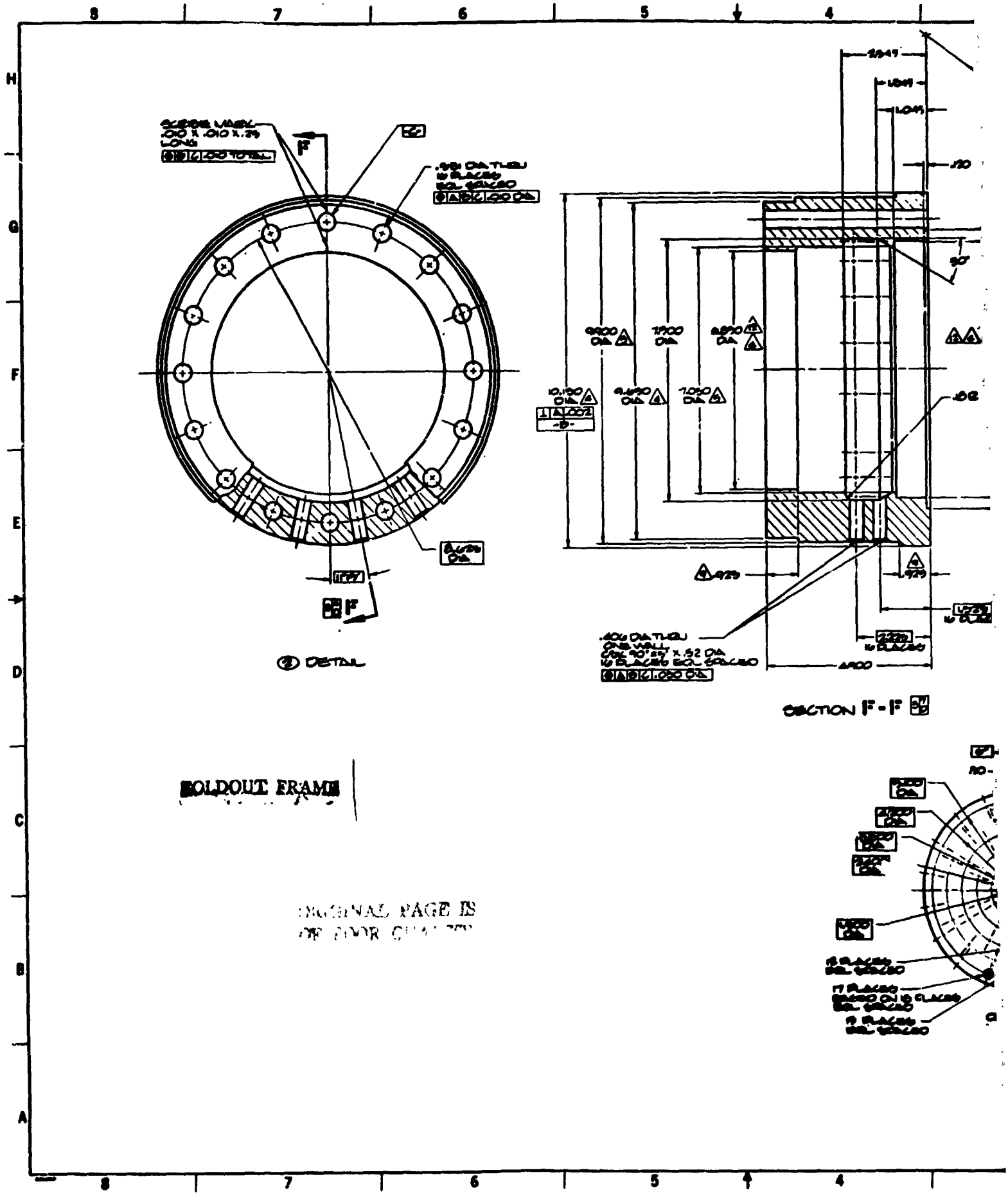

Figure III-1

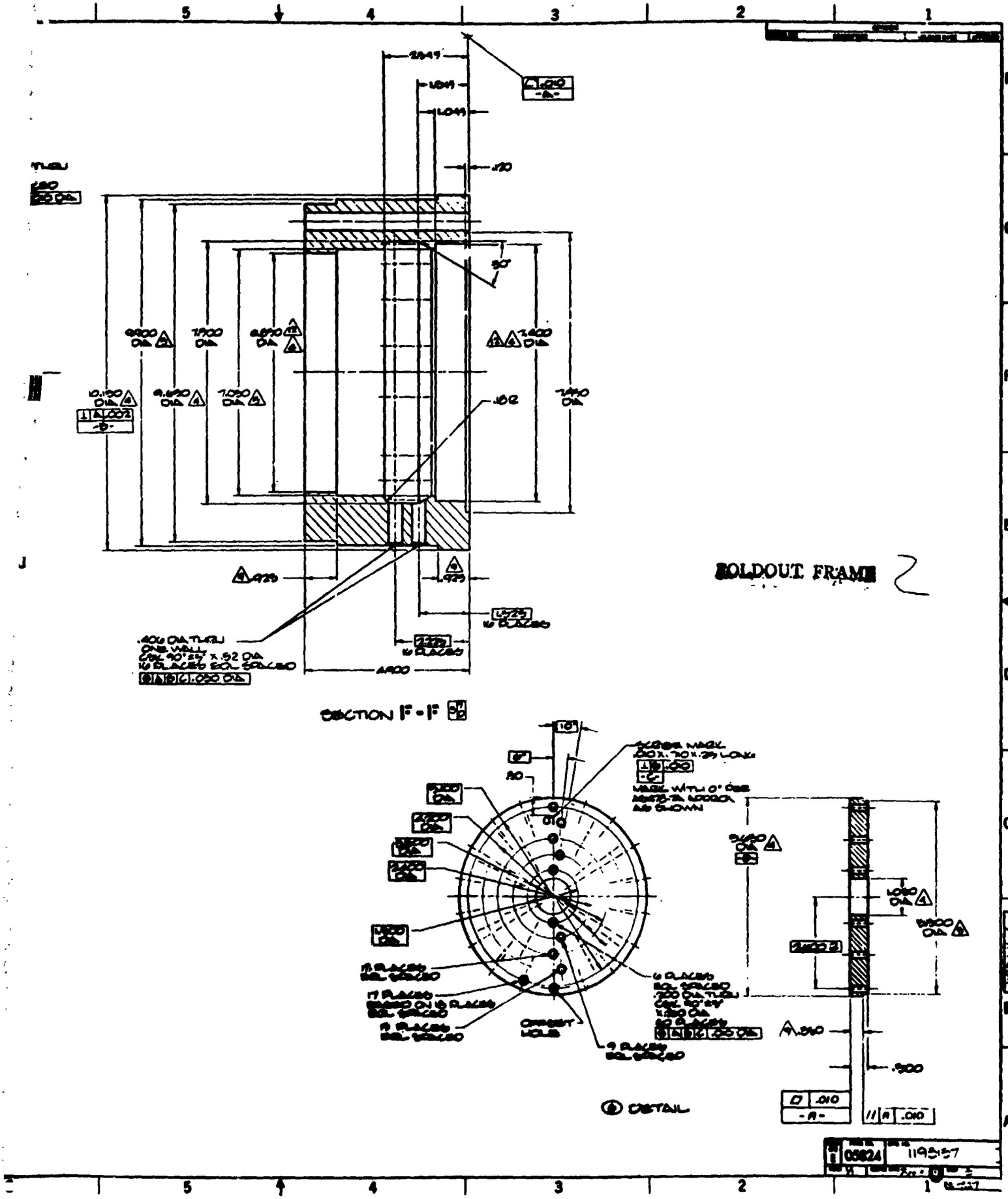

Figure III-11. Injector Components Details (Sheet 3 of 4)

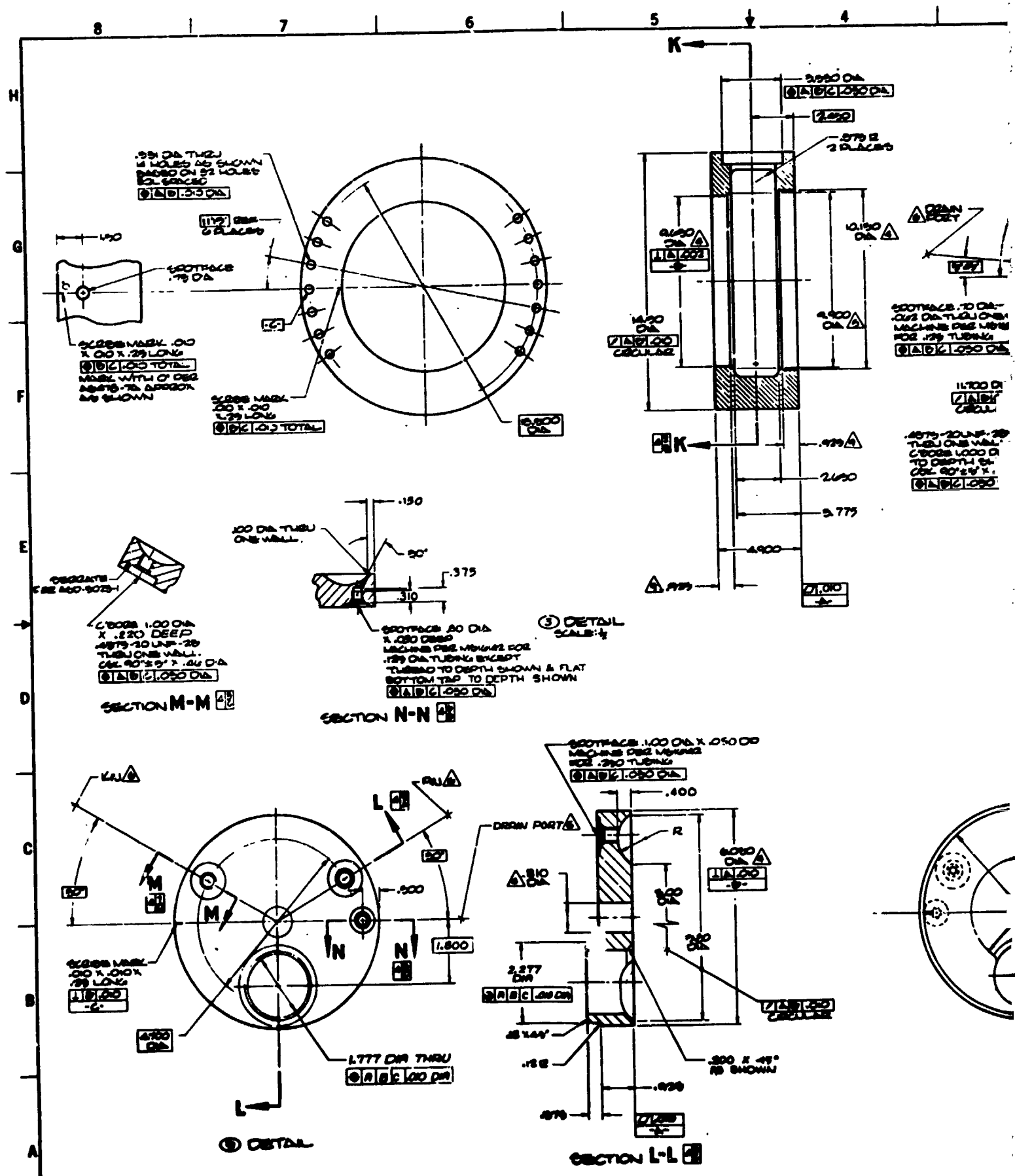

FOLDOUT FRAME

ORIGINAL PAGE IS OF POOR QUALITY

Figure I

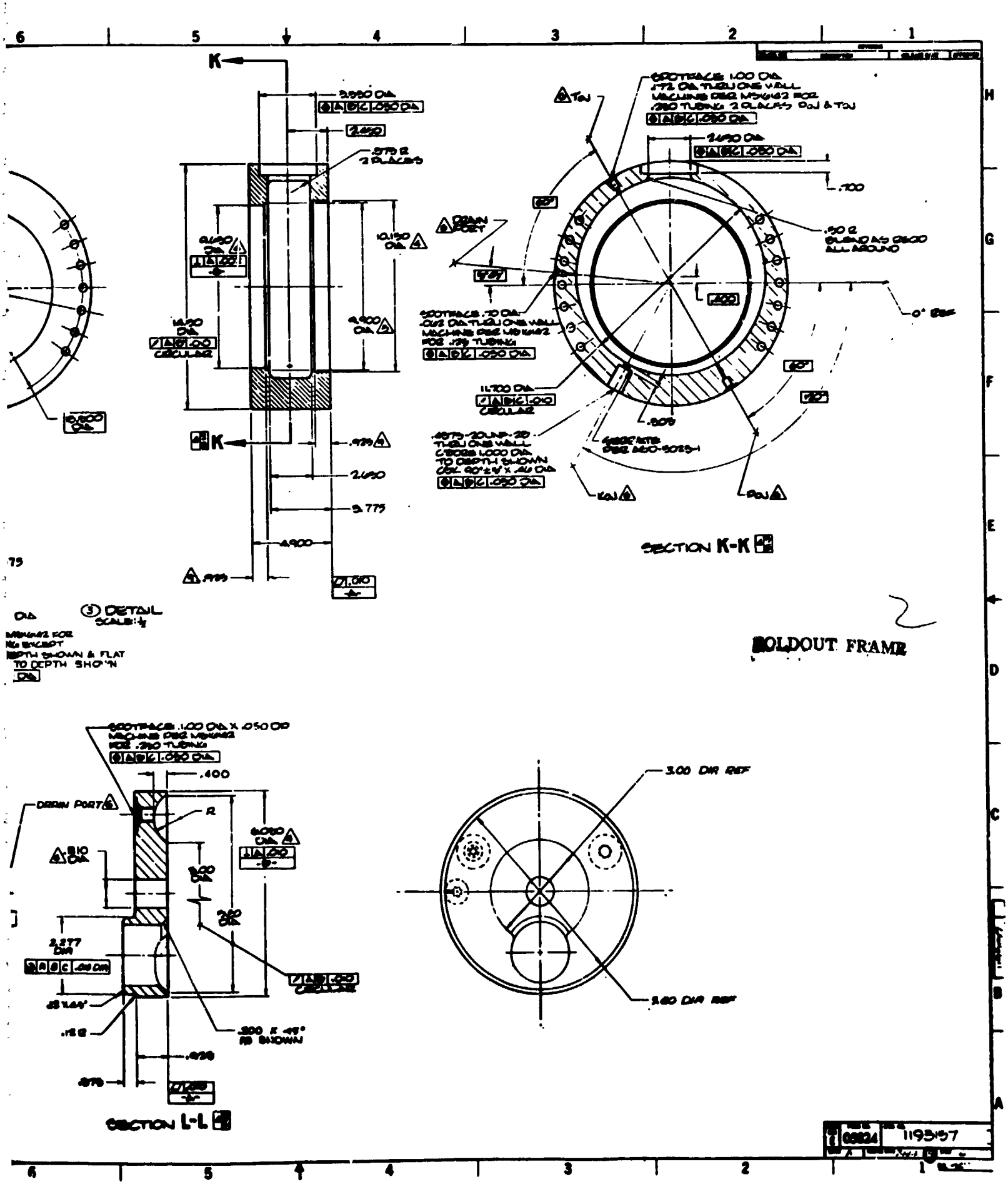

Figure III-11. Injector Components Details (Sheet 4 of 4)

0381 SP 026

Figure III-12. Fuel Coverplate PN 1193157-5

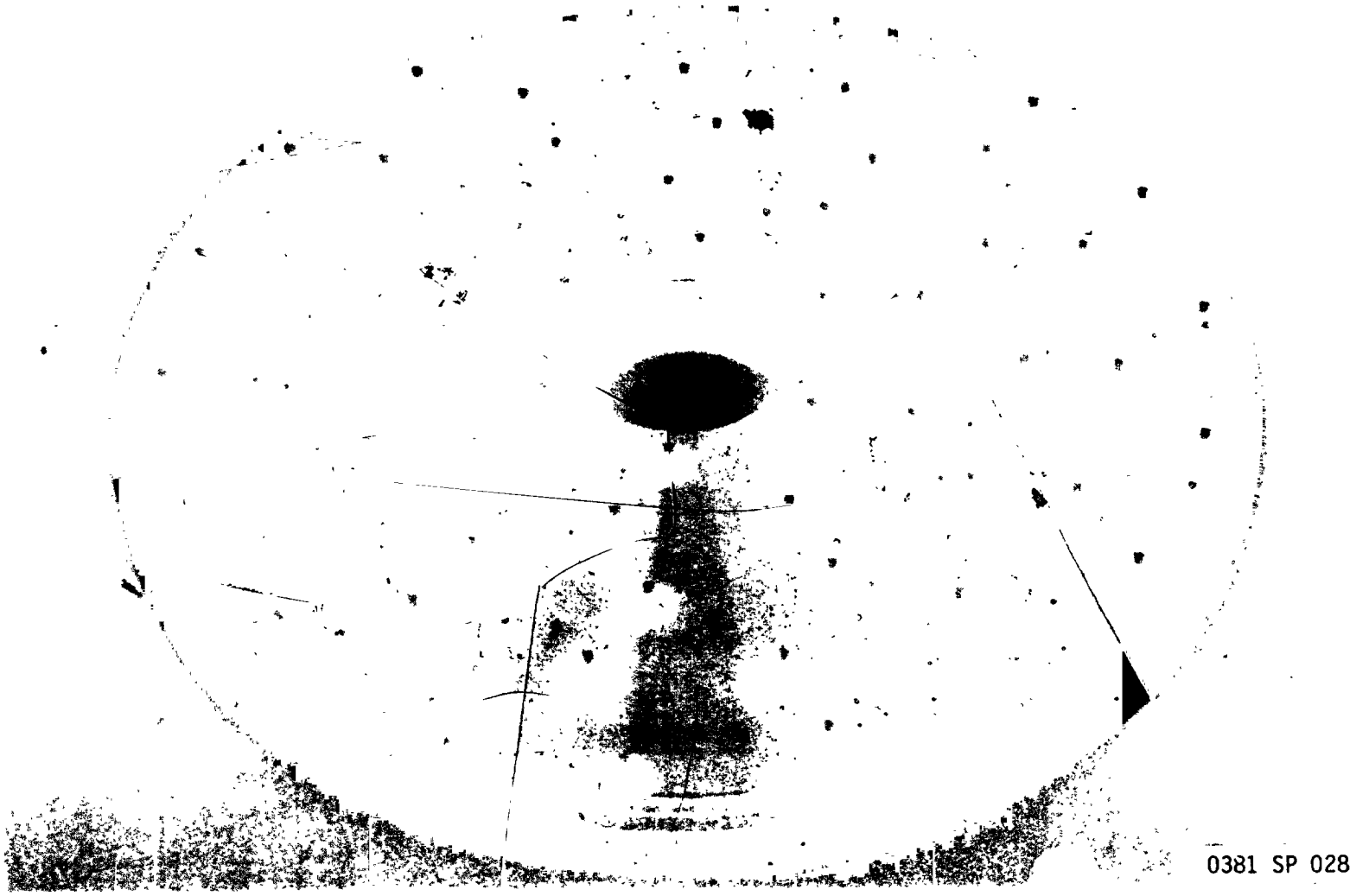

Figure III-13. Fuel Distribution Plate PN 1193157-6

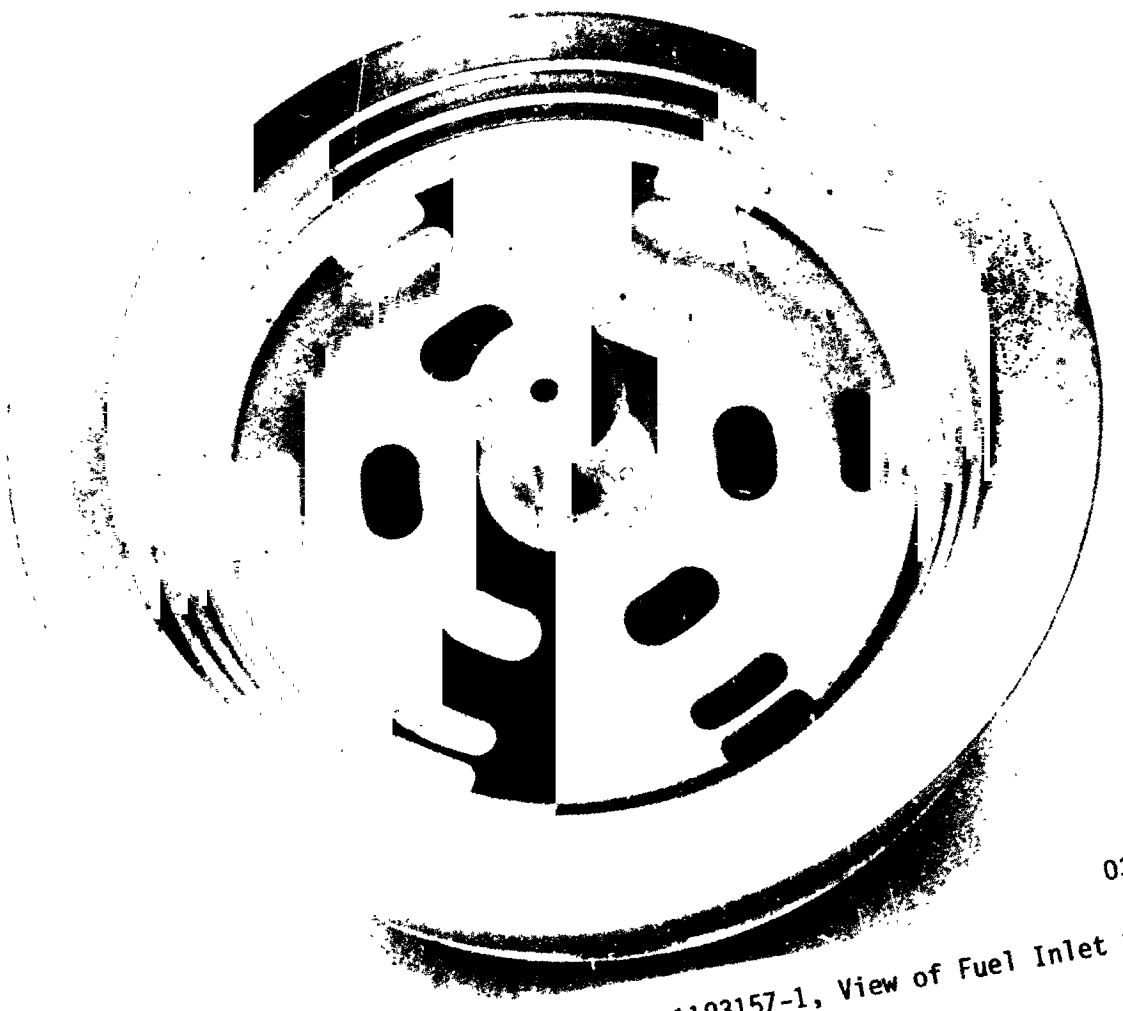

0381 SP 031

Figure III-14. Injector Body Core PN 1193157-1, View of Fuel Inlet Side

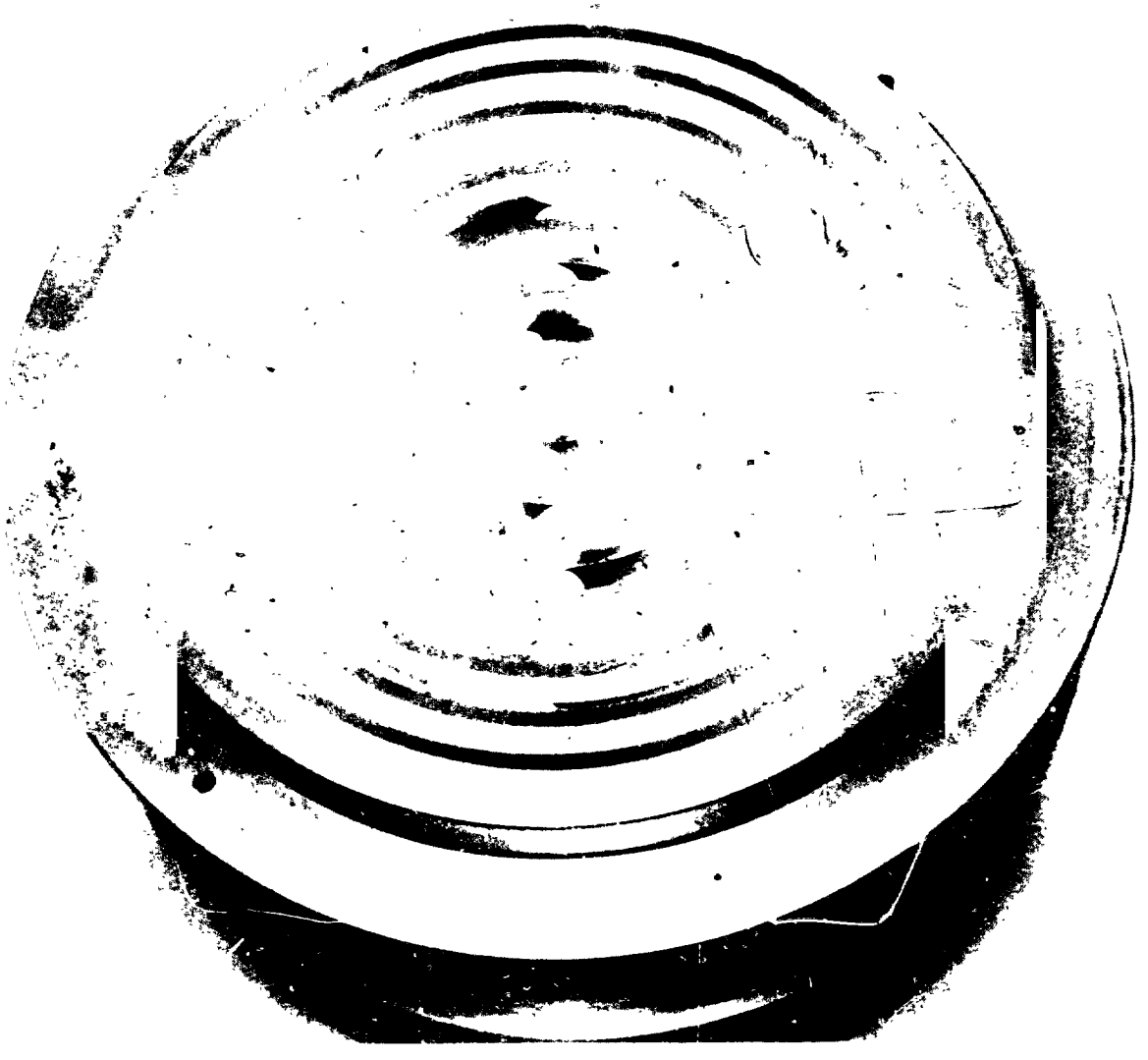

0381 SP 030

Figure III-15. Injector Body Core PN 1193157-1, View of Ring Manifold

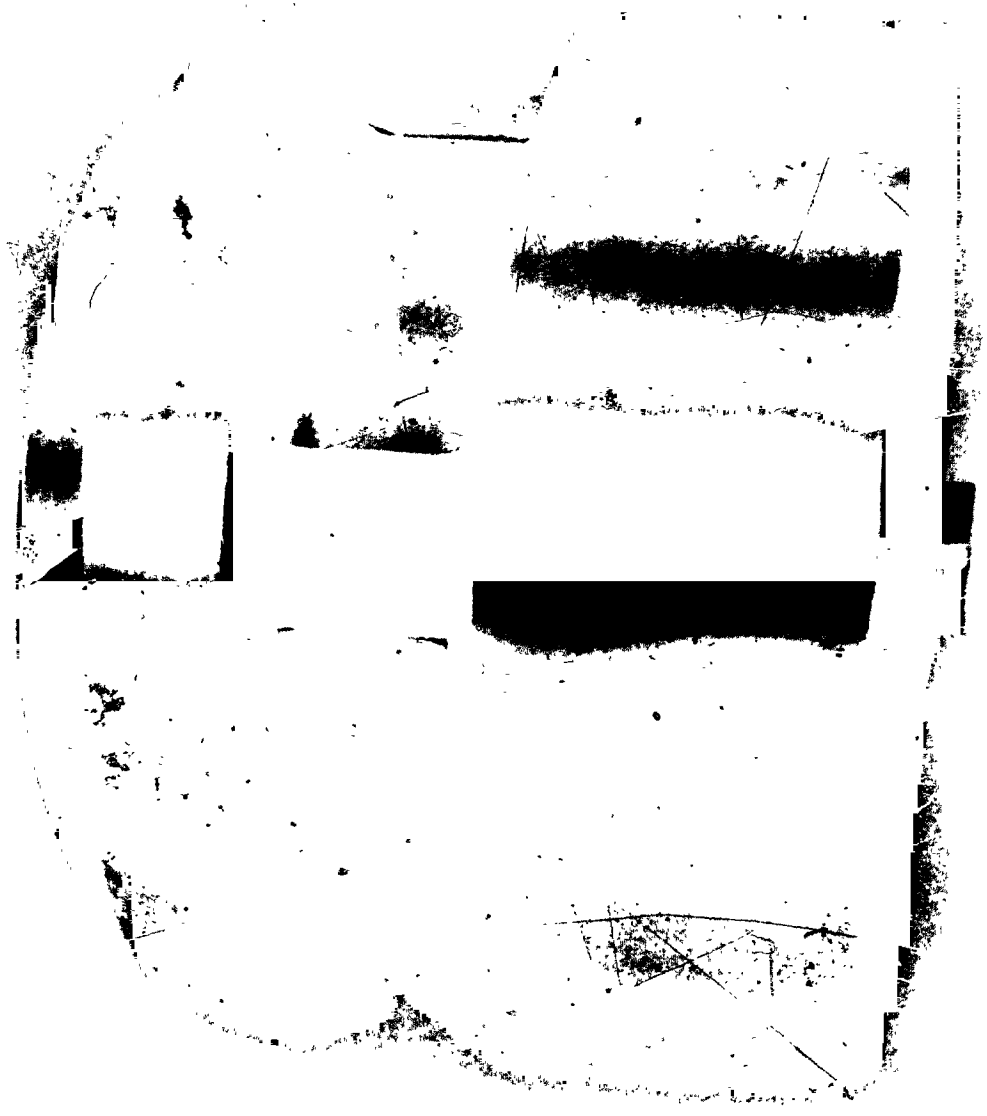

0381 SP 029

Figure III-16. Injector Body Core PN 1193157-1, Side View of Oxygen Inlet

Figure III-17. Subassembly of Core, Fuel Distribution Plate, and Fuel Cover

0781 SP 127

0381 SP 027

Figure III-18. Oxidizer Manifold PN 1193157-3

Figure III-19. Oxidizer Distribution Manifolding

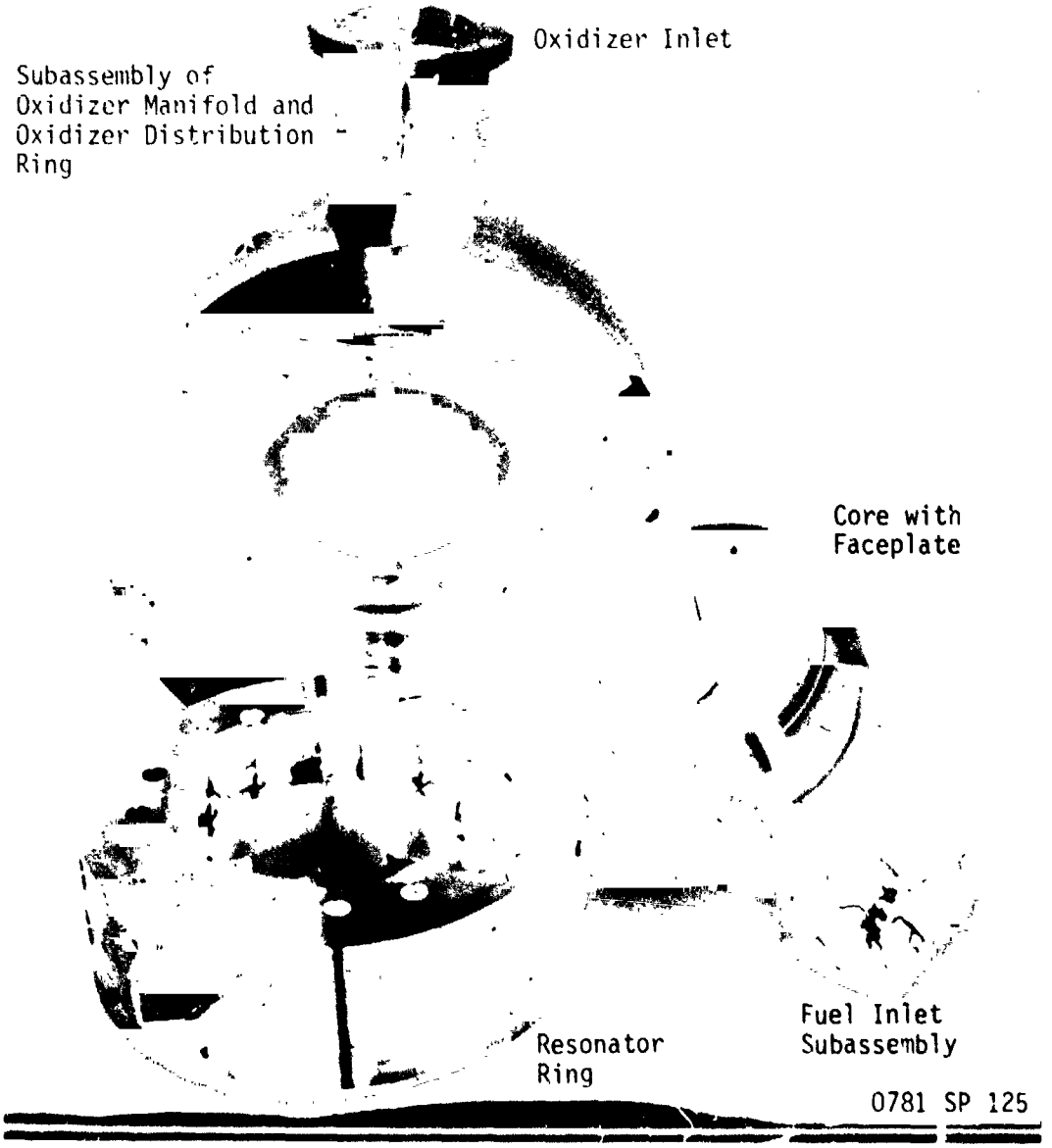

Figure III-20. Injector Subassemblies and Resonator Ring

The oxygen then flows radially inward through a primary flow distribution ring which can be seen in Figure III-19. The secondary plenum, located on the downstream side of the distribution ring, supplies a series of six cross-flow passages which intersect downcomers EDM-machined into the bottom of the face rings. These can be seen in Figures III-15 and III-16. The second, fourth, and sixth ring supply oxygen to the injection elements.

The flow distribution uniformity expected to result from this manifolding design is shown in Figure III-21, which provides data obtained from other contracts utilizing similar manifolding and flow distribution plates and rings.

4. Acoustic Resonator

The acoustic resonator design (PN 1193155) is shown in Figure III-22. A photograph of the flange portion of the resonator is provided in Figure III-20.

5. Selected Injector Element Pattern

Detailed drawings of the selected injector mixed-element pattern are shown in Figure III-23. A photograph of the finished faceplate following welding to the body is provided in Figure III-24.

C. FABRICATION

The fabrication methods employed in the manufacture of the injector body and resonator ring involved conventional machining and electrical-discharge machining (EDM) of the non-circular manifold and downcomer passages seen in Figures III-14 -15, and -16. Electron-beam (EB) welding was

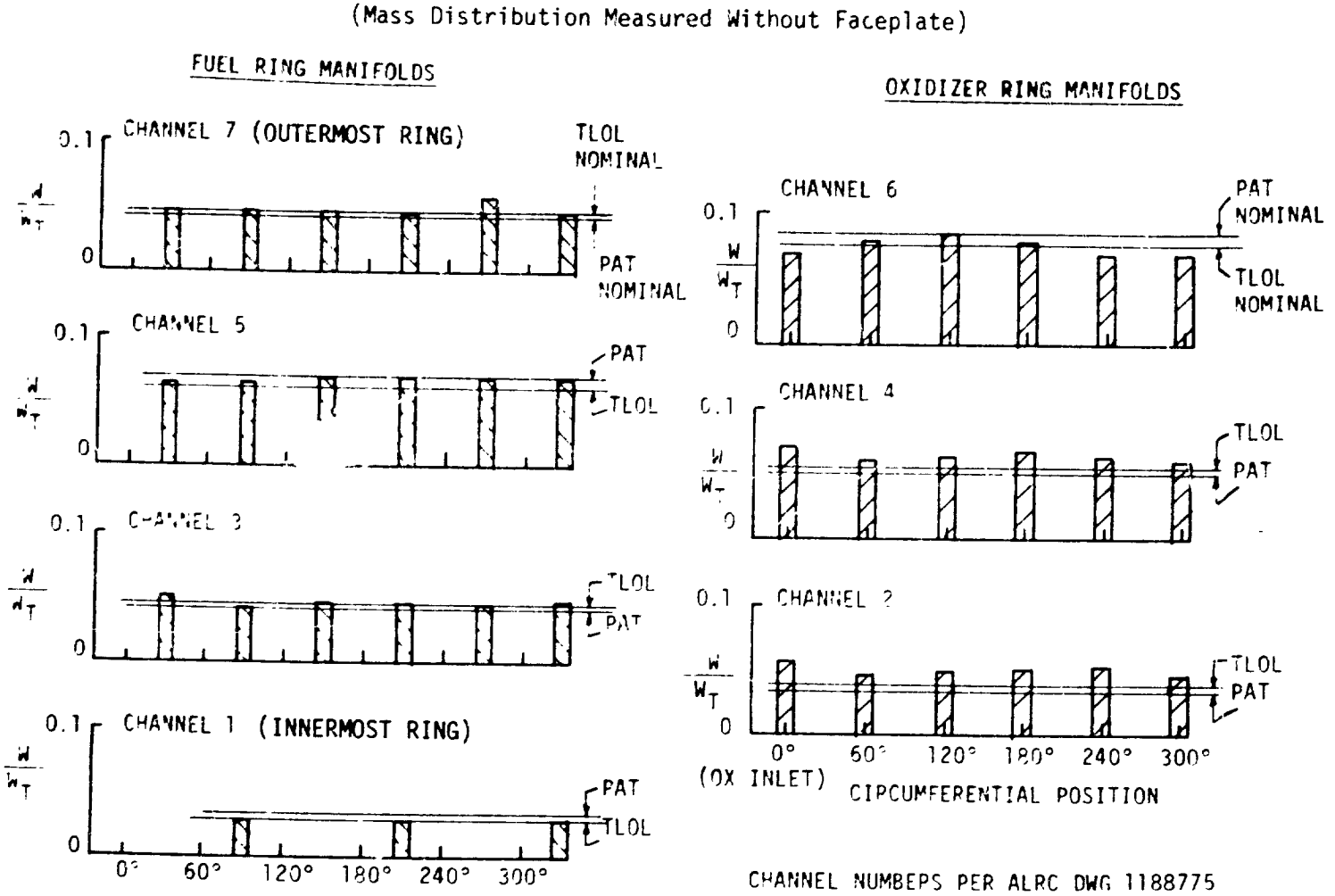

Figure III-21. Expected Injector Manifold Hydraulic Distribution

8 7 6 5 4

...SPECT DRAWING PER ALRC-STD-9026.

DIAMETERS ON A COMMON AXIS TO BE ... [B] .010 CIRCULAR UNLESS OTHERWISE NOTED.

... PER AS478-29 WITH 1103155 AND APPLICABLE ... NUMBER.

... ALL INSTRUMENTATION REFERENCE DESIGNA- ...S NEAR PORT PER AS478-7A. DO NOT MARK ON ... SEAL SURFACE. 2 PLACES

... MATING SURFACES TO BE PROTECTED FROM ...OTION AND SCRATCHES DURING WELDING AND ...INING PHASES.

HOLE LOCATIONS ARE BASIC AND ... [B][C] .010 DIA UNLESS OTHERWISE NOTED.

... PER ALRC-00201.

ULTRASONIC INSPECT WELDS PER ALRC-STD-9002. ...PE I, METHOD A, ACCEPTANCE CRITERIA PER ...C-STD-9005, CLASS I.

...IGHT ANNEAL PER MIL-H-6875 WITH VACUUM OR ...Y HYDROGEN GAS PER MIL-P-27201 OR DRY HYDRO- ...N GAS WITH DEW POINT -60°F OR BETTER.

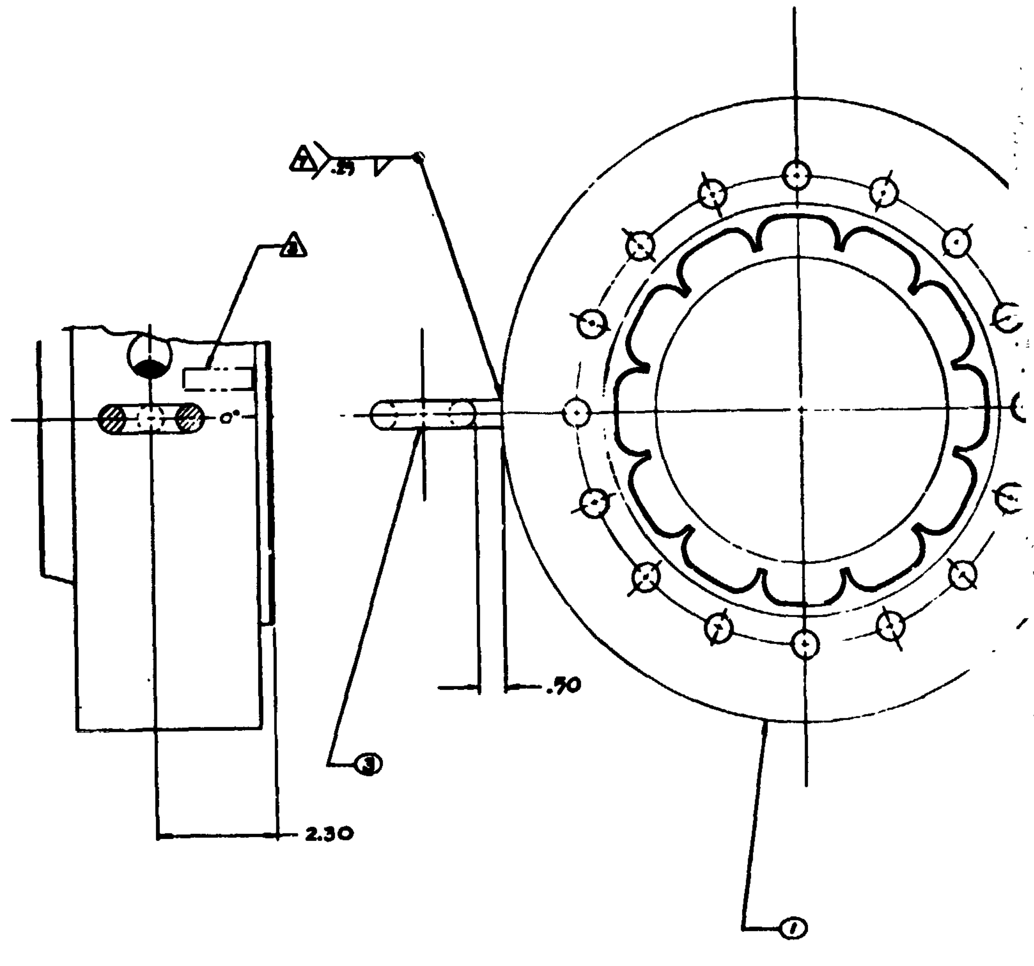

D

C

B

-9 ASSY

FOLDOUT FRAME

A

8 7 6 5 4

Figur

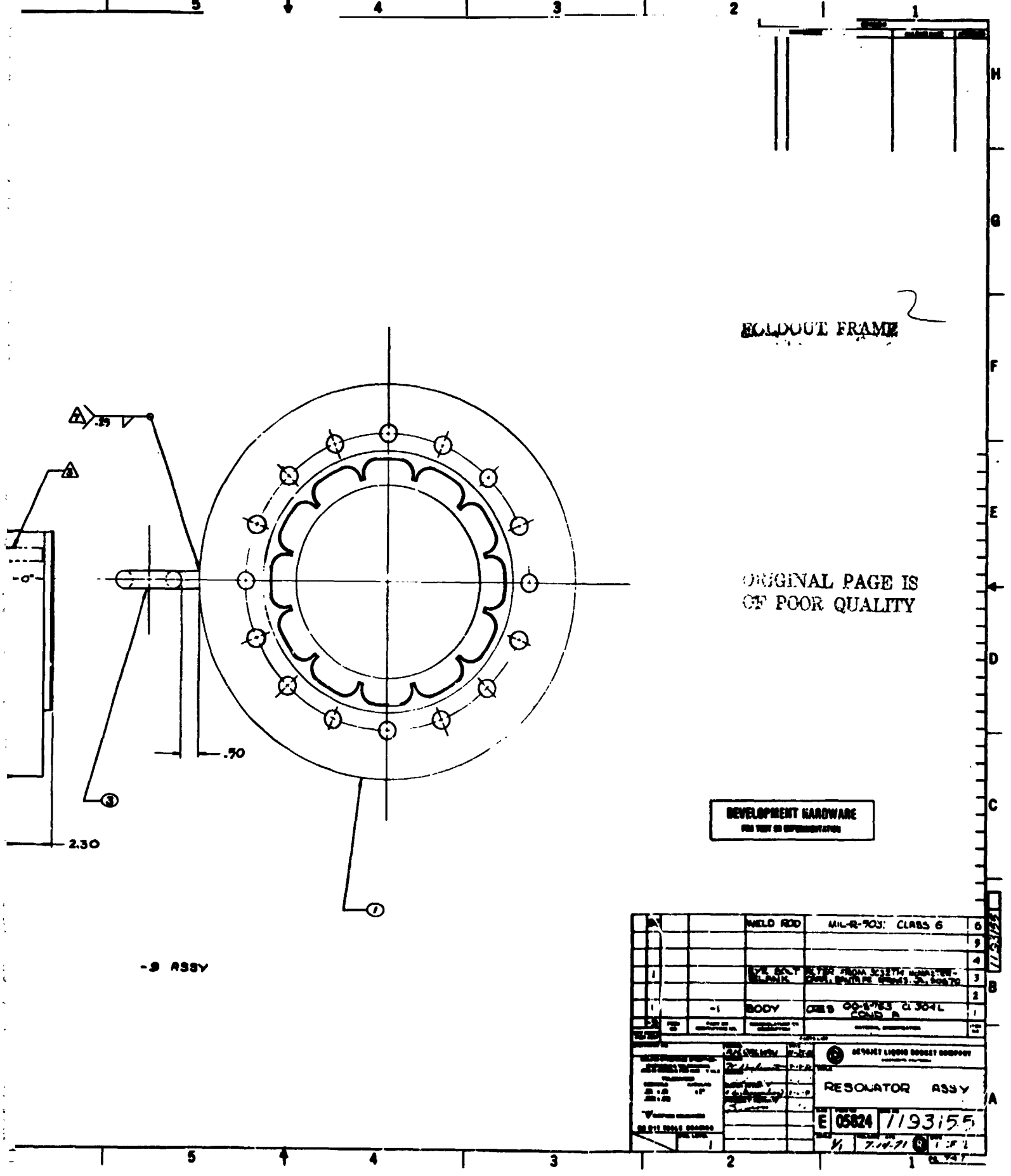

BLOWOUT FRAME

ORIGINAL PAGE IS
OF POOR QUALITY

Figure III-22. Resonator Assembly (Sheet 1 of 2)

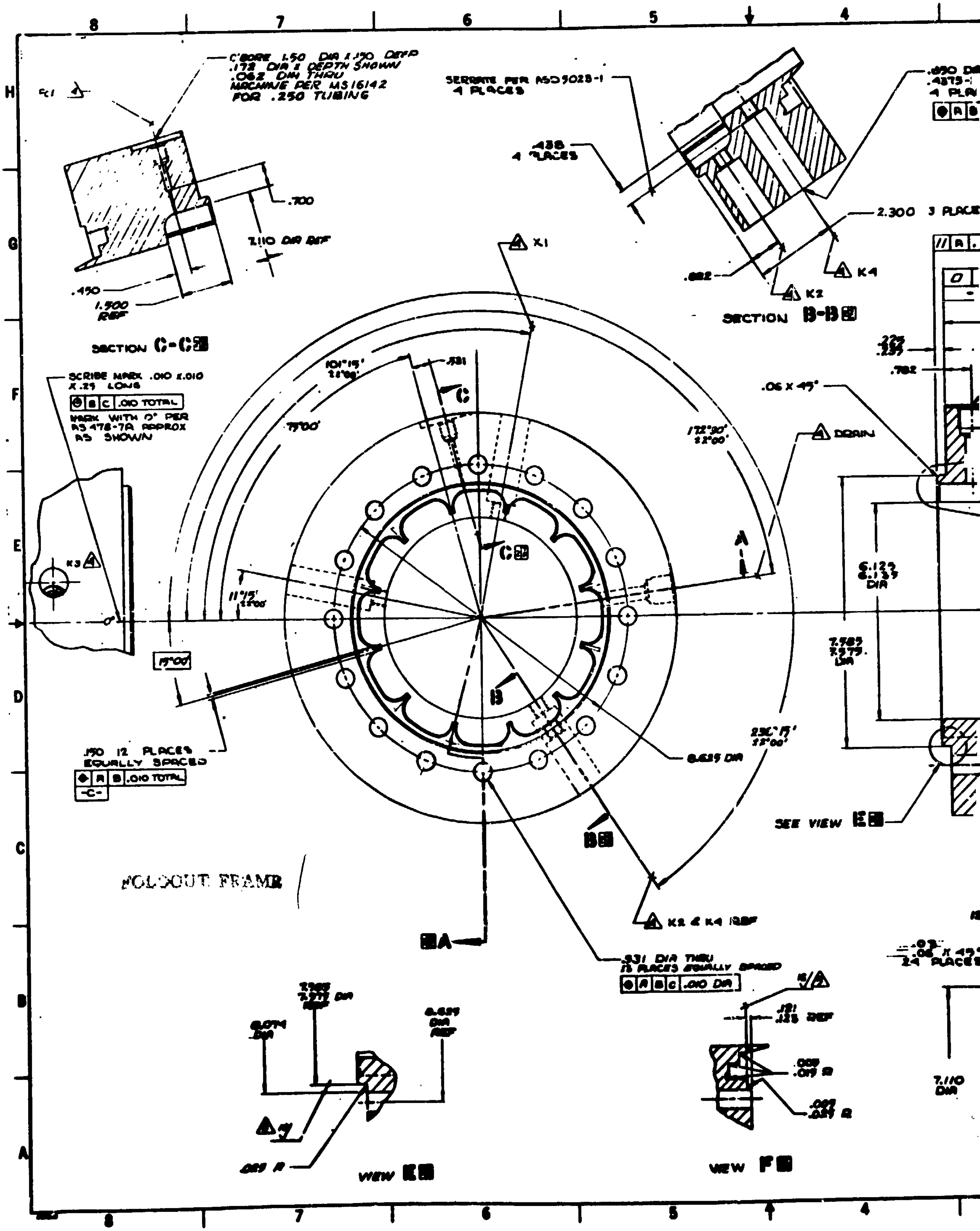

C'BORE 1.50 DIA X .150 DEEP
.172 DIA X DEPTH SHOWN
.062 DIA THRU
MACHINE PER MS16142
FOR .250 TUBING
SERRATE PER NSD5028-1
4 PLACES
.438
4 PLACES
.700
7.110 DIA REF
.450
1.500 REF
SECTION C-C
SECTION B-B
2.300 3 PLACES
K4
K2
X1
SCRIBE MARK .010 X.010
X.25 LONG
.010 TOTAL
MARK WITH 0° PER
AS 478-7A APPROX
AS SHOWN
.531
.06 X 45°
DRAIN
K3
6.125
6.137
DIA
7.585
7.575
DIA
.150 12 PLACES
EQUALLY SPACED
.010 TOTAL
-C-
8.625 DIA
SEE VIEW E
FOLDOUT FRAME
K2 & K4 REF
.331 DIA THRU
.010 DIA
7.110
DIA
VIEW E
VIEW F
.005 R
.025 R
24 PLACES

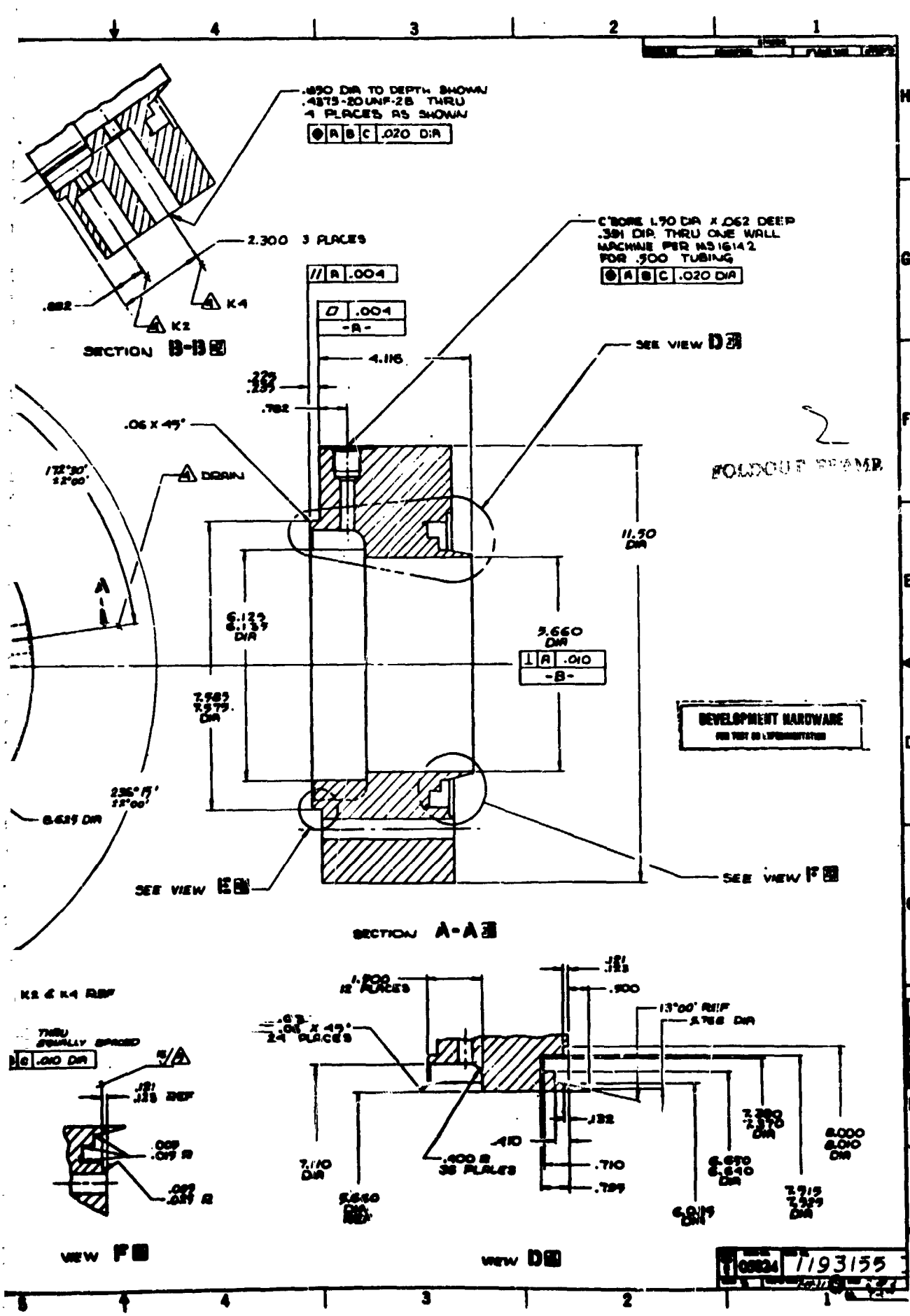

Figure III-22. Resonator Assembly (Sheet 2 of 2)

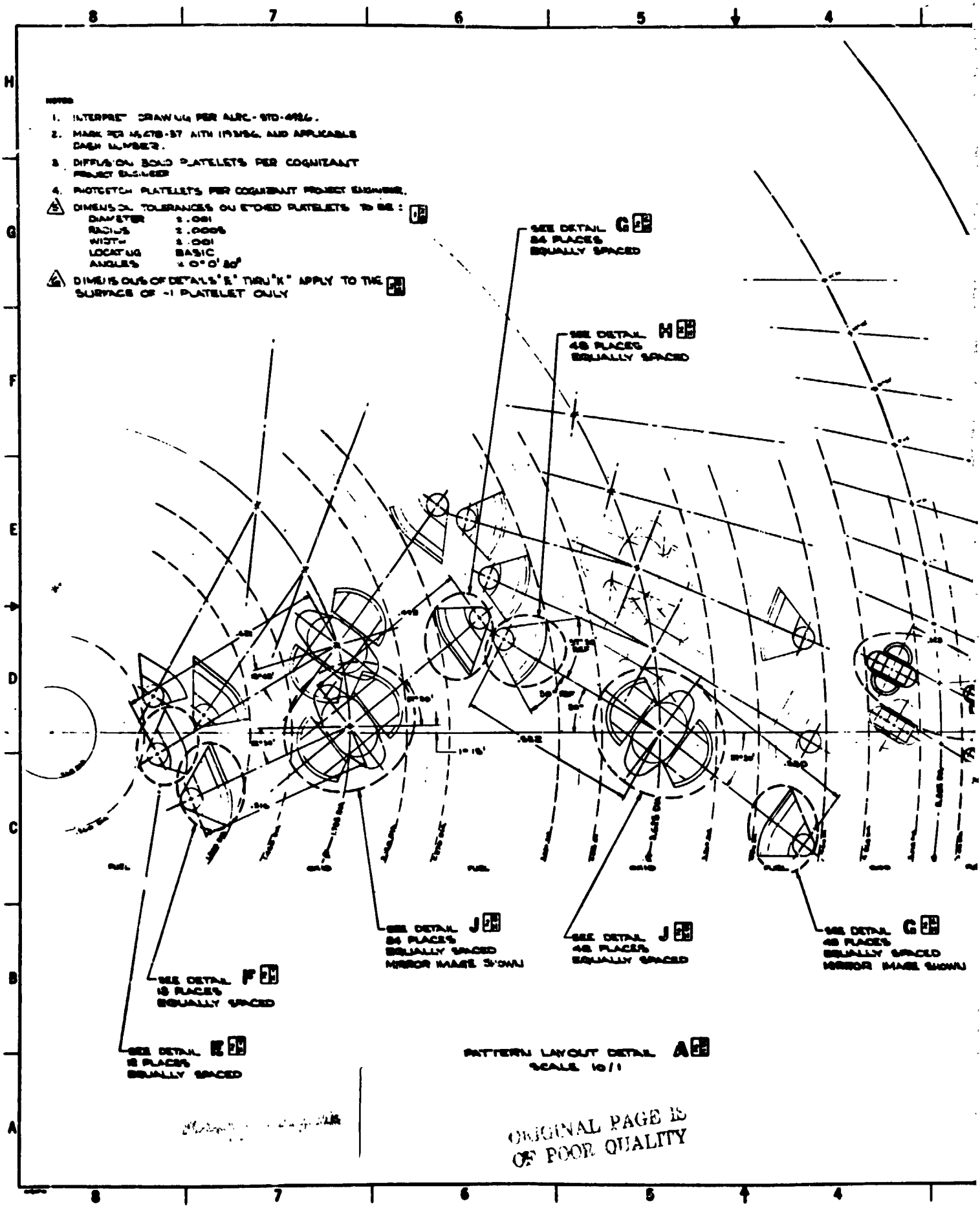

ORIGINAL PAGE IS
OF POOR QUALITY

Figure III-23. Inj

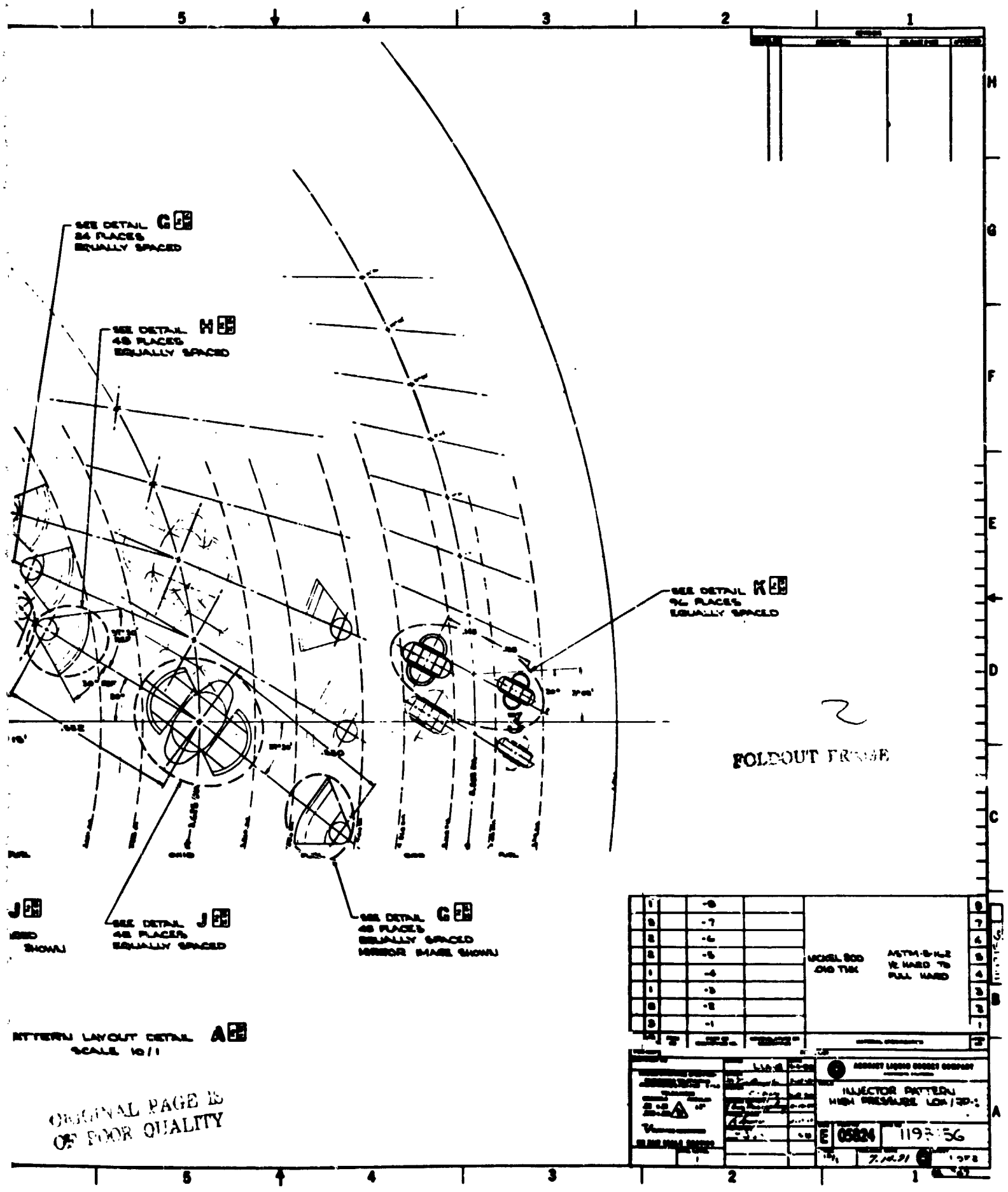

Figure III-23. Injector Pattern, High-Pressure LOX/RP-1 (Sheet 1 of 2)

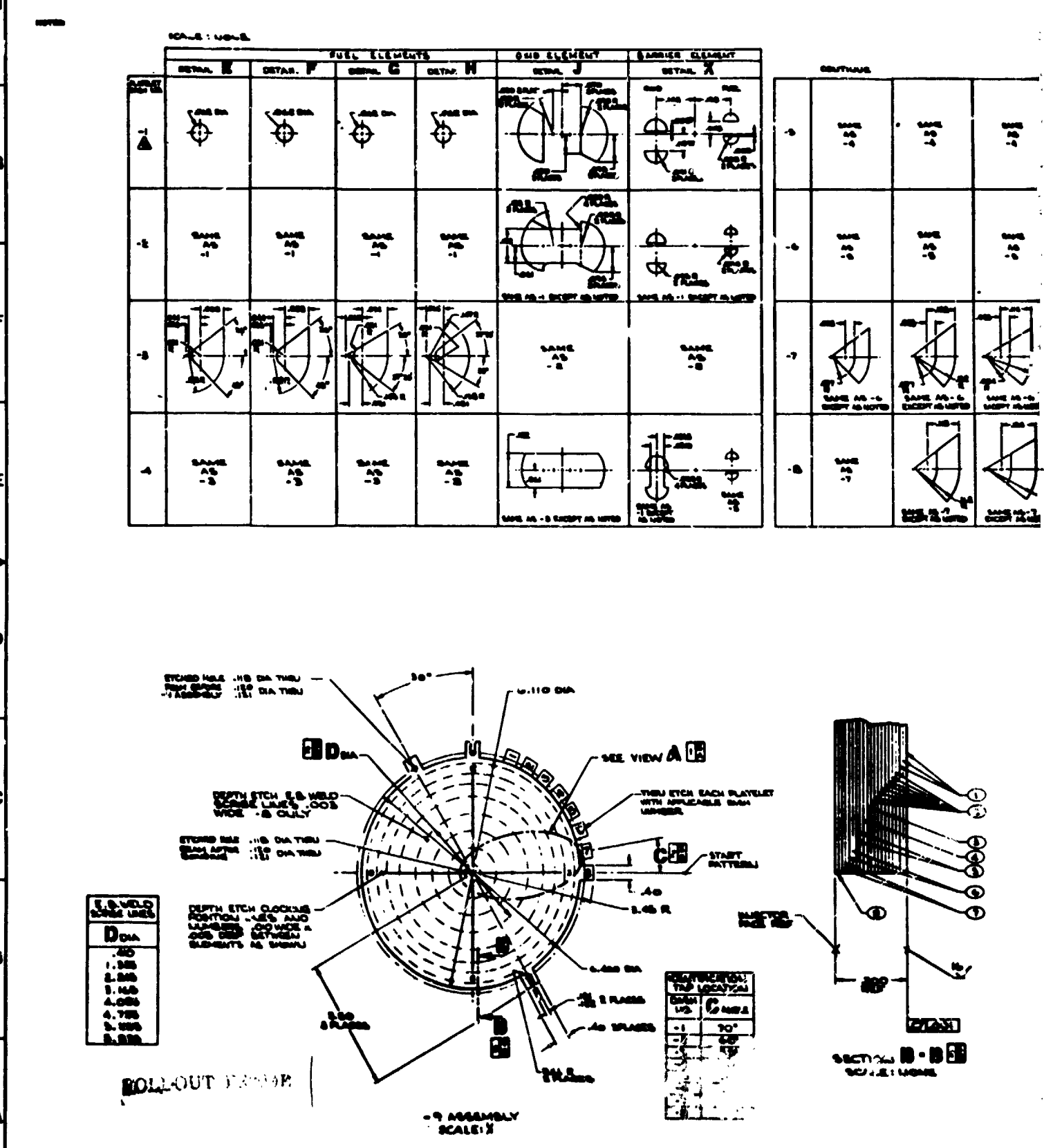

Figure III-23. Injec

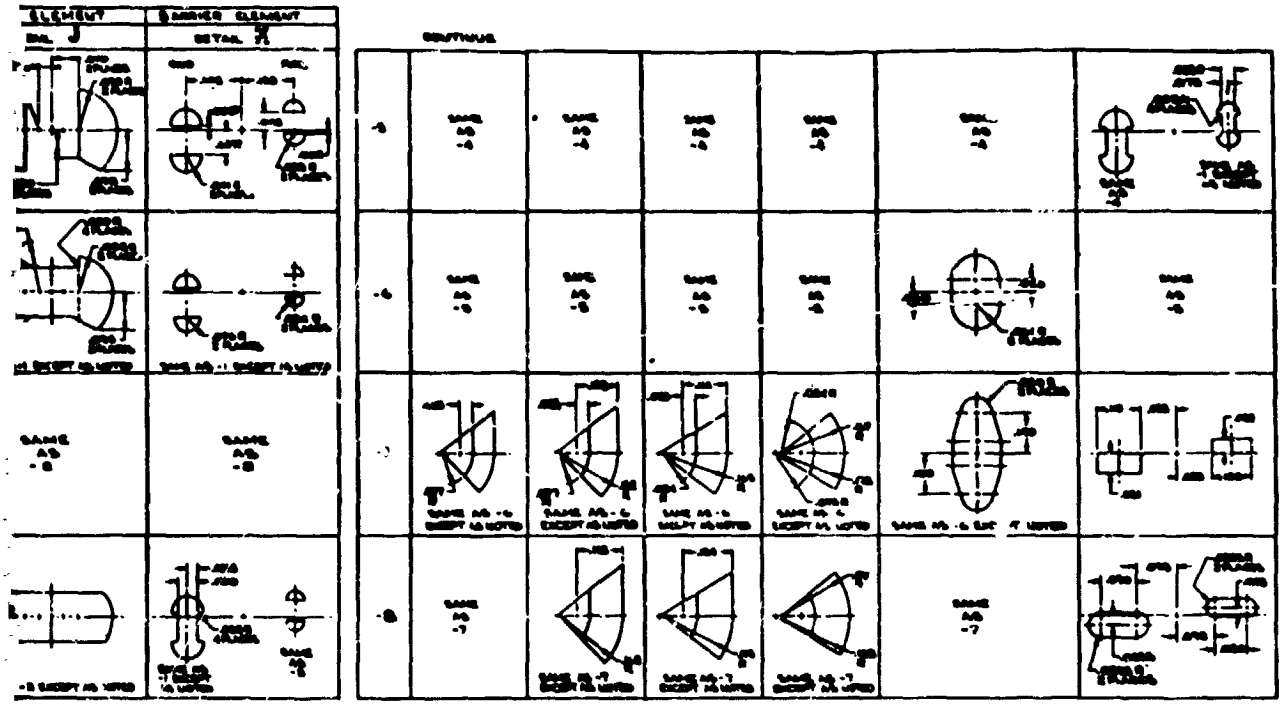

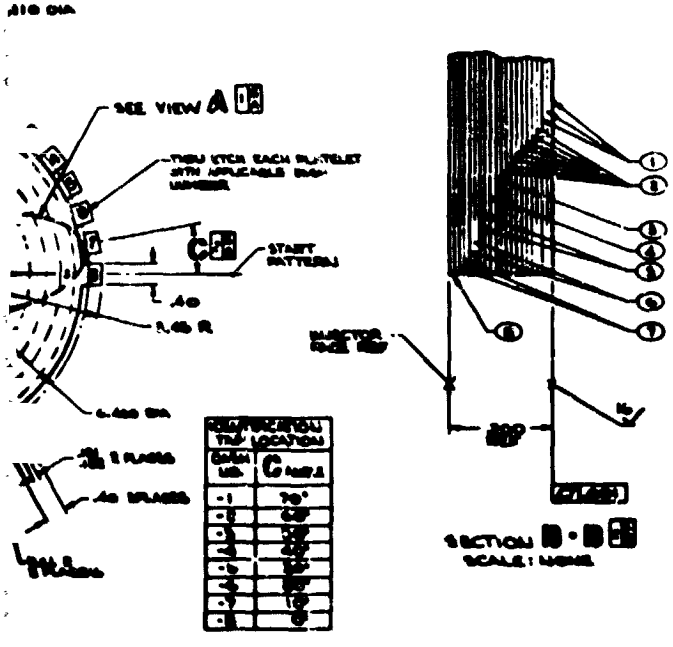

BOLDOUT FRAME

Figure III-23. Injector Pattern, High-Pressure LOX/RP-1 (Sheet 2 of 2)

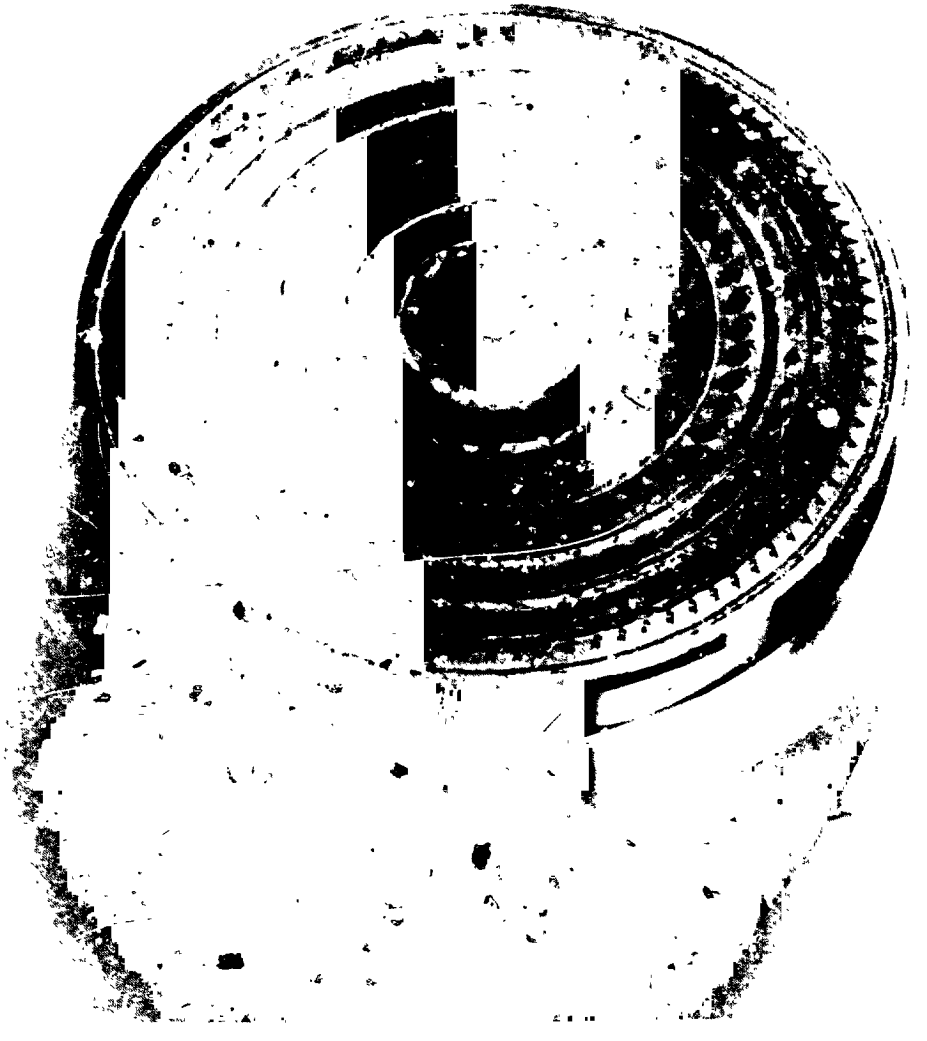

0781 SP 128

Figure III-24. Faceplate Following Welding to Body

employed to join the major flange and core subassemblies. These welds can be seen in Figures III-17 and III-20.

The nickel faceplates were etched and bonded according to proprietary ALRC processes. The stack of face platelets was prebonded, and the unitized assembly was then electron-beam-welded to the face rings as shown in Figure III-24. The initial EB-weld specimens employed to check out the Ni-200 to Cres 304L blind T welding parameters (see Figure III-25) indicated that this joint could not be satisfactorily completed because of the excessive thickness of the Ni stack (0.508 cm (0.2 in.)) relative to the 304L ring manifold (0.318 cm (0.125 in.)). The energy levels required to penetrate the nickel resulted in overheating the stainless steel and produced voids at the interface.

Contractual fabrication activities were temporarily stopped while ALRC explored various options to overcome these limitations. Satisfactory results were obtained by the addition of an intermediate material at the interface between the Ni-200 platelet stack and the Cres 304L body.

Photographs and photomicrographs of the test sections containing an intermediate filler are shown in Figure III-26. Additional full-scale simulated manifold fabrication weld verification testing was conducted prior to welding the deliverable injector. A full-scale manifold used for these tests is shown in Figure III-27. The resulting assembly was pressure-tested to provide a 20,682 kPa (3000 psi) pressure across the face

D. COLD-FLOW CHARACTERIZATION AND CHECKOUT

To ensure that the injector would perform as predicted hydraulically, several cold-flow tets with water were performed.

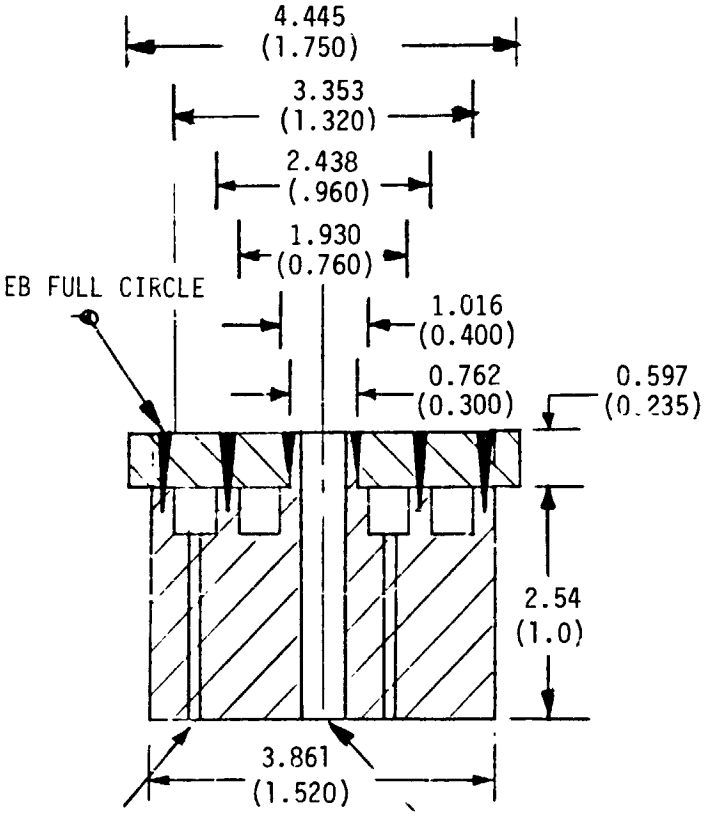

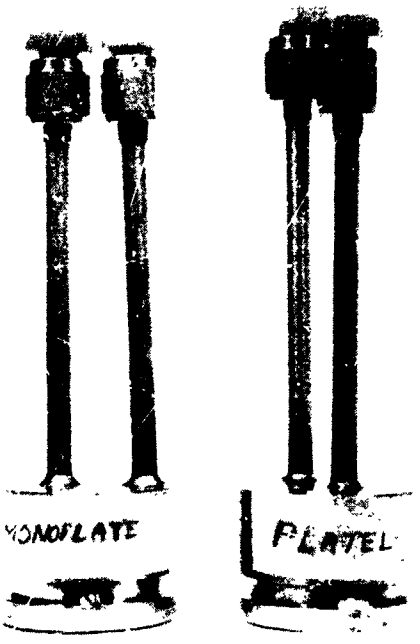

2 SPECIMENS - 20682 kPa (3000 psia)
PROOF "0" LEAKAGE GN_2 @ 1034 kPa
(150 psia)

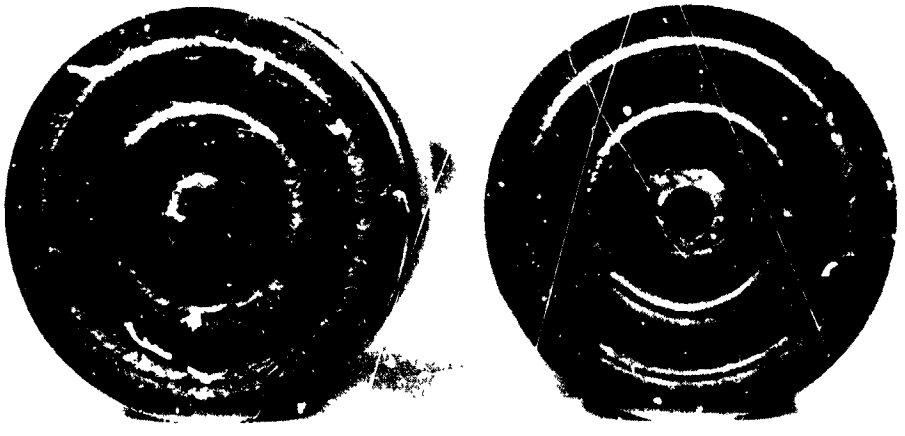

Ni-200 FACE
TO
Ni-200 LAND

NICKEL-200/PLATELET FACE
TO
Ni-61 OVER CRES 304L

Figure III-25. Experimental Evaluation of Circular Weld Specimens

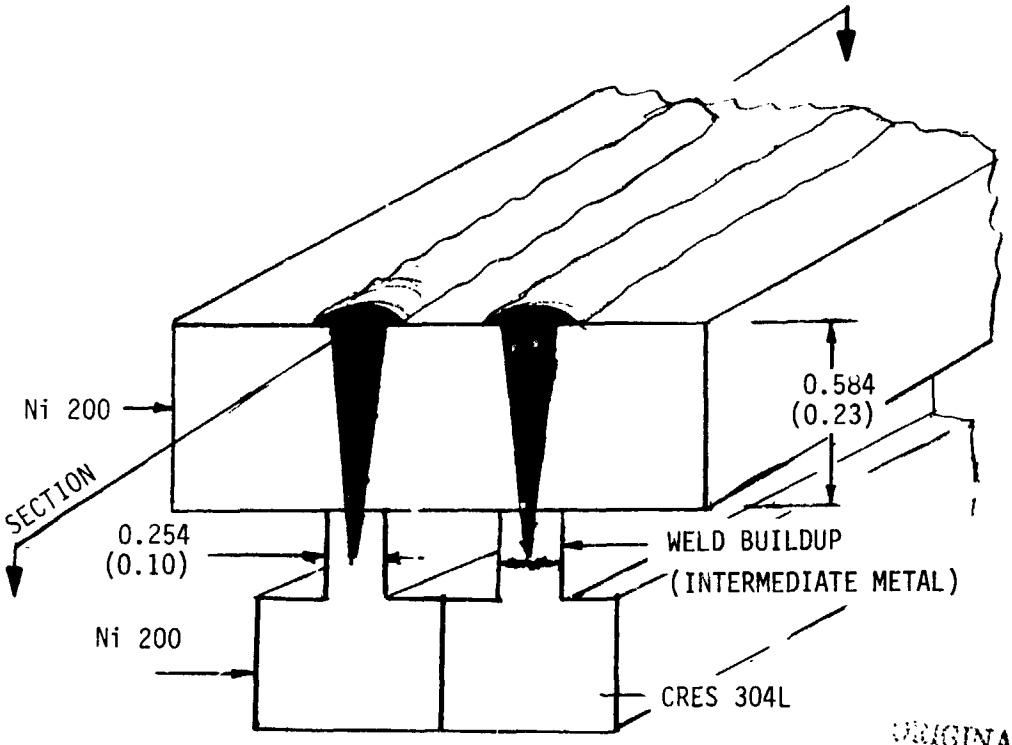

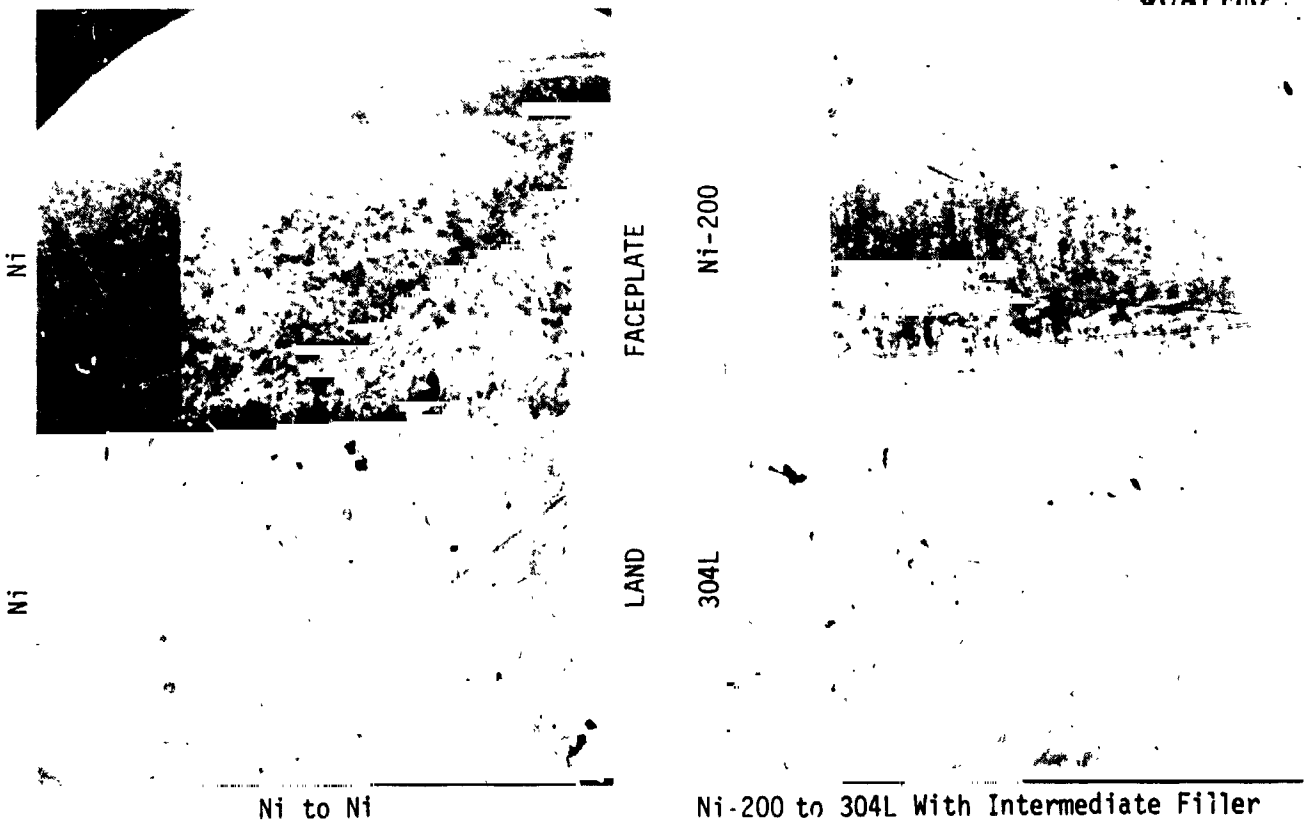

Figure III-26. T Bar Linear Weld Samples

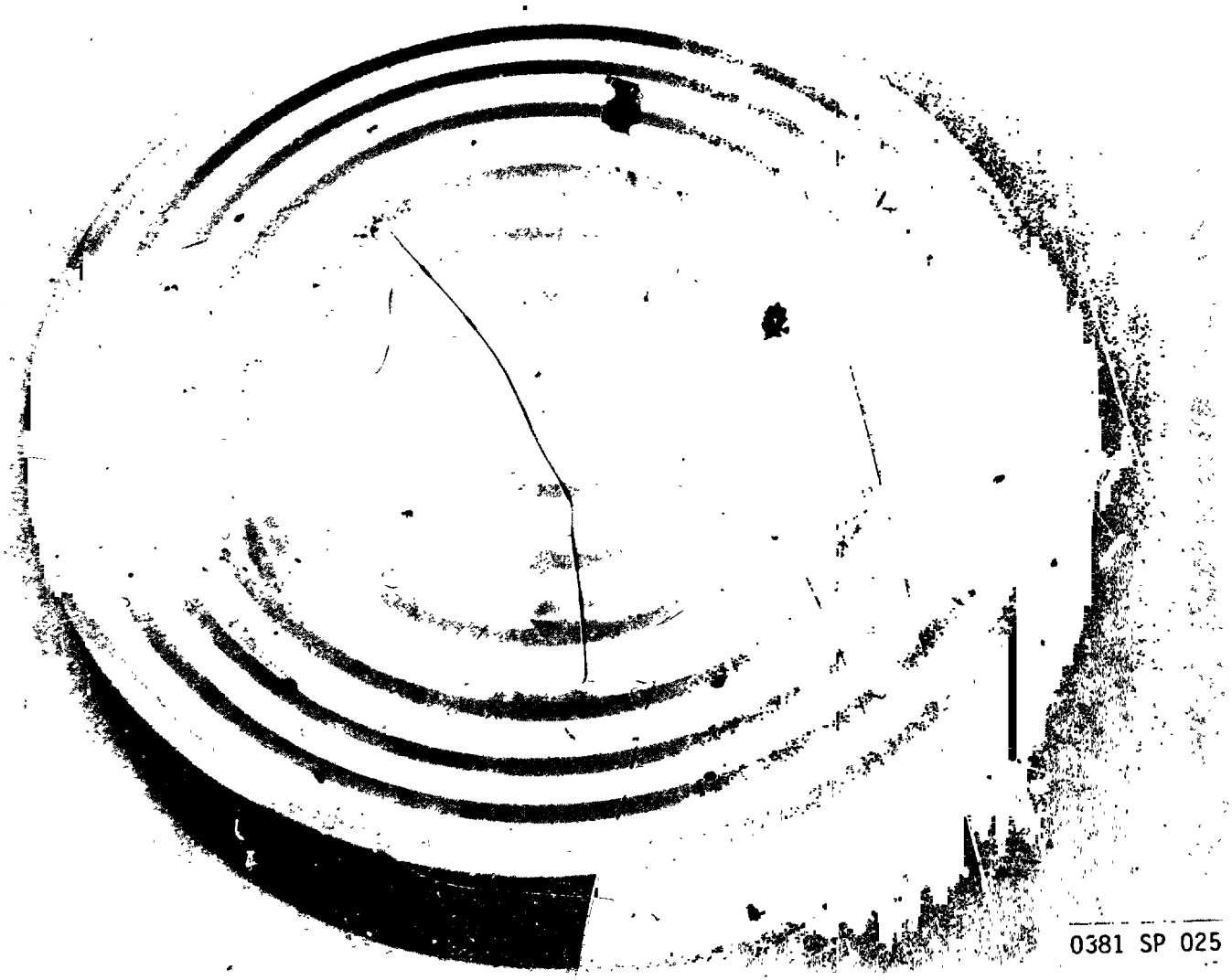

Figure III-27. Full-Scale Manifold Used for Weld Verification Tests

III, D, Cold-Flow Characterization and Checkout (cont.)

1. Pressure Drop and Pattern Check

Early in the fabrication process, prior to bonding the platelet stack, a mechanically clamped loose stack (Figure III-28) was flow-tested with a simulated manifold body. The purpose of the test was to verify the spray pattern and predicted pressure drop.

Initial flow tests indicated that the operational pressure drop was less than the expected 4,136 kPa (600 psi) target (see Table III-IV). A new flow metering platelet (PN 1193156-1) was etched, using a modified procedure to obtain a sharp-edged rather than a chamfered inlet. Reflow of the assembly with the replacement part provided the desired results, as indicated in Table III-V.

2. Injector Assembly Cold-Flow Testing

After final weld assembly and following a successful proof test of 31,023 kPa (4500 psia) and leak checks of 13,788 kPa (2000 psia) with GN_2, the oxidizer and fuel circuits were independently flow-tested with water. These data are provided in Table III-VI. Based on the test results, it is predicted that, at the lower operating point of Pc = 13,788 kPa (2000 psia), the fuel inlet line pressure will be 15,234 kPa (2210 psia) and the oxidizer inlet line pressure will be 15,427 kPa (2237 psia). At the maximum operating pressure of 20,682 kPa (3000 psia) Pc, the fuel inlet line pressure is estimated to be 23,935 kPa (3472 psia) and the oxidizer inlet line pressure is estimated to be 24,371 kPa (3535 psia).

3. Mixture Ratio Distribution

The cold-flow data indicated that 80% of the mass flow would be in the injector core and that the core MR is 2.83. The remaining 20% mass flow is in the barrier, at a MR of 2.76.

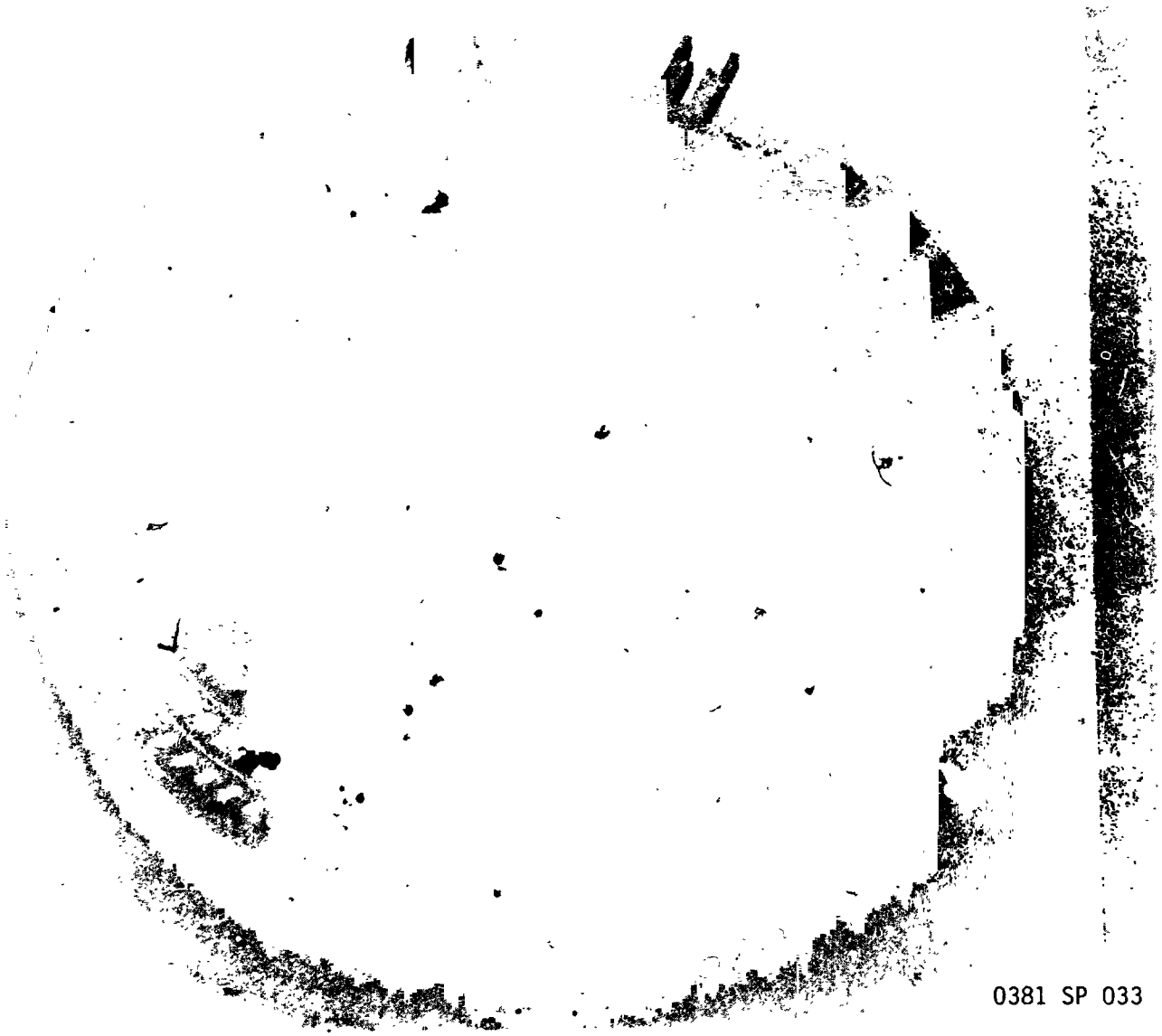

Figure III-28. Assembly of Loose Platelets Prior to Cold-Flow Testing

TABLE III-IV

LOOSE-STACK COLD-FLOW

TEST #1 - LARGE CHEVRON

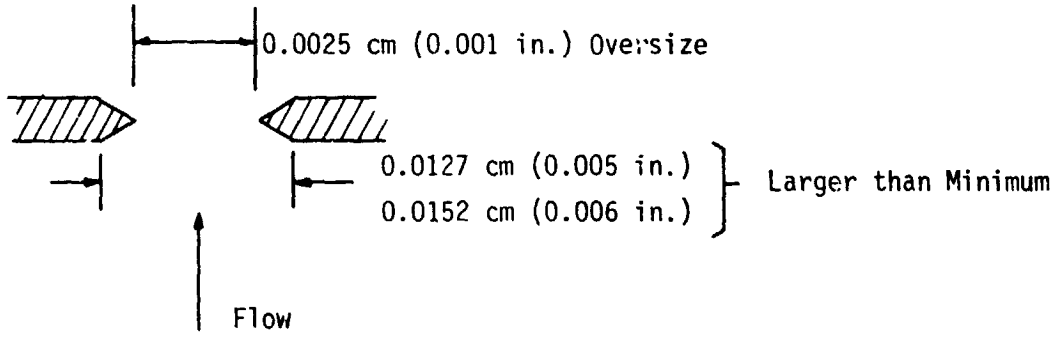

Single-Element Flow

Location	ΔP, kPa (psi)	$\dot{W}$, kg/sec (lb/sec)	Kw*
Outer Fuel	68.9 (10)*	0.0068 (0.0149)	0.00081 (0.00471)
	172.4 (25)	0.0103 (0.0226)	0.00078 (0.00452)
	344.7 (50)	0.0143 (0.0315)	0.00077 (0.00445)
Outer Oxidizer	68.9 (10)	0.0133 (0.0293)	0.00160 (0.00926)
	172.4 (25)	0.0206 (0.0455)	0.00157 (0.00910)
	344.7 (50)	0.0293 (0.0645)	0.00158 (0.00912)
Oxidizer Main	68.9 (10)	0.0833 (0.1837)	0.01002 (0.0580)
	131.0 (19)	0.1075 (0.2369)	0.00940 (0.0544)
Fuel Main	68.9 (10)	0.0174 (0.0383)	0.00209 (0.0121)
	172.4 (25)	0.0271 (0.0597)	0.00206 (0.0119)

All Elements, Calculated

Kw Oxidizer	Core =	0.699 (4.046)	82%
	Barrier =	0.152 (0.879)	18%
	Total =	0.851 (4.926)	O/F Barrier = 2.47
	ΔPox =	2875 kPa (417 psi)	O/F Core = 2.88
Kw Fuel	Core =	0.299 (1.728)	80%
	Barrier =	0.0756 (0.438)	20%
	Total =	0.375 (2.166)	
	ΔP Fuel =	2613 kPa (379 psi)	

$$*(Kw) = \left(\frac{\dot{w}\ (kg/sec)}{\sqrt{\Delta P\ (kPa)\ Sg}}\right) \text{ or } \left(\frac{\dot{w}\ (lb/sec)}{\sqrt{\Delta P\ (psi)\ Sg}}\right)$$

*SI Units (English Units)

TABLE III-V

LOOSE STACK COLD-FLOW

TEST #2 - SHARP-EDGED ORIFICE

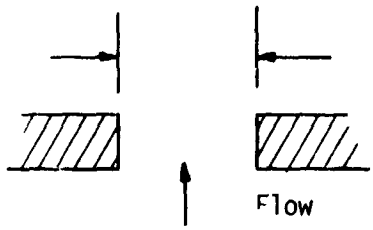

Single-Element Flow

Location	ΔP, kPa (psi)	$\dot{W}$, kg/sec (lb/sec)	Kw*
Outer Fuel	68.9 (10)*	0.00638 (0.01407)	0.00077 (0.00445)
	172.4 (25)	0.00989 (0.0218)	0.00075 (0.004365)
	344.7 (50)	0.01374 (0.0303)	0.00074 (0.00429)
Outer Oxidizer	68.9 (10)	0.01330 (0.02932)	0.00160 (0.00927)
	172.4 (25)	0.02075 (0.04575)	0.00158 (0.00915)
	344.7 (50)	0.02975 (0.06559)	0.00160 (0.00928)
Oxidizer Main	68.9 (10)	0.07099 (0.1565)	0.00885 (0.0495)
	172.4 (25)	0.11249 (0.248)	0.00857 (0.0496)
	344.9 (50)	0.16198 (0.3571)	0.00872 (0.0505)
Fuel Main	68.9 (10)	0.01642 (0.0362)	0.00199 (0.0115)
	172.4 (25)	0.02567 (0.0566)	0.00195 (0.0113)
	344.7 (50)	0.03624 (0.0799)	0.00195 (0.0113)

All Elements Calculated

Kw Oxidizer	Core = 0.620 (3.586)	80%
	Barrier = 0.153 (0.886)	20%
	Total = 0.773 (4.472)	O/F Barrier = 2.76
	ΔPox = 3485 kPa (506 psi)	O/F Core = 2.83
Kw Fuel	Core = 0.281 (1.627)	80%
	Barrier = 0.072 (0.416)	20%
	Total = 0.353 (2.043)	
	ΔP Fuel = 2937 kPa (426 psi)	

$$*(Kw) = \left(\frac{\dot{w}\ (kg/sec)}{\sqrt{\Delta P\ (kPa)\ Sg}}\right) \text{ or } \left(\frac{\dot{w}\ (lb/sec)}{\sqrt{\Delta P\ (psi)\ Sg}}\right)$$

*SI Units (English Units)

TABLE III-VI

FINAL ASSEMBLY COLD-FLOW

OX CIRCUIT

$\dot{w}_{H_2O}$ Flow kg/sec	lb/sec	ΔP gage kPa	psi	$\Delta P(P_{fg}-P_{back})$ kPa	psi	Kw (ΔP)(gage)	Kw (absolute gage)
16.6	36.6	458.5	66.5	1082-600	157-87	4.49	4.38
19.4	42.8	654.9	95.0	1517-855	220-124	4.39	4.37
22.9	50.4	882.4	128.0	2103-1213	305-176	4.45	4.44
FUEL CIRCUIT						Expected Value = 4.4	
Water Flow $\dot{w}$ kg/sec	lb/sec			$\Delta P(P_{oj}-P_{back})$ kPa	psi		
8.89	19.59	710.1	103.0	951-241	138-35	1.93	1.93
9.97	21.99	879.0	127.5	1193-296	173-43	1.95	1.93
10.72	23.63	1013.4	147.0	1379-345	200-50	1.95	1.93

Expected Value 2.043

IV. OPERATION

The LOX/RP-1 injector design requirements and predicted operating parameters are contained in Table IV-I. Also included are maximum allowable operating pressure values that should be incorporated into test operating procedures. It has been predicted that all of the design requirements will be satisfied. In addition, ALRC feels confident that other important factors such as chamber heat flux can also be met satisfactorily.

A. IGNITION SYSTEM AND START SEQUENCE

In order to achieve a smooth, reliable start, ALRC recommends the use of a 0.15/0.85 mixture of TEA/TEB. In the event of a TEB availability problem, TEA will achieve satisfactory ignition; however, TEA does leave heavy deposits that may have to be removed.

A suggested igniter plumbing schematic is shown in Figure IV-1. A low-flow oxygen supply line which parallels the main valve is shown as a typical method of limiting the preignition pressure drop across the injector face during the start transient to a maximum of 13,788 kPa (2000 psia). Other methods, such as a preprogrammed valve opening rate, would also be acceptable. This suggested ignition system would provide the capability of loading a predetermined quantity of igniter fluid into an accumulator. A small purge flow should be maintained through the igniter, following its cut-off, to ensure proper cooling of the igniter port and the central portion of the injector face. The purge can be GN_2, as shown, or RP-1. This purge pressure should be sufficiently high to preclude backflow into the igniter in the event of an instability. A check valve is required to preclude backflow. Figure IV-2 shows the ignition sequence and start transient employed in the 13,788-kPa (2000-psia) High-Density Fuel Program. A 0.02-ms (minimum) ox lead start is recommended for a soft start. The valve opening rates should be controlled to prevent the ΔP across the injector face from exceeding 13,788 kPa (2000 psia).

TABLE IV-I

DESIGN REQUIREMENTS AND PREDICTED OPERATION (SI Units)

	Requirement	Prediction	Maximum Operating Value
Chamber Pressure(Pc), kPa	13788/20682	13788/20682	
Fuel:	RP-1		
Temperature, °K	Ambient		
Maximum Interface Pressure, kPa	15450/24129		27576[2]
Flowrate, kg/sec	11.39/17.10	11.39/17.10	
Oxidizer:	LOX		
Temperature, °K	358		
Maximum Interface Pressure, kPa	15856/25508		27576[2]
Flowrate, kg/sec	31.93/47.90	31.93/47.90	
Propellant Mixture Ratio	2.8		
Characteristic Velocity Efficiency	>97%		
Allowable Chamber Pressure Oscillations	$\pm$ 5%[1]		
Combustion Chamber:			
Throat Diameter, cm	8.407		
Chamber Diameter, cm	14.376		
Length(Injector to Throat), cm	35.484		
Ignition Fluid:		TEA/TEB	
Temperature, °K		Ambient	
Flowrate, kg/sec		TBD	
Pressure Drop:			
P_{FJ} - Pc, psia		1447/3254	17235
P_{OJ} - Pc, psia		1639/3688	17235

(1) <5% after tuning of resonator cavity with actual test data

(2) Proof pressure test (31023 kPa)

TABLE IV-I (cont.)

DESIGN REQUIREMENTS AND PREDICTED OPERATION (English Units)

	Requirement	Prediction	Maximum Operating Value
Chamber Pressure(Pc), psia	2000/3000	2000/3000	
Fuel:	RP-1		
Temperature	Ambient		
Maximum Interface Pressure	2244/3500		4000[2]
Flowrate, lbm/sec	25.1/37.7	25.1/37.7	
Oxidizer:	LOX		
Temperature, °R	185		
Maximum Interface Pressure	2300/3700		4000[2]
Flowrate, lbm/sec	70.4/105.6	70.4/105.6	
Propellant Mixture Ratio	2.8		
Characteristic Velocity Efficiency	>97%		
Allowable Chamber Pressure Oscillations	≤± 5%*	1	
Combustion Chambers:			
Throat Diameter, in.	3.310		
Chamber Diameter, in.	5.660		
Length (Injector to Throat), in.	13.97		
Ignition Fluid:		TEA/TEB	
Temperature		Ambient	
Flowrate, lbm/sec		TBD	
Pressure Drop:			
P_{FJ} - Pc, kPa		210/472	2500
P_{OJ} - Pc, kPa		233/535	2500

(1) <5% after tuning of resonator cavity with actual test data

(2) Proof pressure test (4500 psia)

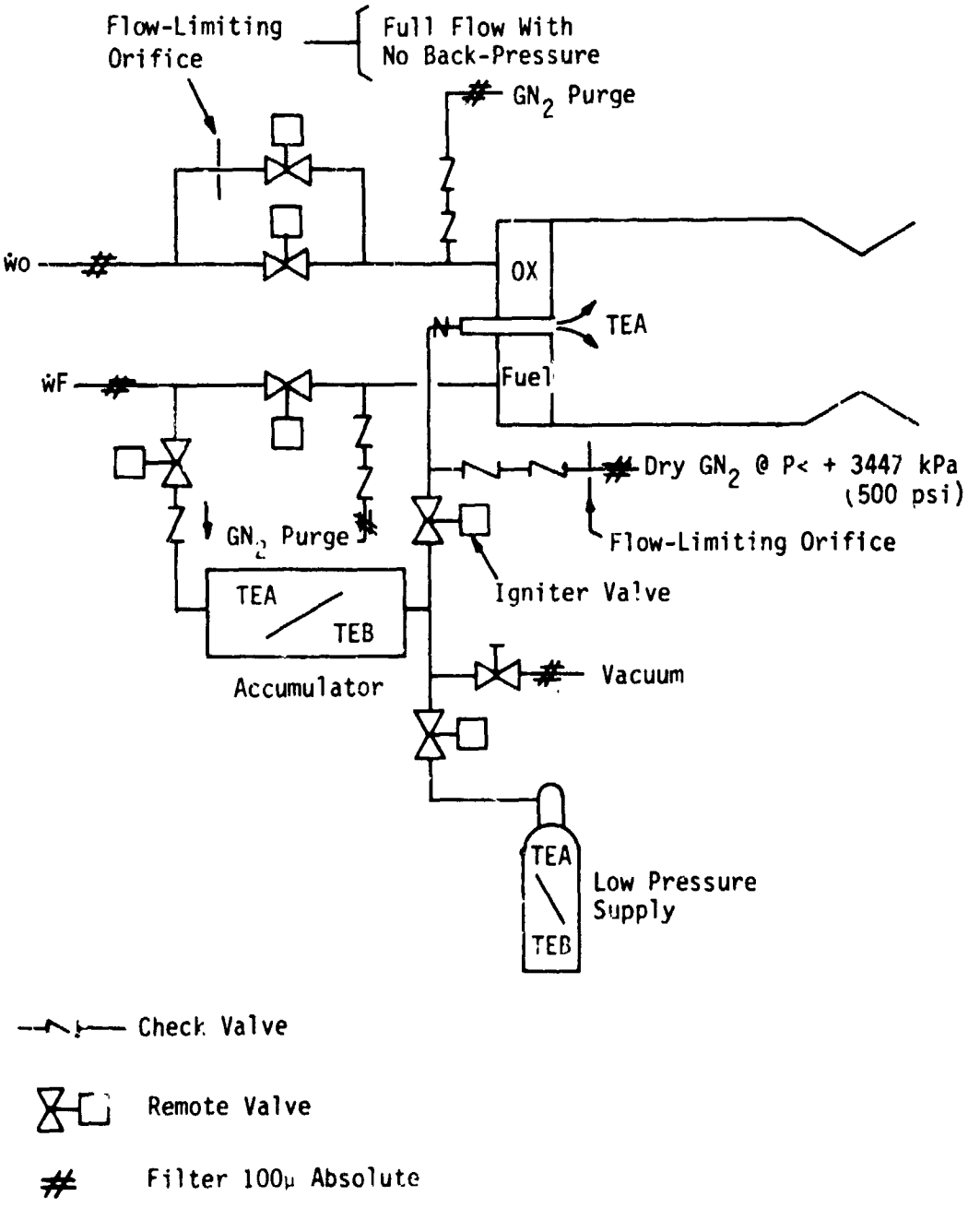

Figure IV-1. Suggested Propellant Supply for the Ignition System

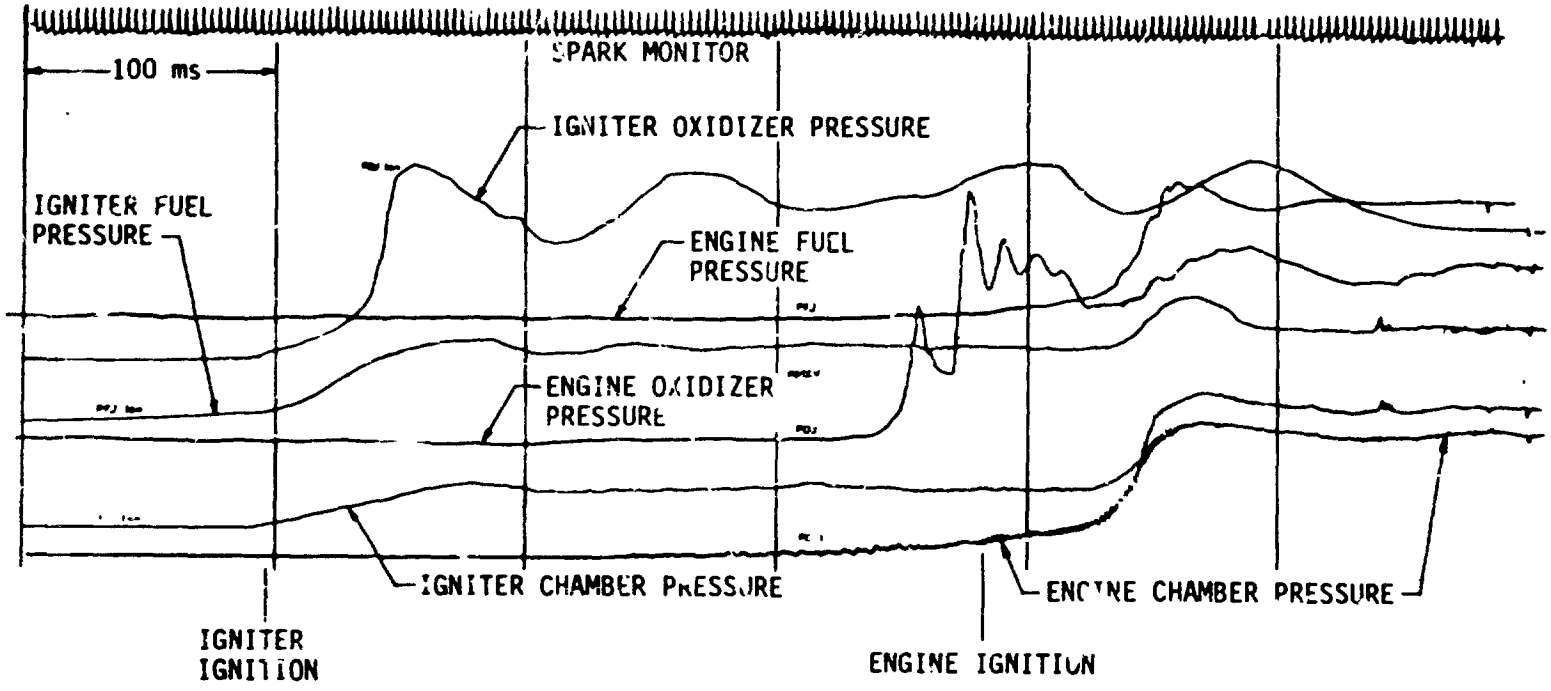

Figure IV-2. Ignition Transient of 2000 psia LOX/RP-1 Engine

IV, A, Ignition System and Start Sequence (cont.)

The recommended test sequence is as follows:

Start

a. Make sure all valves are closed.

b. Open igniter system vacuum valve to remove any air from system.

c. Close vacuum valve.

d. Open TEA/TEB low-pressure supply valve to fill accumulator to selected capacity.

e. Close supply valve.

f. Open fuel valve to accumulator. Accumulator should now be at fuel supply pressure.

g. Perform facility sequencing.

h. Start signal.

i. Open secondary oxidizer valve. LOX flowrate should be 45.36 kg/sec (100 lb/sec) at full thrust.

j. Open igniter valve.

k. Sample chamber pressure for ignition. Shut down if ignition is not achieved prior to fuel valve initiation.

l. Initiate fuel valve opening.

m. Initiate main oxidizer valve opening.

n. Sample for chamber pressure; shut down if full Pc is not achieved.

o. If recommended GN_2 purge circuit is used, close igniter valve.*

*Dumping of fuel through igniter port during test will reduce performance.

IV, A, Ignition System and Start Sequence (cont.)

Shutdown

a. Close oxygen valve.
b. Close fuel valve.

B. CARE AND HANDLING

The LOX/RP-1 injector assembly PN 1193106 comprises two major components:

Injector Body Subassembly PN 1193138
Resonator Ring Assembly PN 1193155

In addition, there are the small igniter components plus various seals, fasteners, and extra tuning blocks for the acoustic resonator.

The following suggestions and comments may be helpful during the handling operation of this unit. They are as follows:

1. The unit was slipped with a protective face cover. This cover should remain in place during all handling operations to protect the soft, fully annealed nickel face. In addition, LOX cleaning processes which are not compatible with nickel, such as picklings, should not be employed.

2. The injector assembly weighs approximately 160 kg (350 lb) and should be handled accordingly. A lifting eyebolt has been provided for this purpose. Drain ports have been placed to function properly when the eyebolt is in the vertically upward position.

C-2

IV, B, Care and Handling (cont.)

3. The high-strength nuts and bolts supplied with the unit are subject to galling and should be lubricated with a propellant-compatible lubricant such as Fel-Pro.

4. The unit should be LOX-cleaned prior to firing.

5. The propellant, RP-1, and the oxidizer should be filtered to 100 microns absolute or less.

6. The unit was delivered with the resonator cavity ring installed and tuned to dampen the most likely modes of combined 1T/2T instability. It may be necessary to resize the cavities if the actual gas sound speed in the cavities differs from the estimated values. The high-frequency pressure measuring ports provided allow the necessary data for resizing these ports to be obtained.

7. Once a stable cavity configuration has been obtained and verified by several short 1/2- to 1-sec tests, the tuning blocks should be tack-welded in place at the screw head and in the corners. Experience has shown that the screws (regardless of torque and locking compounds used) work themselves loose due to the thermal and vibration effects encountered in long-duration tests.

ALRC Post-Test LOX Cleaning Procedure

Normal high pressure post-test GN_2 purges are employed to remove excess propellant from the feed system following valve closure at the end of a test. Before each test, both the fuel and oxidizer circuits are degreased with GN_2-atomized 1,1,1-trichloroethane (TCL). Hot GN_2 at 353 to 367°K (175 to 200°F) is recommended. Before introducing the cleaning

solvent, the cryogenic oxidizer line is allowed to warm to ambient temperature. This warming prevents the cleaning solvent from freezing in the line. LOX and solid trichloroethane can detonate on contact, causing extensive damage.

Following verification that collected samples of the TCE are free of hydrocarbon, the LOX system is purged with hot GN_2-atomized Freon TF. The Freon will replace the TCE; the manifold drain ports and resonator cavity drain ports remain open during these cleaning operations. (California and ALRC environmental regulations require that liquid TCE be collected and disposed of in accordance with toxic waste standards for this material.) A hot GN_2 dry purge at 353 to 367°K (175 to 200°F) is maintained until it is evident that all residual cleaning solvents have been removed.

Dry GN_2 trickle purges are maintained during the LOX line chill-down operation to prevent contamination and potential frost deposits within the engine.

The trickle purges remain in effect until the prefire high-pressure purge sequence is initiated.

C. INSTRUMENTATION

The following instrumentation ports have been provided:

Injector

Fuel Manifold Pressure	P_{FJ}
Oxidizer Manifold Pressure	P_{OJ}
Oxidizer Manifold Temperature	T_{OJ}

IV, C, Instrumentation (cont.)

High-Frequency Manifold

Oxidizer	K_{OJ}
Fuel	K_{FJ}

Resonator Capacity and Ring

Chamber Pressure	Pc-1	(Kistler Model 601)
High-Frequency Chamber Pressure	K-1	
High-Frequency Chamber Pressure	K-2	
High-Frequency Chamber Pressure	K-3	
High-Frequency Chamber Pressure	K-4	

The Kistler ports have been designed to utilize a 7-mm to 7/16-20 standard thread adapter fitting. This fitting (PN 1183588) is shown in Figure IV-3. PN 1183588-1 contains a 0.157-cm (0.062-in.) diameter restrictor to protect the Kistler diaphragm and is for use in the hot gas stream. PN 1183588-2 is recommended for use in the propellant lines.

D. PROPELLANT FILTRATION REQUIREMENTS

The minimum passage sizes in the injector are as follows:

Fuel Circuit	0.061 cm (0.024 in.)
Oxidizer Circuit	0.089 cm (0.035 in.)

These occur in the barrier elements (see Figure III-23). The recommended filtration sizes for the propellant are 100 microns absolute for both fuel and oxidizer.

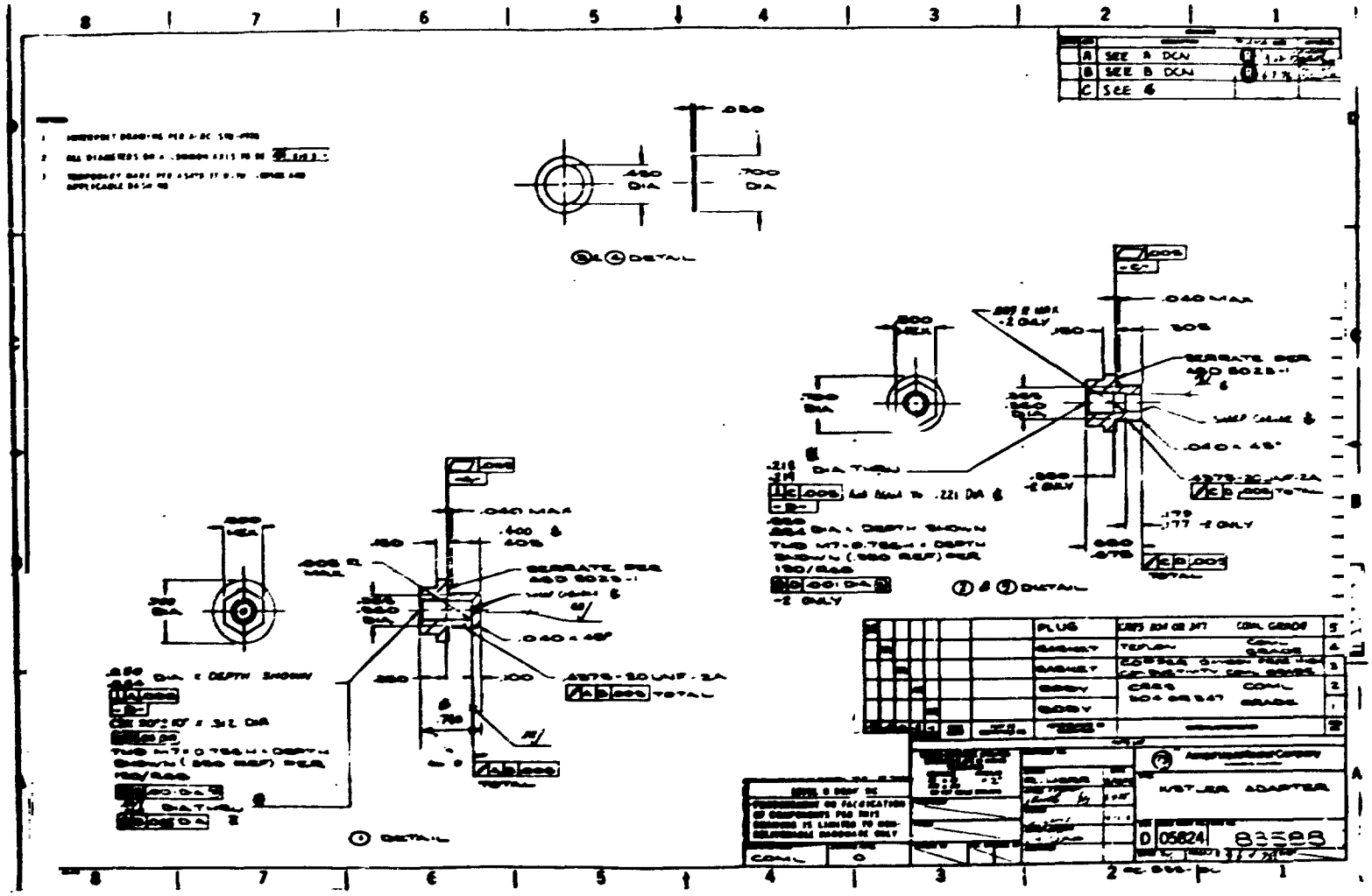

Figure IV-3. Kistler Adapter

REFERENCES

1. LaBotz, R.J., D.C. Rousar, and H.W. Valler. High-Density Fuel Combustion and Cooling Investigation. Final Report, ALRC, NAS 3-21030, NASA-CR 165177, 1981.

2. Priem, R.J. and Heidman, M.F. Propellant Vaporization as a Design Criterion for Rocket Engine Combustion Chambers, NASA TR-67, 1960.